

4-23-2021 10:30 AM

Mitigation of Fluid Coker Cyclone Fouling with Consideration to Reactor Performance

Andrew J. Heaslip, *The University of Western Ontario*

Supervisor: Pjontek, Dominic, *The University of Western Ontario*

A thesis submitted in partial fulfillment of the requirements for the Master of Engineering Science degree in Chemical and Biochemical Engineering

© Andrew J. Heaslip 2021

Follow this and additional works at: <https://ir.lib.uwo.ca/etd>

 Part of the [Petroleum Engineering Commons](#)

Recommended Citation

Heaslip, Andrew J., "Mitigation of Fluid Coker Cyclone Fouling with Consideration to Reactor Performance" (2021). *Electronic Thesis and Dissertation Repository*. 7768.
<https://ir.lib.uwo.ca/etd/7768>

This Dissertation/Thesis is brought to you for free and open access by Scholarship@Western. It has been accepted for inclusion in Electronic Thesis and Dissertation Repository by an authorized administrator of Scholarship@Western. For more information, please contact wlsadmin@uwo.ca.

Abstract

FLUID COKING™ is a continuous process to thermally upgrade heavy hydrocarbons into lighter, higher-value products. Fouling of the cyclones in commercial Fluid Coker reactors significantly reduces unit runtimes. The main objective of this thesis is to improve unit reliability by identifying process levers that can mitigate against this phenomenon while minimizing reductions in product quality. This thesis expanded a previous freeboard region model to consider vapour phase cracking and adsorption and developed a novel reactor region model to consider the impact of liquid and vapour phase cracking, vapour-liquid equilibrium, and residence time distribution on product composition. By changing the temperature and flowrate of key process inlets, these two parallel models noted the impact of raising specific process temperatures on increased light end yields, while identifying increasing steam and scouring coke flows as the most effective methods to reduce cyclone fouling while minimizing the impact on Fluid Coker products.

Keywords: Process modelling, Aspen Plus, thermal cracking, vacuum residues, vapour condensation, residence time distribution

Summary for Lay Audience

Canada has an abundance of natural resources, including the third largest oil reserve in the world. However, this oil is found in a thick, heavy, tar-like form, referred as bitumen, which cannot be used in its natural state. By taking this heavy oil and heating it up to high temperatures (between 500 and 550°C), the large hydrocarbon molecules can break, or crack, into smaller, useful compounds like gasoline and diesel. One reactor that is used for this conversion is called a Fluid Coker, which can run continuously as long as it is fed heavy oil and sufficient heat is provided. However, droplets of the heavy oil can form, adhere and solidify at the wall of the reactor outlet, causing it to be plugged and shut down. Previous studies showed that increasing the reactor temperature would prevent the droplets from forming and clogging the outlet, thus increasing the unit run length. Nonetheless, if the feed into the reactor is heated too much, it will continue to react, thus breaking down into smaller molecules like propane or natural gas, which have a lower value, instead of the desired products. This thesis therefore investigates methods to prevent the droplets from forming and plugging the reactor outlet without overheating the feed in the reactor. This thesis builds two process models, one that investigates near the reactor outlet to study droplet formation, and a second which investigates the products made inside the reactor. Both model predictions are analyzed to ensure that the changes made to prevent fouling at the reactor outlet do not significantly reduce the reactor product quality.

Co-Authorship Statement

Chapters 1, 2, 3 and 5 entitled “Introduction”, “Literature Review”, “Fluid Coker Freeboard Model” and “Conclusions and Recommendations” were written by A. Heaslip. Dr. D. Pjontek reviewed and edited these chapters.

Chapter 4 entitled “Fluid Coker Reactor Region Model” was written by A. Heaslip. Residence time distribution equations were developed in collaboration with Niall Murphy. Dr. D. Pjontek reviewed and edited this chapter.

Acknowledgments

I certainly would not have reached the finish line of this thesis had it not been for the support and encouragement of many individuals which I would be remised to not mention when given the chance.

First, I would like to thank my supervisor, Dr. Dominic Pjontek for giving me this opportunity to step away from the workplace and back into academia with this project. I am grateful for your patience and support throughout the many challenges this thesis faced during these unconventional times.

I'd also like to thank Dr. Jose Herrera and all members of the Pjontek-Herrera research group, who listened to countless talks on FLUID COKING™ and provided invaluable feedback and questions from a fresh perspective which undoubtedly furthered my own understanding of the project. Niall, working with you was a pleasure, and I wish you all the best in your future endeavours.

The opportunity to expand my knowledge in the classroom supplemented my research very well, and I would like to thank Dr. Kibret Mequanint, Dr. Franco Berruti and Dr. Hugo de Lasa for their teachings throughout my graduate studies.

The support of my parents and family through out my Master's and life as a whole cannot be understated. Although I know I don't get home nearly enough, the support you send from a distance is felt and appreciated every day. Neither can the support of my closest friends – you're each like a brother to me, and I think I speak for all of us when I say I can't wait to celebrate with the boys of summer once things go back to normal.

Finally, Julia – you've made this experience one to remember. Thank you for the continued support and care throughout the highs and lows of this journey, and I hope I can return the favour as you finish your own Master's degree and beyond.

Table of Contents

Abstract	ii
Summary for Lay Audience.....	iii
Co-Authorship Statement.....	iv
Acknowledgments.....	v
Nomenclature	xiv
Chapter 1: Introduction.....	1
1.1 Problem Overview.....	1
1.2 Research Objectives	3
1.3 Thesis Outline	4
Chapter 2: Literature Review.....	6
2.1 Heavy Oil Upgrading	6
2.2 FLUID COKING™.....	8
2.2.1 Fluid Coker Cyclone Fouling	10
2.2.2 Recent Work on Cyclone Fouling.....	12
2.2.3 Related Fluid Coker Studies	13
2.3 Kinetic Modelling	13
2.3.1 Thermal Cracking Kinetics.....	14
2.3.2 Hydrocarbon Adsorption Kinetics	18
Chapter 3: Fluid Coker Freeboard Model.....	20
3.1 Background information	20
3.2 Modelling in Aspen Plus.....	22
3.2.1 Component Specification.....	23
3.2.2 Method Specification	27
3.2.3 Pressure Drop Calculations.....	28

3.2.4	Endothermic Cracking Reactions	28
3.2.5	Hydrocarbon Adsorption Estimates.....	33
3.2.6	Flowsheet Setup	34
3.2.7	Base Case Parameters	36
3.3	Results and Discussion.....	37
3.3.1	Preliminary Analysis of Model Assumptions	37
3.3.2	Scouring Coke Flowrate	42
3.3.3	Fluid vs Flexicoke Adsorption.....	45
3.3.4	Transfer Line Temperature	47
3.3.5	Fluidized Bed Coke Entrainment.....	50
3.3.6	Bed Steam Flowrate.....	52
3.3.7	Case study comparison	54
3.4	Summary	55
Chapter 4:	Fluid Coker Reactor Region Model.....	56
4.1	Background Information	56
4.2	Fluid Coker Reactor Model.....	57
4.2.1	Residence Time Distributions.....	58
4.2.2	Kinetic Equations.....	60
4.2.3	Application of RTD and Rate Equations	65
4.3	Software Selection.....	66
4.4	Base Case Conditions.....	68
4.4.1	Fluid Inputs	68
4.4.2	Average Residence Time Estimates.....	69
4.4.3	Reaction Products and Stoichiometry	71
4.5	Results and Discussion.....	72

4.5.1	Basic CSTR Model	72
4.5.2	Reactor Ring Model.....	76
4.5.3	Complex Vapour Residence Time	79
4.5.4	Impact of hydrocarbon vapours on VLE	82
4.5.5	Impact of mixing between gas and liquid-solid phases	83
4.5.6	Impact of Bed Temperature	85
4.5.7	Impact of bed steam flowrate.....	86
4.6	Summary	87
Chapter 5: Conclusions and Recommendations		89
5.1	Freeboard Model	89
5.2	Reactor Model.....	90
5.3	Recommendations for Future Work.....	90
5.3.1	Freeboard Model.....	90
5.3.2	Reactor Model.....	91
Bibliography		93
Appendix.....		97
Curriculum Vitae		104

List of Tables

Table 1. Boiling point range for crude oil fractions [9].....	6
Table 2. Arrhenius constants for first order residue cracking reactions as reported by Olmstead and Freund [24].....	15
Table 3. Kinetic Parameters fit to experimental data for reaction network shown in Figure 5 [26]	15
Table 4. Composition of Light Ends [8,20].	24
Table 5. Lumped assay definition and mass distribution based on Gray kinetics. Mass fractions are based on the listed condensable hydrocarbon fractions, excluding all other species present.	26
Table 6. Cyclone Pressure Drop Calculations [33].....	28
Table 7. Thermal cracking reaction simulation parameters used by Glatt et al. [8,24]	29
Table 8. Summary of base case parameters and operating envelopes for case studies.	37
Table 9. Predicted cyclone liquids, per cyclone, with increasing scouring coke flow with and without hydrocarbon adsorption.	46
Table 10. Arrhenius constants for the liquid phase cracking reactions [26].....	61
Table 11. Equilibrium Values for the heavy residue, light residue and coker gas oil fractions as predicted by Aspen Plus. Mass transfer coefficient as reported by Gray is assumed to be independent of temperature and constant for all fractions [25].	62
Table 12. Composition of vacuum residue feed to the Fluid Coker [26].	69
Table 13. Volume of each control volume for the commercial reactor based on dimensions of 1/20th scale lab model [4].	70
Table 14. Average residence time of each reactor control volume.....	71
Table 15. Composition of product exiting the Fluid Coker based on data reported by Jankovic [20].	72
Table 16. Liquid phase reaction stoichiometry used in each case study.	72
Table 17. Composition of the vapour products exiting the single CSTR Fluid Coker Model. Overall, model shows a reasonable alignment with operational data, providing an initial baseline to compare further models against.	75
Table 18. Vapour composition of the tanks-in-series vapour phase compared to operational data reported by Jankovic [20].	79

List of Figures

Figure 1. Fluid Coker schematic and key regional names, modified from [3].	2
Figure 2. Schematic of a Fluid Coker (modified from [3]).....	9
Figure 3. Schematic of Exxonmobile Flexicoking Process, modified from [3].	10
Figure 4. Location of Fluid Coker Cyclone Fouling [17]	11
Figure 5. Updated lumped kinetic model modified from Radmanesh [26]	16
Figure 6. Fluid Coker Model Control Volumes.....	23
Figure 7. CGO and OTSB assays based on data from Jankovic, where the filled data points represent extrapolated values [20].	25
Figure 8. Combined CGO and OTSB Assay.	26
Figure 9. Summary of vapour phase cracking kinetics used in the Aspen Plus freeboard model. Kinetics reported by Radmanesh are used for the residue fractions and kinetics by Bu for the CGO fraction. The products were adapted to match the vapour phase cracking reported by Bu [26,27].	31
Figure 10. Block flow diagram representation of calculation steps for a single control volume.	35
Figure 11. Aspen flowsheet for the first two control volumes, BD1 and BD2. Green streams indicate inputted values, pink and blue streams indicate exported and imported data from excel respectively, black streams indicate an intermediate process stream while red indicate the final control volume composition and operating conditions.	36
Figure 12. Resulting pressure drop due to reduction in cyclone gas outlet tube diameter.	38
Figure 13. Estimated unit runtime based on hydrocarbon deposition rate assuming maximum pressure drop of 90 kPa before unit shutdown.....	39
Figure 14. Freeboard temperature profile with (bottom) and without (top) vapour cracking.	40
Figure 15. Impact of vapour cracking on model prediction of cyclone liquids.....	41
Figure 16. Comparison of pore volume-based adsorption estimates to first order kinetics. Solid lines represent pore volume kinetics, dashed lines represent first order kinetics.	42
Figure 17. Comparison of sensible and reaction heat as a function of scouring coke flowrate....	43
Figure 18. Impact of scouring coke flow on cyclone temperature and liquids.....	43

Figure 19. Inlet and resulting gas outlet tube products with varying scouring coke flowrate. The majority of cracking occurs without the presence of scouring coke, with minor increase in cracking as scouring flowrate is increase.	45
Figure 20. Hydrocarbons adsorbed by fluid and flexicoke in the freeboard region. Adsorption done by entrained hot coke (5 ton/min) and variable scouring coke flow rates. Entrained hot coke is primary contributor due to its increased residence time compared to the scouring coke.	46
Figure 21. Predicted composition of adsorbed hydrocarbons on fluid and flexicoke. The composition of the adsorbed hydrocarbons remains comparable for both coke samples. As the adsorption was assumed to follow the same mass distribution of the hydrocarbons in the vapour phase, the CGO fraction dominates the adsorbed phase.	47
Figure 22. Impact of transfer line temperature on control volume temperature.	48
Figure 23. Change in cyclone liquids due to varying the transfer line temperature. Change in liquids reported relative to liquids predicted in the base case with a transfer line temperature of 610°C.	49
Figure 24. Impact of increasing transfer line temperature on products exiting the gas outlet tube. An additional 3.5 wt% of light and distillate products formed as a result of increasing the temperature to 650°C compared to the base case.	50
Figure 25. Cyclone temperature vs bed coke entrainment rate. Reducing entrained coke improves the ability of the hot and scouring coke lines to heat the freeboard region, resulting in an increase in cyclone temperature.	51
Figure 26. Change in cyclone liquids relative to the base case as a function of entrained bed coke.	52
Figure 27. Reduction of cyclone liquids compared to change in bed steam flow rate relative to the base case flows.	53
Figure 28. Impact of increased steam flowrate on the Ranque-Hilsch cooling predicted in the cyclone.	53
Figure 29. Comparison of the relative change of cyclone liquids and light product formation for each of the four case studies investigated. Arrows indicate the direction of increased	

flow, with the upper and lower limits the extremes of the case studies as shown in Table 8.....	54
Figure 30. Residence time distributions modelled with a tanks-in-series approach for an average residence time of 15 seconds. As the number of tanks increases from 1 to 50, the model behaviour shifts from that of an ideal CSTR to an increasingly PFR like output.....	60
Figure 31. Thermal cracking reaction network diagram based on the weight fraction of each lump, modified from Radmanesh [26]. Stoichiometry (s_{ij}) and first order reaction rate constants determined with Arrhenius constants as presented by Radmanesh, while equilibrium values (K) estimated based on Aspen Plus estimates.	61
Figure 32. Vapour Phase Reaction model, including kinetic parameters.	65
Figure 33. Schematic of Fluid Coker reactor (left) and proposed MATLAB model block flow diagram (right), with detailed schematic of Ring 2. Fresh liquid feed of a known composition enters a given ring, where liquid and vapour cracking reactions are applied using a series of ODE solvers, with vapour products exiting the cyclone, while liquid products carry on down to next ring.	68
Figure 34. Resulting liquid and vapour phase products as a function of time due to liquid phase cracking of residue feed. The left plot reflects the remaining liquid film and solids formed from the initial residue feed, while the right shows the increasing vapours composition over time.	73
Figure 35. Change in predicted hydrocarbon fractions over time as a product of vapour phase cracking.	74
Figure 36. Predicted mass flowrates of hydrocarbon lumps for a two-phase ideal CSTR Fluid Coker model. Cracking reactions converted the feed into lighter fractions, with CGO, light ends and distillates dominating the final composition. Minimal products remained in liquid phase lost to the burner, while CGO, light gases and distillates dominate the vapour product.	75
Figure 37. Product distribution between solids and liquids exiting bottom of reactor and vapours exiting top when modelling liquid-solid phase as the tanks-in-series approximation with 1, 5 and 50 tanks.	77
Figure 38. Composition of the vapour phase products when modelling the liquid-solid phase as the tanks-in-series approximation with 1, 5 and 50 tanks.	77

Figure 39. Comparison of ideal CSTR model (left, $n=1$) and tanks in series (right, $n=50$) on vapour phase residence time distribution for products of each ring before exiting the cyclone outlet tube.....	78
Figure 40. Composition of vapour products with varying tanks-in-series for the vapour phase components.	79
Figure 41. Block flow diagram for complex RTD based on modeling individual control volumes as either a CSTR or PFR.	80
Figure 42. RTDs for each ring based on complex CSTR-PFR vapour model.....	81
Figure 43. Overall vapour phase residence time distributions for the ideal CSTR, 50- tanks-in-series and complex flow pattern approximations.	82
Figure 44. Impact of complex RTD on vapour products, compared to CSTR and PFR (50 tanks-in-series) cases.	82
Figure 45. Impact of updated VLE on Fluid Coker products. By considering the vapours flowing upwards through the reactor, there is a reduction in vapours predicted compared to the original model, resulting in increased coke yield.....	83
Figure 46. Block flow diagram for one ring of the proposed Simulink model to estimate RTD with 5% mixing of vapours between each region as prepared by Niall Murphy.	84
Figure 47. RTD for vapour phase for each ring with 5% mixing between solid-rich and gas-rich phases. Results part of a collaboration with Niall Murphy.	85
Figure 48. Impact of vapour-solid mixing on Fluid Coker products. Mixing of the vapours into the solid phase increases the resulting residence time, and ultimately the light products formed.	85
Figure 49. Change in coke formation and liquids lost to the burner and distribution of vapour products with increasing reactor temperature.	86
Figure 50. Change in coke formation and liquids lost to the burner and distribution of vapour products with variable steam flowrate.	87

Nomenclature

A	Arrhenius pre-exponential factor, s^{-1}
CGO	Coker gas oil
$C(t)$	Concentration curve, mol/L
\bar{C}_i	Average exit concentration of component i, mol/L
D_b	Cyclone barrel diameter, m
E_a	Activation energy, kJ/mol
$E(t)$	Residence time distribution function, s^{-1}
f	Fanning friction factor
ΔH_R	Enthalpy of reaction, kJ/kg
k_{Ga}	Mass transfer coefficient, s^{-1}
k_i	Rate constant, s^{-1}
K_i	Equilibrium constant of component i
L	Length, m
m	Mass, kg
\dot{m}	Mass flowrate, kg/s
\bar{m}_i	Average exit mass flowrate of component i, kg/s
n	Number of tanks
ΔP_{as}	Acceleration of solids pressure drop, Pa
ΔP_{bf}	Barrel friction pressure drop, Pa
ΔP_E	Elbow pressure drop, Pa
ΔP_{ec}	Exit Contraction pressure drop, Pa
ΔP_{ic}	Inlet gas contraction pressure drop, Pa
ΔP_{gf}	Gas outlet tube friction pressure drop, Pa
ΔP_{sc}	Snout contraction pressure drop, Pa
q^*	Equilibrium adsorption capacity, mg/g
q_t	Adsorbed mass at a given time, mg/g
ρ_i	Density of component i, kg/m^3
ρ_g	Gas density, kg/m^3
r_i	Rate of change of component i, s^{-1}

R	Gas Constant, kJ/mol•K
τ	Time constant, s
OTSB	Once through scrubber bottoms
s_{ij}	Stoichiometric coefficient of component i forming component j
t	Time, s
T	Temperature, K
u	Gas velocity, m/s
V_{pore}	Pore volume, mL/g
w_i	Wight fraction of component i

Subscripts

CGO	Coker Gas Oil
DIST	Distillates
EC	Extrinsic coke
HR	Crackable heavy residue
HR-IC	Intrinsic coke forming heavy residue
IC	Intrinsic Coke
LR	Light residue
p	Product exiting Fluid Coker
v	Flashed Vapour

Chapter 1: Introduction

1.1 Problem Overview

With global energy consumption projected to grow 50% by 2050, increased production from sources including oil, natural gas, hydro, nuclear and renewables will be required to fulfill the market demand [1]. Despite the emergence of alternative energy sources, oil remains a key contributor in the energy market, providing, 34% of global energy in 2018, particularly within the petrochemical, freight, aviation and shipping industries [2]. The Canadian oil sands are the third largest reserve in the world, totalling 171 billion barrels extractable using current technology [3]. However, these reserves are primarily in the form of bitumen, a highly viscous hydrocarbon mixture which contains over 50 wt% vacuum residues. The vacuum residue fraction is a low value product with limited applications in its natural state. In order to extract value from this resource, the vacuum residue must be upgraded, or cracked, into the lighter high value products the global market demands. This upgrading reduces the carbon to hydrogen ratio, resulting in a more valuable, energy dense product.

As conventional crude oil contains low quantities of vacuum residue, these sources can be directly fed to traditional refineries where the desired products can be separated and sold. This places heavy Canadian oil at a disadvantage due to the extra upgrading step, which must be completed before being fed to a refinery. Therefore, there is interest in maximizing the efficiency of the upgrading process, thus reducing the amount of energy required per unit of upgraded material, to increase the viability of Canadian oil reserves. FLUID COKING™ is a continuous upgrading process that uses carbon rejection as a method to decrease the carbon to hydrogen ratio of the cracked product. Alongside the desired products, the coke by-product is used as a fuel to heat the cracking reactions as shown in Figure 1.

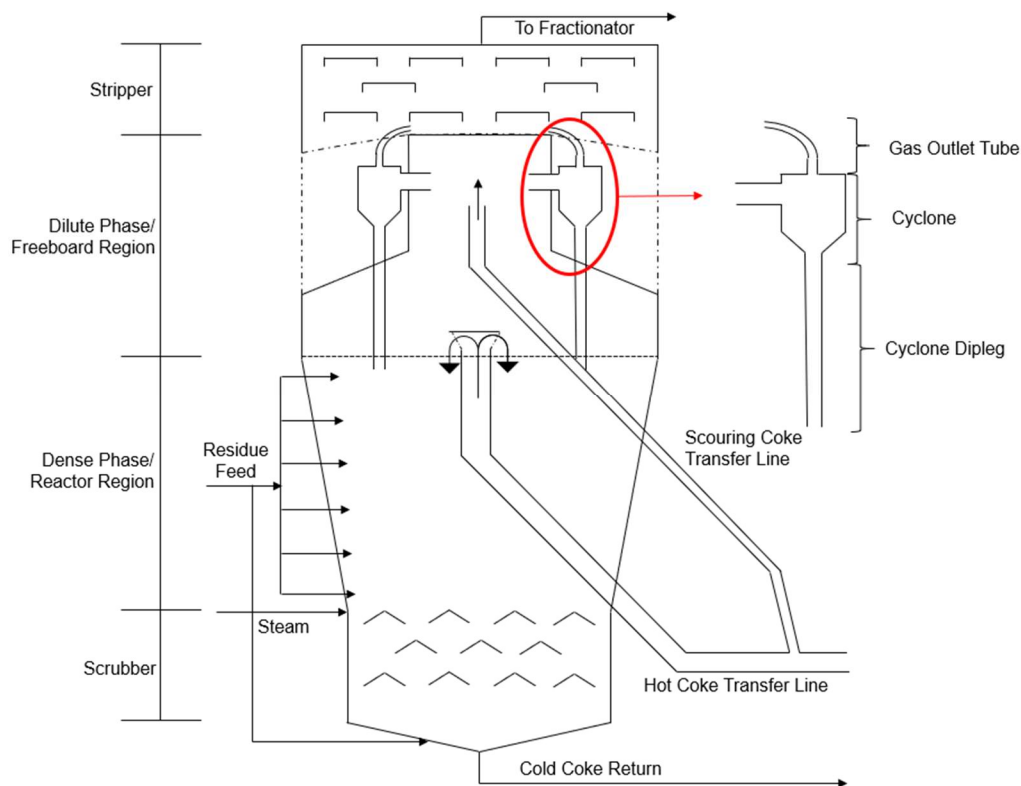


Figure 1. Fluid Coker schematic and key regional names, modified from [3].

The Fluid Coker operates at near atmospheric pressures and at a bed temperature of 510-540 °C [4]. Within the reactor fluidized bed, residue feed is injected and contacts hot coke particles. After coating the particles, endothermic cracking occurs and the product vapours flash off the surface. These vapours travel upwards through the bed, exiting the reactor through a series of cyclones at the top of the unit, and are sent to a fractionator for further processing [3]. Coke is simultaneously removed from the bottom of the fluidized bed reactor and sent to a burner unit, which heats the coke particles via combustion with air before being sent back to the reactor. The partial combustion of coke in the burner heats the coke particles to 590-650°C [3], providing the heat that drives the endothermic cracking reactions.

During operation, fouling within the cyclone gas outlet tube is one of the most common limiting factors for the unit run time [3]. As premature unit shutdown reduces productivity and the economics of the process, there is an incentive to research and mitigate against this cyclone fouling phenomenon. Several studies investigated potential cyclone fouling mechanisms, concluding that condensation of hydrocarbon vapours with boiling

points exceeding 650°C was the dominant mechanism [5–7]. After cracking, some of the flashed products are near their dew point at the reactor pressure. Small changes in temperature, pressure, or composition could result in condensation to occur for the heavier compounds. If this condensation occurs downstream of the reactor region, it is possible that droplets could deposit on the cyclone surfaces, thus fouling the outlet tubes. A recent study from this research group aimed to identify process levers to minimize cyclone fouling. Aspen Plus modelling done by Glatt et al. considered the impact of vapour-liquid thermodynamics, fluid dynamics, cooling from cracking reactions and the Ranque-Hilsch effect to predict the quantity of condensed vapours, particularly within the gas outlet tube [8]. It was found that process levers, which are controllable parameters on the industrial Fluid Coker, that increased the cyclone temperature were the most effective strategies to reduce cyclone fouling; however, operating the Fluid Coker at a higher temperature is known to lead to over cracking, reducing the quality of the Fluid Coker products. As this model did not include the fluidized bed reactor section or compositional changes due to cracking reactions, an expanded model is required to monitor product quality in addition to cyclone fouling, while modifying key process levers.

A final consideration for the expanded model is the inclusion of hydrocarbon adsorption by the coke particles. The heaviest hydrocarbon vapours are most likely to adsorb on coke, while also being the most likely compounds to condense in the cyclone. Hydrocarbon adsorption leading up to or within the cyclone region could reduce fouling; however, adsorption would also be present within the fluidized bed. Hydrocarbons adsorbed to the coke near the bottom of the reactor could be sent to the burner, resulting in a loss of product. Adsorption modeling in this system should thus consider and predict the impact on fouling reduction as well as lost product to the burner.

1.2 Research Objectives

The primary objective of this research is to develop a Fluid Coker model which identifies optimal process levers to mitigate cyclone fouling, while also considering the impact on reactor performance. A combination of process and numerical modelling are used to achieve this goal, which includes a novel model of the fluidized bed while expanding upon the previously modelled freeboard and cyclone regions. These

developments allow for kinetic modelling of thermal cracking reactions, as well as considerations for non-ideal flow patterns within the fluidized bed, which were not previously studied. Experimental data for hydrocarbon adsorption kinetics is considered and adsorption estimates are included within the model. With the expanded model, case studies are used to:

- 1) Determine the impact on product quality resulting from increased reactor and freeboard temperature to reduce cyclone fouling,
- 2) Determine the effect of adsorption on expected fouling rate,
- 3) Determine the benefit or detriment of varying flow patterns within the Fluid Coker (e.g., core-annular flow) on the product quality.

Recommendations to mitigate cyclone fouling while considering reactor performance, as well as future studies, are made in an effort to improve Fluid Coker run times.

1.3 Thesis Outline

This thesis follows the monograph format outlined by the School of Graduate and Postdoctoral Studies at the University of Western Ontario. The remaining chapters within this thesis are described as follows:

- Chapter two provides a literature review on the FLUID COKING™ process. This includes a summary of previous modelling efforts for the unit, as well as the applicable kinetic models for the thermal cracking of vacuum residues and hydrocarbon adsorption kinetics.
- Chapter three presents the developed freeboard model, which allows for the impact of changing key operating parameters on cyclone fouling and product yield to be determined. This model applies the cracking and adsorption kinetics identified in Chapter two while also considering pressure drops and vapour-liquid equilibrium to identify effective process levers to reduce cyclone fouling while considering Fluid Coker product quality.
- Chapter four presents a novel numerical model of the reactor region of the Fluid Coker. This model considers both liquid and vapour phase cracking, vapour-liquid equilibrium and residence time distribution of both phases to predict the product

yields from the Fluid Coker. Case studies were performed to study the impact of temperature and flow pattern on reactor performance.

- Chapter Five provides a summary of the work completed and recommendations for future studies.

The included appendix includes copyright permissions for a figure included in the thesis.

Chapter 2: Literature Review

2.1 Heavy Oil Upgrading

With global energy demand projected to grow 50% by 2050, increased production from sources including oil, natural gas, hydro, nuclear and renewables is required [1]. Despite the emergence of alternative energy sources, oil derived products continue to fulfill global product demands. In 2018, 34% of global energy was provided by oil, particularly within the petrochemical, freight, aviation and shipping industries [2]. Traditionally, this demand is filled through the processing of conventional crude oil in refineries. Conventional crude oil is a mixture of hydrocarbons that are characterized by their density, viscosity and yield of extractable fractions [3]. The extractable fractions are summarized in Table 1, categorized by their boiling points and end use applications.

Table 1. Boiling point range for crude oil fractions [9]

Name	Boiling Range (°C)	Applications
Naphtha	26 – 193	Reformed for gasoline
Kerosene	165 – 271	Jet fuel or gasoline blending
Light Gas Oil	215 – 321	Diesel or jet fuel
Heavy Gas Oil	321 – 426	Feedstock for catalytic or hydro cracking
Vacuum Gas Oil	426 – 524	Feedstock for catalytic or hydro cracking
Vacuum Residue (Resid or residuum)	>524	Asphalt or feedstock for upgrading units

Canada has the third largest known oil reserve in the world, where the highest reserves are found in Saudi Arabia and Venezuela [10]. The Canadian oil reserves total an estimated 171 billion barrels that are extractable using current technology. 97% of the Canadian oil reserves are located in northern Alberta and Saskatchewan in the Athabasca, Cold Lake and Peace River deposits, commonly known as the oil sands [3]. Unlike conventional crude oil fed to refineries, however, the hydrocarbons extracted from the oil sands are in the form of bitumen, a highly viscous and tar-like substance which contains over 50 wt% vacuum residues. As crude oil refineries are designed to treat feedstocks with a lower density and viscosity, bitumen must be upgraded before being refined. Such

upgrading processes convert the low value residue into naphtha and gas oil fractions, thereby increasing its value and making its properties within the specifications required for refinery processing. The vacuum residue upgrading reactors fall within two categories: hydroconversion or thermal/coking processes. The goal of these reactors is to increase the hydrogen to carbon ratio of its products, thus increasing the value of the products as they will be lighter and more energy dense hydrocarbons.

Hydroconversion is the general process of cracking residues at elevated pressure and temperature (in excess of 9500 kPa and 400°C) in the presence of hydrogen to produce lighter, higher quality products [11]. Hydroconversion is a desirable upgrading pathway due to its high yield of the most valuable and in demand hydrocarbon fractions. Hydroconversion processes include trickle beds, ebullated beds (commercially known as the LC-Fining or H-Oil process), or slurry-phase hydrocrackers [11]. Although these reactors produce a higher quality product, they require significant capital and operational costs due to the pressure and temperature requirements and hydrogen consumption. Furthermore, these reactors require monitoring of the feedstock composition to prevent asphaltene agglomeration and premature unit shutdown. This is of higher concern for heavier feedstocks, as these units are better suited for atmospheric residues, rather than the heaviest vacuum residues. A more detailed review of these technologies can be found in the literature, such as work by Gray and Sahu [3,12].

Thermal cracking and coking are the most common methods to convert vacuum residue to distillable fractions worldwide [3]. These processes “crack” large hydrocarbon chains using elevated temperatures without a catalyst, thus improving the hydrogen to carbon ratio by removing coke as a by-product. Thermal cracking processes can be further classified based on their respective operating conditions and resulting product yields, which are reviewed and compared by various authors [3,11,13]. The most common method of cracking vacuum residues is delayed coking, a semi-batch process using two drums in tandem. At a given time, one drum is filled with heated residues, which crack to form the desired products and coke. This process continues until the drum is filled with coke, at which time the feed is switched to the second drum, allowing the first to be emptied. An

alternative process which is the focus of this thesis is FLUID COKING™, which was developed and patented by Esso (Exxon) in the 1950's [14].

2.2 FLUID COKING™

FLUID COKING™ is a continuous reactor that operates at near atmospheric pressures and at bed temperatures of 510-540 °C [4]. A schematic of a FLUID COKING™ unit is provided in Figure 2. Liquid vacuum residues are injected into the fluidized bed via steam and high-velocity nozzles. Within the fluidized bed, the residue feed contacts a downward flow of hot coke particles which provide the heat for the endothermic cracking reactions. After coating the coke particles, the residues crack and flash off the particle surface. The coke particles are fluidized based on the thermal cracking product vapours as well as steam injected throughout the reactor. The cracked hydrocarbon vapours travel upwards through the fluidized bed, before exiting through cyclones in a parallel configuration at the top of the unit. These cyclones remove entrained coke particles and return them to the fluidized bed. The products vapours are quenched in the scrubber at the top of the unit, before being sent to a fractionator for further processing [3]. FLUID COKING™ inherently produces coke as a by-product. Coke is removed from the bottom of the reactor and sent to a separate fluidized bed burner unit. The burner is fed with a controlled amount of air, allowing for the partial combustion of coke to heat the remaining solids to the required 590-650°C, while also reducing the amount of coke requiring disposal [3]. This heated coke is fed back into the reactor through one of two transfer lines. The hot coke transfer line provides the majority of coke to the bed for the cracking reactions. The remaining coke is fed through the scouring coke transfer line and inserted near the cyclone inlets. The purpose of this coke is to reduce fouling in the cyclones by scouring the cyclone surfaces [15].

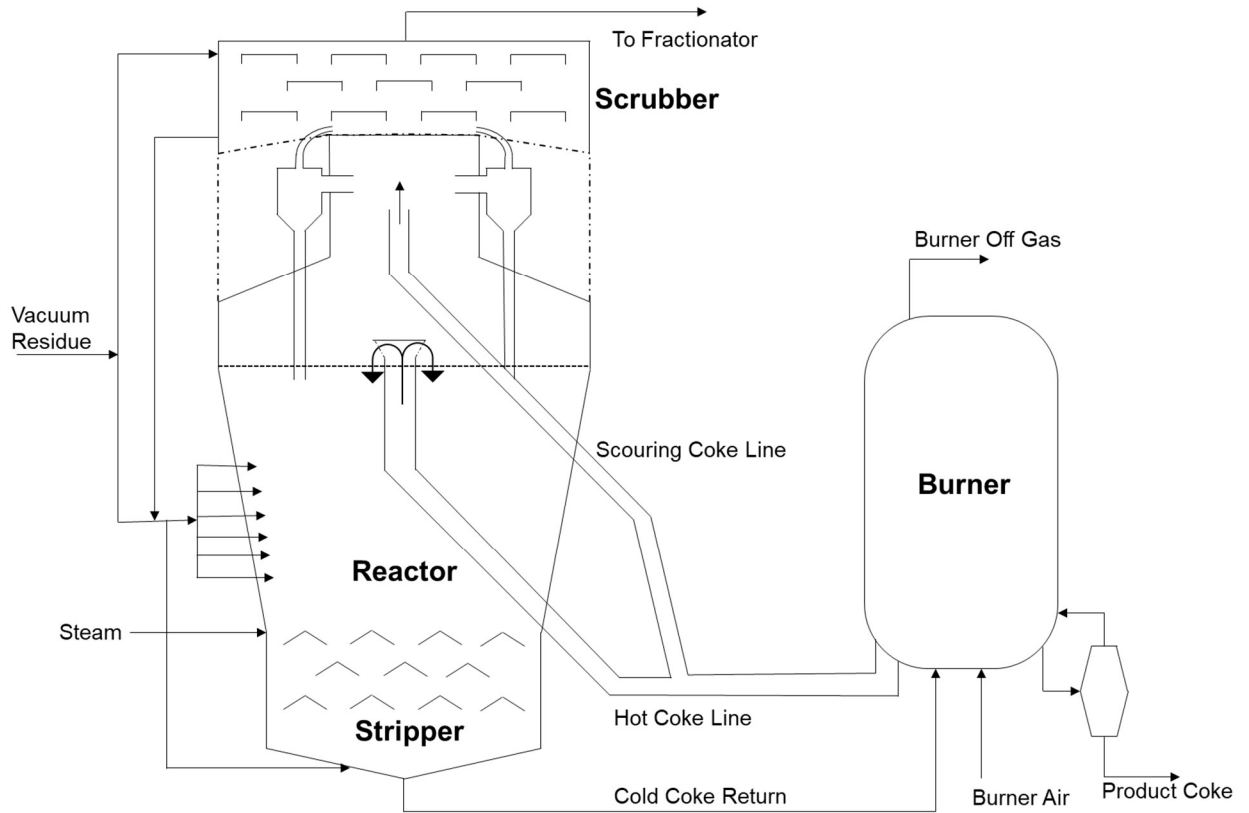


Figure 2. Schematic of a Fluid Coker (modified from [3])

Although FLUID COKING™ is the focus of this thesis, a similar process to be aware of is Flexicoking, which is shown in Figure 3. The key difference between the two processes is the method of heating the coke before feeding it to the reactor. Compared to the partial combustion of coke in a burner as shown in the FLUID COKING™ process, Flexicoking uses a heater and gasifier in tandem. A fraction of the cold coke returned from the reactor is sent to the gasifier, where it is heated to 830-1000°C. This coke is then mixed with the remaining cold bed coke, resulting in the mixture reaching the required 590-650°C for the transfer lines. Flexicoking produces an off gas from the heater, due to coke gasification, which can be scrubbed and used as a gaseous fuel. Despite using similar feed and operating conditions, Flexicoker run time is typically limited by the downstream fractionator rather than the reactor itself, suggesting the fouling phenomenon is not as prevalent [16].

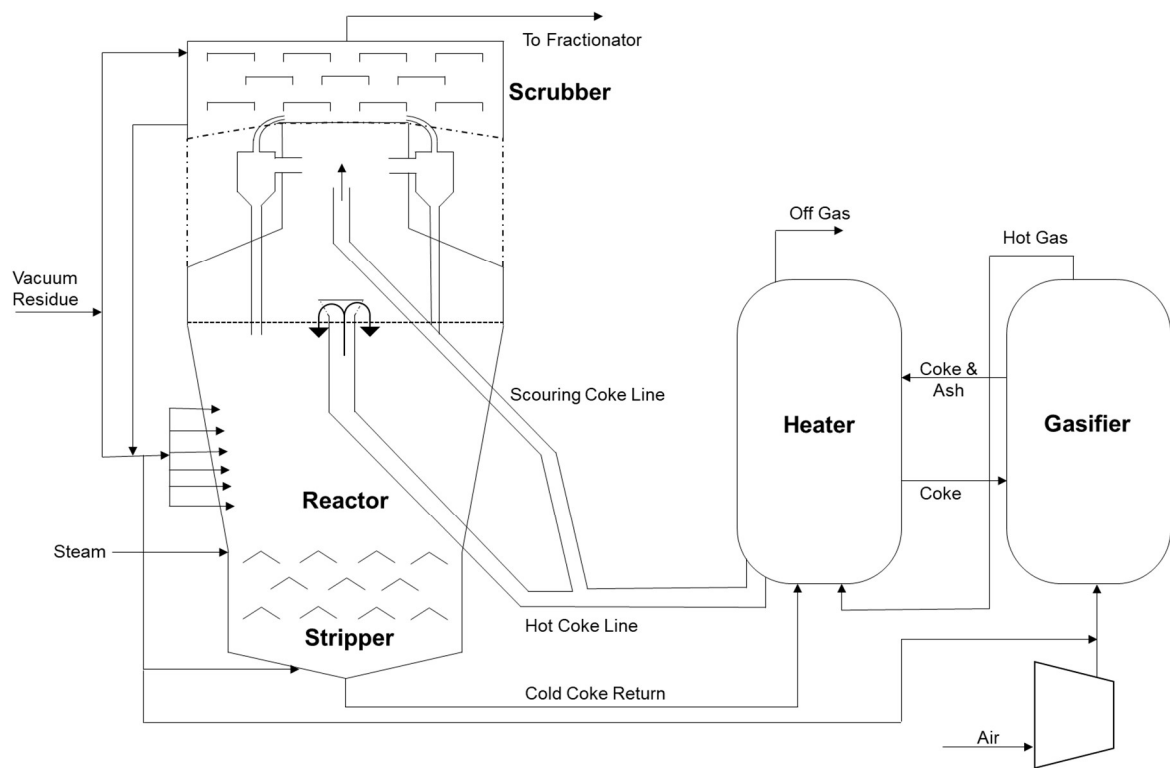


Figure 3. Schematic of Exxonmobile Flexicoking Process, modified from [3].

2.2.1 Fluid Coker Cyclone Fouling

Run lengths for the Fluid Coker are generally dictated by fouling or coke deposition within the cyclones. Throughout operation, coke deposits form throughout the cyclone, as shown in Figure 4, with the gas outlet tube being of particular concern [17]. Extensive research has been done to investigate the fouling mechanism. This research can be categorized into three unique fouling mechanisms, being:

- 1) Feed droplet entrainment [5,6]
- 2) Chemical reaction forming condensable species [18]
- 3) Heavy end condensation [5–7]

The feed droplet entrainment method hypothesized that a fraction of the vacuum residue being fed to the Coker became entrained in the vapour bubbles travelling upwards to the cyclones. This vacuum residue thus did not react and would ultimately deposit and form coke on the cyclone surfaces. Alternatively, the second pathway proposed that vapour phase cracking produced highly reactive radicals that could recombine to form heavier compounds. These compounds would then condense, due to their higher normal boiling

point, resulting in fouling. A detailed summary of the past studies completed on these mechanisms is included in the work by Glatt et al., which focuses on the condensation of heavy ends as the dominant fouling mechanism [8].

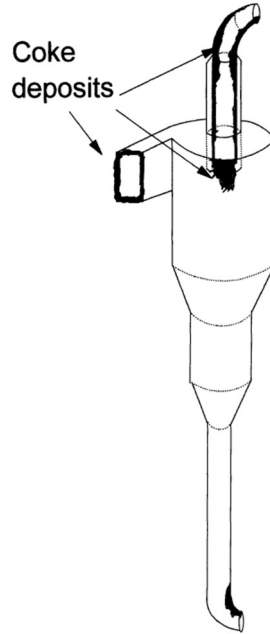


Figure 4. Location of Fluid Coker Cyclone Fouling [17]

The remaining fouling mechanism involved the condensation of heavy hydrocarbon products from the Fluid Coker. The composition of the hydrocarbon vapours produced in the fluidized bed reactor ranges from light gases (such as methane and butane) to heavy hydrocarbons that are in vapour-liquid equilibrium when they flash off from the hot coke particles. It is possible that these components, which are close to their respective dew points, could condense due to minor changes in composition, temperature and/or pressure. If this condensation occurs while still in the fluidized bed, the vapours could contact the coke surface and further crack. However, if these vapours exit the bed before condensing, deposition in the cyclone could occur.

A series of experimental studies were completed to investigate the applicability of this fouling mechanism. Experimental and mathematical studies done by Zhang and Watkinson investigated the impact of temperature and vapour dilution on deposition rate. It was found that reducing the temperature increased the deposition rate as a result of more favourable condensation conditions, while there was also a strong correlation between

vapour dilution and a reduction in deposition due to the physical dilution of the vapours [5,6]. Alternatively, an analytical study to characterize the deposition of hydrocarbons in the cyclone diplegs of a residue fluidized catalytic cracking (FCC) unit was done by Kim et al [7]. Although not identical to a Fluid Coker due to the use of a catalyst and a lighter feedstock, the trends seen in this unit can be used as an analogy for the Fluid Coker. Samples of deposits formed in the cyclone dipleg of commercial FCC reactors were collected and categorized based on an elemental analysis and morphology. Here, the deposits were comprised of both inorganic catalyst fines and hydrocarbons. A review of the deposit structure and formation mechanism identified the condensation and polymerization of heavy oil droplets as a factor for the deposit formation [7]. These past studies demonstrate that condensation of heavy oil vapours is the prominent mechanism for cyclone fouling.

2.2.2 Recent Work on Cyclone Fouling

A recent Aspen Plus model by Glatt [8] of the Fluid Coker upper bed and cyclone region was developed to identify process levers to minimize cyclone fouling. This model considered the impact of vapour-liquid thermodynamics, pressure drops, cooling from cracking reactions, and the Ranque-Hilsch effect to predict the quantity of condensed vapours within six control volumes, most notably the cyclone gas outlet tube [8]. By changing key process variables, a set of operating conditions could be established to minimize condensation and thus fouling. It was found that increasing the rate of scouring coke flow, as well as increasing the transfer line temperature (i.e., the coke temperature from the burner) were the most effective strategies to reduce cyclone fouling [8]. These methods reduced fouling by increasing the temperature within the cyclone, shifting the vapours away from their respective dew points. Although this simulation was effective in identifying a strategy to reduce fouling, it did not consider the impact these changes had on reactor performance. The liquid phase cracking heat of reaction in those control volumes was estimated, however the resulting composition change was not quantified. Furthermore, vapour phase cracking was not considered. Increasing the reactor temperature is known to reduce the product quality due to over cracking, further studies are thus required to determine the impact of increased temperature on product quality. A kinetic model to estimate the cracking reactions is therefore required.

2.2.3 Related Fluid Coker Studies

A combination of experimental, Computational Fluid Dynamics modelling (CFD) and process modelling have been completed in past studies related to the Fluid Coker. Although these studies were not directly addressing cyclone fouling, useful parameters and modelling trends can be taken. Solnordal et al. built a CFD model of a lab scale Fluid Coker to investigate the distribution of coke amongst the ring of cyclones and characterized the flow of coke entering from the hot coke transfer line. Their work found the CFD model was able to replicate their simplified lab scale apparatus and predict the impact of changing transfer line geometry on coke distribution amongst the cyclones [15]. The geometry of this lab-scale model can be used to estimate the dimensions of the commercial unit in this study. The deposition of heavy hydrocarbon droplets on a circular disk was also modeled using CFD by Lakghomi et al. Their model was validated with experimental data at room temperature and allowed for the impact of temperature and physical properties on hydrocarbon deposition to be predicted. This model found that deposition decreased with increasing temperature, while the effects of temperature on the physical properties contributing to droplet deposition was small [19]. As temperature changes did not appear to increase the affinity of droplet deposition, the rate of fouling can be predicted based solely on the presence of liquids, independent of temperature. Process modelling using Aspen HYSYS was studied by Jankovic investigating the scrubber section of a Syncrude Fluid Coker. This work investigated the effects of key operating and design parameters on the scrubber performance. This work found that by using two pseudo-component assays provided by Syncrude, HYSYS was able to replicate the operating data well. Although the scrubber is located downstream from the cyclones, these results provide confidence in process modelling for Fluid Coker applications [20]. Furthermore, Jankovic defines the hydrocarbon products exiting the cyclones, which can be used as a baseline for the input or products from the developed models.

2.3 Kinetic Modelling

Developing an effective kinetic model presents several challenges due to variations in composition and physical properties of vacuum residues. As residues are a complex mixture of hydrocarbons, typically characterized by a boiling point curve, it is challenging to predict the composition of the cracked products for a given feed. As a result, lumped

kinetic models are the prominent technique for describing these cracking reactions [21]. Lumped kinetic models aggregate or differentiate many molecules into defined lumps, typically based on boiling points, but can also be based on solubility, adsorption capacity, or other physical properties. More lumps can lead to more accurate representation of the physical properties, however, this comes at the cost of additional model complexity [21]. Lumped models are also highly dependent on the feed material used to determine the kinetic parameters. Nonetheless, this is a common method to model bitumen cracking, having been used to quantify cracking kinetics in hydrocracking and FCC processes, as well as thermal cracking in delayed and FLUID COKING™. Many such studies are highlighted in a review by Singh [21]. As this thesis involves the modelling of thermal cracking in a Fluid Coker, a summary of recent cracking models relevant to FLUID COKING™ will be provided in greater detail.

2.3.1 Thermal Cracking Kinetics

Early work on thermal cracking kinetics focused on the rate and mechanism for coke formation, as well as the overall rate of residue conversion. Through experimental work and kinetic modelling, Wiehe proposed a phase separation kinetic model to quantify coke formation [22]. This model was further studied, resulting in the classifications of intrinsic and extrinsic coke formation. Intrinsic coke is the result of large and aromatic cores which are unable to crack and are too large to vaporize. These carbon-rich molecules remain in the liquid phase until they form solid coke. Alternatively, the recombination or polymerization of lighter hydrocarbons leads to extrinsic coke formation. Dutta et al [23] demonstrated that the larger aromatic cores required for coke formation could be produced through the combination of smaller aromatic groups. Preliminary kinetic estimates for residue conversion were done by Olmstead and Freund by measuring the weight change during cracking via thermogravimetric analysis (TGA) [24]. Arrhenius constants, shown in Table 2, were estimated to model the rate of reaction/disappearance of the residues. An inherent limitation in this work is the lack of product quantification. As products were not analyzed upon vaporization, further studies would be required to develop a kinetic model to predict the quantity and quality of products formed.

Table 2. Arrhenius constants for first order residue cracking reactions as reported by Olmstead and Freund [24].

	Arab Heavy Residue (698°C+)	Cold Lake Heavy Residue (706°C+)
$\log A, \text{s}^{-1}$	13.24	13.21
$E_a, \text{kJ mol}^{-1}$	215.5	212.8

More recent studies have proposed kinetic models for cracking of residues under hydrocracking or at lower temperature conditions. Mirroring the conditions seen in the Fluid Coker (i.e., open reactor, at low pressures and between 450-530°C), Gray et al investigated a reaction network that would estimate the products formed by cracking thin films of vacuum residue [25]. This lumped kinetic model minimized mass transfer limitations by using thin films and sweeping volatized products with an inert gas. Products were collected and analyzed, allowing for the quantification of the cracked products and fitting to stoichiometric and Arrhenius constants. In addition to this work, Radmanesh et al fitted the same data, with a slightly modified reaction network (Figure 5) while considering the liquid side mass transfer resistance [26]. This updated network also distinguished between intrinsic and extrinsic coke formation, aligning with the previously determined coke formation mechanism. The Radmanesh et al model thus provided a better fit between predicted and experimental results when considering thicker films, which have an increase in the recombination reactions required for extrinsic coke formation. The associated kinetic parameters are summarized in Table 3.

Table 3. Kinetic Parameters fit to experimental data for reaction network shown in Figure 5 [26]

Parameter	Value	Parameter	Value
$E_{\text{AHR}} (\text{kJ/mol})$	230	$\log A_{\text{HR}} (\text{s}^{-1})$	14.00
$E_{\text{ALR}} (\text{kJ/mol})$	188	$\log A_{\text{LR}} (\text{s}^{-1})$	11.00
$E_{\text{AIC}} (\text{kJ/mol})$	33.7	$\log A_{\text{IC}} (\text{s}^{-1})$	1.0
$E_{\text{AEC}} (\text{kJ/mol})$	99.6	$\log A_{\text{EC}} (\text{s}^{-1})$	5.0
$S_{\text{HR-LR}}$	1	$S_{\text{LR-CGO}}$	0.2
$S_{\text{HR-CGO}}$	0	$S_{\text{LR-DIST}}$	0.8

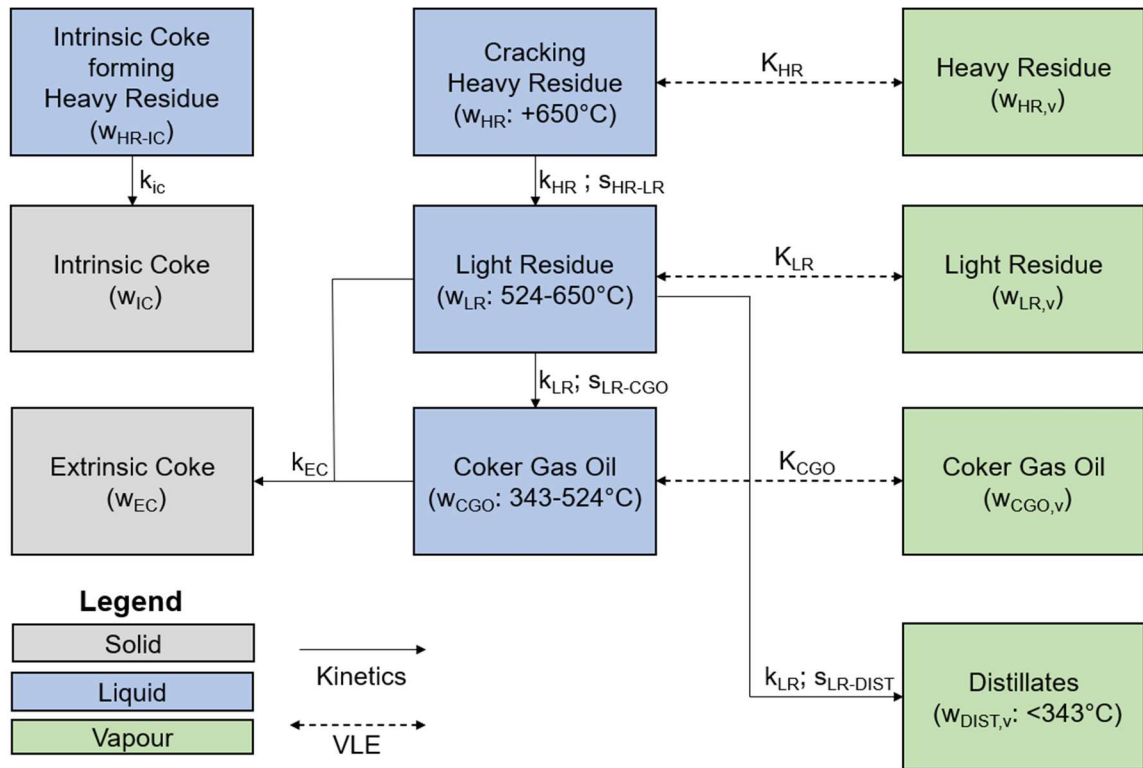


Figure 5. Updated lumped kinetic model modified from Radmanesh [26]

Thermal cracking kinetic studies presented so far have focused on the liquid phase reaction of residues under FLUID COKING™ conditions. However, after the liquid residue cracks and vaporizes, the vapours are subjected elevated temperatures in the reactor until they enter the scrubber. It is possible for these vapours to continue cracking, producing progressively lighter products. Work by Bu and Gray determined Arrhenius kinetic parameters to quantify the thermal cracking of heavy gas oil in the vapour phase [27]. Compared to liquid phase cracking, it was found that negligible amounts of coke were formed. Vapour phase cracking removed side chains from the larger vapour product, increasing the yield of light gases and reducing the hydrogen to carbon ratio of the gas oil product. With a pre-exponential factor ($\log A$) of 12.4 s^{-1} and activation energy of 215 kJ/mol, the reaction rate was shown to be slower than the unreacted vacuum residue, but could still impact the product composition based on Fluid Coker residence times.

For both the liquid and vapour phase cracking reactions, it should be noted that each reaction is assumed to be first order. As such, the rate of reaction is dependent only on the concentration of the given reactant and its respective rate constant. Following the definitions provided in Radmanesh et al, the kinetics for cracking of residues is defined on a mass or mass fraction basis rather than molar as seen in traditional reactions. The general rate equation, excluding mass transfer, is shown in Equation 1:

$$\frac{dw_i}{dt} = -k_i w_i \quad (1)$$

Where the rate of change of mass fraction of component i (dw_i/dt ; [1/s]) is given as the product of the rate constant and mass fraction of a given component. As the rate is dependent on the reaction temperature, the rate constant, k_i [1/s], is estimated based on the Arrhenius equation (Equation 2) based on experimentally determined activation energy (E_a) and preexponential factor (A) [28].

$$k = Ae^{-\frac{E_a}{RT}} \quad (2)$$

It is also important to note the key fundamental equations for reactor modelling, being the continuous stirred tank reactor (CSTR) and plug flow reactor models. Although non-ideal conditions are considered in Chapter 4, these two ideal cases provide an initial estimate that can be used in reactor analysis. In a CSTR, the contents of the reactor are assumed to be well mixed such that the overall reactor concentration is equal to the exit concentration, as shown in Equation 3. Conversely, a plug flow reactor describes a system where each fluid element passes through the reactor in a definite amount of time, as shown in Equation 4.

$$V = \frac{F_{A_o} - F_A}{-r_A} \quad (3)$$

$$\frac{-dF_A}{dV} = -r_A \quad (4)$$

2.3.2 Hydrocarbon Adsorption Kinetics

Another area of interest for this thesis is hydrocarbon adsorption on the coke particles. The heaviest hydrocarbons leaving the Fluid Coker are the closest to their dew points, therefore are the most susceptible to condensation and fouling. However, they are also the most likely to adsorb onto coke particles. If these hydrocarbons were to adsorb, they would no longer be available to condense, thereby reducing the prevalence of cyclone fouling. This raises the question of whether the amount of adsorption that could occur under Fluid Coker conditions and the relevant timescales could sufficiently impact fouling in the cyclone region. Furthermore, adsorption considerations could determine whether changing the porosity via process changes (e.g., Fluid versus Flexi Coking) would have a significant reduction potential for cyclone fouling.

A recent study by Pazoki investigated the adsorption kinetics of n-decane, n-dodecane and mesitylene on coke adsorbents and activated carbon [29]. The study found that each hydrocarbons and adsorbents followed first order kinetics, with Flexicoke and Fluid Coke having comparable time constants. Coke samples with higher porosities were observed to have higher equilibrium adsorption capacities. This trend includes a coke sample from the heater of a Flexi Coker, with a pore volume of 0.02 mL/g adsorbing 40 wt% more hydrocarbons than a sample from a Fluid Coker with a pore volume of 0.006 mL/g. Although residence times in the Fluid Coker are not long enough to achieve equilibrium, first order kinetics predict a difference in adsorption, nonetheless. Although this work demonstrated the effect of increased porosity on adsorption, it is not clear if the difference is sufficient to impact cyclone fouling.

This thesis aims to implement novel changes to improve upon previous process modelling efforts to mitigate Fluid Coker cyclone fouling. This work will include vapour phase cracking and adsorption estimates to a Fluid Coker freeboard model in Aspen Plus. The freeboard model developed by Glatt et al successfully identified the transfer line temperature and scouring coke flowrate as effective methods to reduce cyclone fouling [8]. My addition of vapour phase cracking estimates will determine whether the resulting temperature increase from these changes notably decrease the product quality. Furthermore, estimating adsorption under Fluid Coker timescales will determine whether

changing coke porosity is an effective method to reduce fouling, while also providing an estimate for products lost due to this phenomenon. Finally, as changes to the transfer line temperature would also impact the Fluid Coker reactor, a numerical model of the reactor will be developed using both the liquid and vapour phase kinetics developed by Bu and Radmanesh to predict the impact of bed temperature on liquid yield [26,27]. This model will also investigate the impact of vapour and liquid/solid residence time distributions on product yield, as well as unreacted feed lost to the burner.

Chapter 3: Fluid Coker Freeboard Model

3.1 Background information

Vacuum residues must be converted or upgraded to a lighter, higher value product which can be used in traditional refinery operations. Technologies to upgrade residues can be categorized by their operating conditions and their respective method to increase the hydrogen to carbon ratio of the products, which is indicative of a higher energy density and higher value product. The first category increases the hydrogen content of the products by cracking residues at elevated temperatures and pressures in the presence of hydrogen. Recent improvements to residue hydrocracking can be found in Sahu [12]. Alternatively, carbon rejection or coking processes reduce the hydrogen to carbon ratio through the removal of carbon from the cracked hydrocarbons. These processes break large hydrocarbons using temperature without a catalyst and are the most common residue upgrading methods worldwide [3]. This study focuses on FLUID COKING™, a continuous upgrading process, previously shown in Figure 2, which operates at a bed temperature of 510 – 540°C and near atmospheric conditions [14].

Vacuum residue is injected through six rings of nozzles, before contacting a fluidized bed of hot coke particles. The residue coats the hot particles, which provide the heat required for the endothermic cracking reactions, while the lighter products flash off the particle surface. The product vapours then travel up the bed, exiting through the cyclones, which return entrained coke particles to the fluidized bed. Coke particles generally travel downwards in the fluidized bed, where they are sent to a parallel fluidized bed burner unit. Partial combustion of coke is carried out in the burner, which heats the particles to the requires temperature of 590-650°C [14]. Most heated particles are sent back to the Fluid Coker reactor through the hot coke transfer line, which adds the hot coke particles above the fluidized bed. A smaller fraction of the transferred coke enters the horn chamber through the scouring coke transfer line, which helps scour cyclone surfaces via erosion [3].

Run lengths for commercial Fluid Coker units generally depend on the rate of cyclone fouling. The parallel cyclones have been observed to experience coke deposition or fouling throughout typical runs. Fouling within the gas outlet tubes decreases the

available flow area, thus increasing the pressure drop across the cyclone [17]. This increased pressure drop results in a pressure buildup through the reactor and burner regions. The air fed into the burner is subsequently reduced due to blower limitations, reducing the available heat for the cracking reactions. The feed rate must be reduced to maintain the required bed temperature. Eventually, the reduced feed rate forces the unit to be shut down for cleaning [3].

Fluid Coker cyclone fouling is primarily the result of physical condensation of heavy hydrocarbon vapours. Along with the lighter cracked products, heavier components can vaporize and travel into the freeboard, horn chamber or cyclone regions. These heavier components would be near their respective dew points and could condense due to minor changes in temperature, pressure, and/or composition. If this condensation occurs in the cyclone, the resulting droplet could contact the surface of the gas outlet tube and form coke on the surface. Experimental and mathematical studies by Zhang and Watkinson investigated the impact of temperature and vapour dilution on residue deposition rate. Their work found that reducing the temperature or vapour dilution increased deposition rates due to the more favourable condensation conditions [5,6]. Analytical studies to characterize the deposits in cyclone diplegs of a fluidized catalytic cracking (FCC) unit by Kim et al observed that deposits were comprised of both inorganic catalyst fines and hydrocarbons [7]. Although not identical to a Fluid Coker (i.e., catalyst use and lighter feedstock), the trends can be used as an analogy for Fluid Coker fouling. A review of the deposit structure and mechanism formation identified the condensation and polymerization of heavy oil droplets as a factor for the deposit formation [7].

Previous work by Glatt et al. developed an Aspen Plus model of the Fluid Coker freeboard and cyclone region to identify the impact of key operating parameters on cyclone condensation. This model considered vapour-liquid thermodynamics, heat of liquid phase endothermic cracking, and pressure changes on a series of defined control volumes [8]. Case studies identified that increasing the scouring coke flow and transfer line temperature would be effective methods to mitigate cyclone fouling [8]. A separate study by Pazoki demonstrated that the more porous Flexicoke had a higher hydrocarbon adsorption capacity compared to Fluid Coke [29]. Hydrocarbon adsorption on coke particles was shown to

follow first order kinetics, with comparable time constants and varying equilibrium capacities between the two coke samples [29]. Despite having similar operating conditions, the Flexicoking run times tend to be limited by the downstream fractionator and not cyclone fouling [16]. Since the heaviest hydrocarbons are most likely to adsorb to coke and are also the components which cause fouling, adsorption may be a factor in reducing cyclone fouling. Due to the short residence times within the freeboard and cyclones, this adsorption must be estimated based on adsorption kinetics and not equilibrium values alone.

This study aims to improve upon previous the previous Fluid Coker modelling by incorporating vapour phase cracking and hydrocarbon adsorption into an Aspen Plus model. These additions will allow for the quantification of over cracking resulting from increased temperature and/or scouring flow in the freeboard and cyclone regions. Overall, we will identify process levers that can be used to mitigate cyclone fouling, while considering their impact on product quality. Hydrocarbon adsorption estimates based on the previous first order kinetics will also be implemented to determine if increased adsorption at the relevant timescales would impact hydrocarbon condensation.

3.2 Modelling in Aspen Plus

Aspen Plus V9.0 is simulation software developed by Aspen Tech which provides methods to design, analyze and optimize chemical processes by providing tools to complete otherwise challenging calculations. The developed model used a series of modules or units to represent six defined regions of interest within the Fluid Coker freeboard, which are then solved sequentially by the software. This allows for the heat of reaction and pressure drops to be calculated and applied, with the model determining the resulting operating conditions and phase equilibrium within each region. This allows for case studies on key operating parameters to be run, determining their relative impact on operating conditions, product quality and ultimately cyclone fouling. These control volumes, illustrated in Figure 6, are defined as:

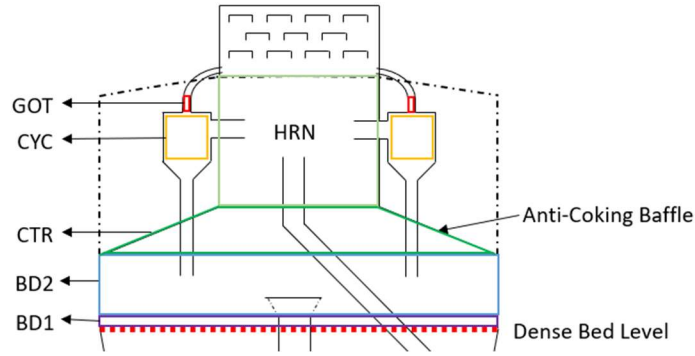


Figure 6. Fluid Coker Model Control Volumes.

- BD1: Region exiting the dense region of the fluidized bed, ending immediately below the hot coke transfer line (HCTL). The region contains steam, hydrocarbons and entrained bed coke.
- BD2: Region beginning immediately below the HCTL and continues until the Fluid Coker contraction. The region contains the components of BD1, as well as the steam from the anti-coking baffle (ACB) and HCTL, as well as a fraction of coke from the HCTL which becomes entrained in the dilute phase.
- CTR: Region extending from immediately below the vessel contraction to the entrance of the horn chamber.
- HRN: Region extending from the bottom entrance of the horn chamber to the midpoint of the cyclone inlets. This region combines the contents of the previous region with additional coke and steam from the scouring coke transfer line (SCTL)
- CYC: Region extending from the midpoint of the cyclone inlets to the inlet of the cyclone gas outlet tube. This region contains the same contents as the previous region.
- GOT: Region from the inlet to the outlet of the cyclone gas outlet tube. This stream contains the same components as the previous region except with the solids removed.

The boundary conditions for this model are defined as being immediately above the dense region of the fluidized bed up to the outlet of the cyclone's gas outlet tubes. For each case study, the hydrocarbon feed entering BD1 is assumed to remain the same. Although changing transfer line temperatures may impact the reactor bed temperature and therefore the vapour composition exiting the dense phase, these changes were outside the scope of this study. They will instead be considered in Chapter 4.

3.2.1 Component Specification

Process streams within the Fluid Coker model are comprised of steam, hydrocarbons and coke. Due to the complexity of the hydrocarbons in the Fluid Coker, specifying the

product composition by chemical species is not viable. Instead, only the light gases (i.e., C₁-C₄) and steam are specified as conventional components. The light gases composition, shown in Table 4, was used by Jankovic and Glatt et al in their Fluid Coker modelling and provides a reasonable estimate for this study [8,20].

Table 4. Composition of Light Ends [8,20].

Light End Component	Weight Fraction (%)
Hydrogen	1
Hydrogen Sulfide	6
Methane	21
Ethane	16
Ethylene	8
Propane	12
Propylene	13
Butadiene	2
Butenes	12
<i>i</i> -butane	1
<i>n</i> -butane	6

The remaining hydrocarbons are defined as assays, which provide a boiling point curve that Aspen Plus uses to model the hydrocarbon component properties. Limited details pertaining to the Fluid Coker products are publicly available; however, work by Jankovic defines the product composition entering the scrubber section as a combination of two hydrocarbon assays [20]. The first assay, Coker Gas Oil (CGO), ranges from normal boiling points of approximately 220-570°C. The remainder of the condensable products are included in the Once Through Scrubber Bottoms (OTSB) assay, which includes components with boiling points approaching 1000°C. The ratio of OTSB to CGO is approximately 1:3 on a weight basis [20]. The boiling point fractions are shown in Figure 7. The final two data points (filled in data), representing the heaviest 10 wt% of the OTSB assay, were extrapolated to obtain sufficient condensation within the model to obtain a representative base case. It should be noted that the light condensable fractions defined such as naphtha and the middle distillates are not included. This omission is due to the limited compositional data available. However, as the condensation phenomena is the result of the high boiling point components present in the OTSB stream, their absence should have minimal impact on the modelling results.

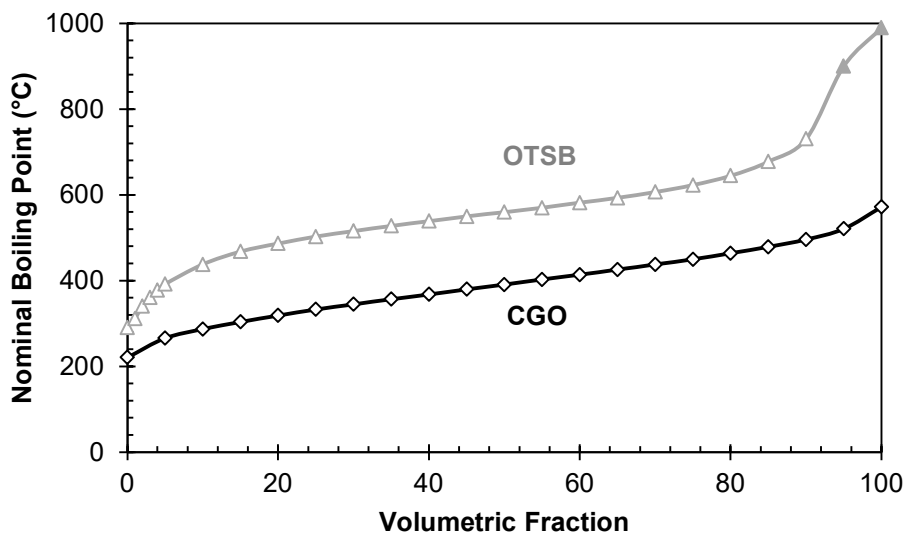


Figure 7. CGO and OTSB assays based on data from Jankovic, where the filled data points represent extrapolated values [20].

Jankovic reported the hydrocarbon composition as two assays with overlapping normal boiling points [20]. The application of thermal cracking reactions to these two assays unnecessarily increases modeling complexity. As such, both assays were combined into a single assay, shown in Figure 8, by considering their respective mass flow rates and boiling point curves. The combined assay was then split into four smaller assays, matching the boiling point ranges of the lumps defined by the Gray kinetic models (shown in Table 5). This splitting is required for cracking kinetics calculations for each individual fraction.

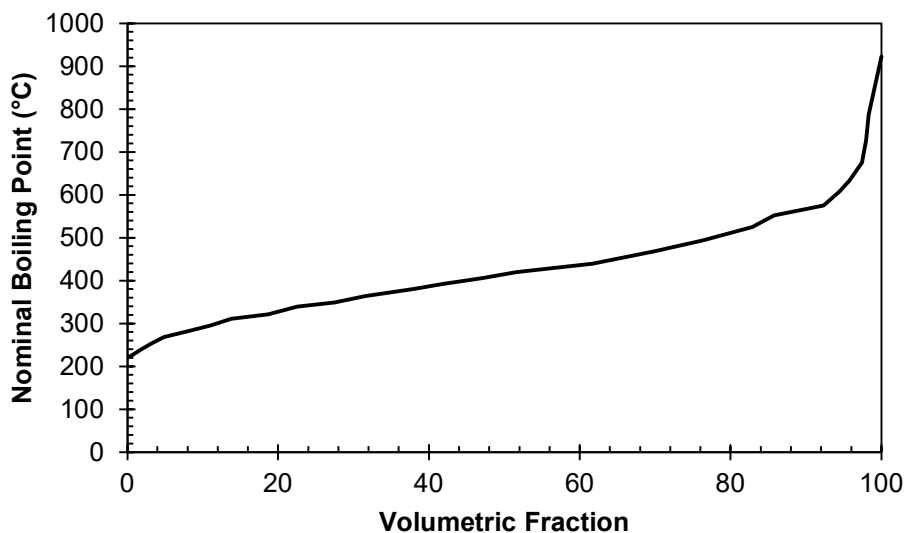


Figure 8. Combined CGO and OTSB Assay.

Table 5. Lumped assay definition and mass distribution based on Gray kinetics. Mass fractions are based on the listed condensable hydrocarbon fractions, excluding all other species present.

Component Name	Boiling Point Range (°C)	Condensable Hydrocarbon Mass Fraction
Heavy Residue	> 650	0.04
Light Residue	524-650	0.15
Gas Oil	343-524	0.59
Distillates	<343	0.22

Coke properties, such as density and heat capacity, were defined using a solids template. Four steam inputs had to be defined in this model. Steam entering from the fluidized bed, and through the hot coke and scouring coke transfer lines were included in the model by Glatt et al [8]. Steam entering from the bed is assumed to match the inlet conditions of BD1, while the hot coke transfer line steam is saturated at a pressure of 150 barg, as shown in Glatt's model [8]. The remaining scouring coke transfer line steam, as well as the newly added anti-coking baffle steam are modeled as superheated to match typical operating conditions.

A final adjustment was made to the previous model for the transfer lines. Glatt's model showed the transfer line steam being added directly to the relevant control volume, along with the coke stream in parallel. This results in a reduction in the predicted temperature following the addition of the HCTL. When the pressure of the saturated steam reduces from 150 barg to the bed pressure, a Joule-Thompson cooling effect was predicted. The impact of this temperature change would be dampened by the HCTL, as the 60 TPM of coke would minimize the observed temperature change. However, because only 5 TPM of the HCTL were assumed to be entrained in the freeboard region, the remaining 55 TPM do not enter the control volumes of the model. This resulted in a larger temperature drop than would normally occur. The updated model in this study mixes the coke and steam in the transfer line first, minimizing the temperature change, before splitting off the entrained coke and steam from the remainder of the coke fraction.

3.2.2 Method Specification

The Peng-Robinson property package was chosen for use in the model due to its applicability to refining, petrochemical and gas processing applications. This equation of state was also found to be effective by Jankovic in their HYSYS simulation of the scrubber section of the Fluid Coker. Our model defined coke as a heterogenous solid with a constant density and heat capacity. The Peng-Robinson property package, in conjunction with the defined coke properties, will allow for phase equilibrium and heat balance calculations. The Aspen Simulation Workbook Add-in is a tool that exchanges process inputs and outputs between the model and Excel. This feature is used to calculate and apply pressure drops through the defined regions, thermal cracking reactions, hydrocarbon adsorption, and Ranque-Hilsch cooling in the cyclone region.

The Ranque-Hilsch effect is a phenomenon where rotating compressed gas is separated into heated and cooled outlet streams. Polihronov and Straatman concluded that the adiabatic expansion of the fluid resulted in a transfer of its internal and rotational energy to the outer fluid, cooling the center vortex in a uniformly rotating duct [30]. In a stationary tube with rotating gases, experimental studies by Parker and Straatman found the pressure ratio between inlet and outlet streams had the best correlation with temperature drop [31]. Although the velocities and pressure changes seen in the Fluid Coker cyclone are not as

high as those in a vortex tube, this phenomenon is still of interest. Vapours present in the cyclones are near their respective dew points, where a small change in temperature could result in condensation. A Ranque-Hilsch prediction derived by Syncrude collaborators, based on the Navier-Stokes equation with adiabatic expansion, was applied to the Fluid Coker model.

3.2.3 Pressure Drop Calculations

The reactor pressure was assumed to apply to both the BD1 and BD2 regions at the top of the fluidized bed. The pressure drops through the CTR, CYC and GOT regions were calculated using proprietary reactor geometry provided by Syncrude collaborators. The pressure drop through the CTR region was calculated using the Bernoulli equation for a contraction in pipe diameter [32]. The pressure-drop equations summarized in Table 6 were used to determine the pressure drop through the cyclone and gas outlet tube regions. As the Mach numbers for the fluid in each of the regions was found to be below 0.3, flow was assumed to be incompressible with pressure drops having negligible impact on temperature change.

Table 6. Cyclone Pressure Drop Calculations [33].

Description	Equation
Inlet Gas Contraction	$\Delta P_{ic} = 0.5\rho_g(U_{ci}^2(1 + K) - U_{fb}^2)$
Acceleration of Solids	$\Delta P_{as} = LU_{pi}(U_{ci} - U_{fb})$
Barrel Friction	$\Delta P_{bf} = \frac{2f\rho_g U_{ci}^2 \pi D_b N_s}{d_{hi}}$
Gas Reversal	$\Delta P_r = \frac{\rho_g U_i^2}{2}$
Cyclone Exit Contraction	$\Delta P_{ec} = 0.5\rho(U_{got}^2(1 + K) - U_{ci}^2)$
GOT Friction	$\Delta P_{gf} = \frac{2f\rho LU^2}{D}$
Elbow	$\Delta P_E = \frac{K\rho U_{got}^2}{2}$
Snout Contraction	$\Delta P_{sc} = \frac{K\rho U_{got}^2}{2}$

3.2.4 Endothermic Cracking Reactions

The previous study estimated first order cracking of the liquid fraction of hydrocarbons present in each control volume [8]. Using the Excel Add-in, the mass of cracked residue and resulting heat of reaction were determined. As assays cannot

participate in reactions in Aspen Plus, the model applied the calculated heat of reaction to the process stream, but did not modify the hydrocarbon assay. Using the Arrhenius constants presented by Olmstead and Freund, the temperature change due to the cracking heat of reaction was estimated using the parameters shown in Table 7 [24]. Although these values provide an estimate of the kinetic parameters and reaction enthalpy for vacuum residue, it should be noted that high variance can be observed between different residue sources and between different fractions within a given feed (up to $\pm 20\%$). The enthalpy of reaction has been assumed to be constant for all hydrocarbon fractions, however this could be improved in future studies.

Table 7. Thermal cracking reaction simulation parameters used by Glatt et al. [8,24]

Parameter	Value	Unit
logA	13.2	s ⁻¹
E _a	213	kJ/mol
ΔH_R	279	kJ/kg

Hydrocarbons within the freeboard region are predominantly present in the vapour phase. The model must thus consider cracking in the vapour phase rather than exclusively in the liquid phase. The kinetic parameters shown in Table 7 are derived using vacuum residue, while hydrocarbons in the freeboard are comprised of the lighter cracked products. Furthermore, resulting products from cracking must be estimated and these predictions must be implemented in Aspen. Available kinetic models will be reviewed and selected for this study. A modelling technique will then be identified to overcome the challenge of changing assay compositions due to reactions in Aspen.

Bu and Gray studied the kinetics of vapour phase cracking of a bitumen derived heavy gas oil (HGO) while analyzing the quality of the derived products [27]. This feed was primarily comprised of the coker gas oil fraction previously defined in Table 2 (i.e., boiling point between 343 and 524°C). By vaporizing, cracking and condensing the products, Arrhenius constants were estimated for thermal cracking of this vapour fraction. This work also showed that the coke yield from vapour phase cracking was low, likely due to the absence of the recombination reactions which are present in liquid phase cracking

[27]. Vapour phase cracking produced permanent gases (C_2 - C_3) while lowering the boiling point of the remaining liquid fraction to below 343°C . The yield and conversion data for the light ends showed a selectivity of 20-40%, with increased selectivity at higher temperatures. As the HGO feed was nearly 80 wt.% CGO, Bu's kinetics would be an effective approximation for that fraction in the model. The feed assumed for this model, however, contains nearly 20 wt.% heavy and light residues. As the heavier fractions tend to be more reactive compared to the light components, it is possible that we may underestimate the rate of cracking of the heaviest components. Although Gray and Radmanesh have completed studies on cracking these heavier fractions, these studies were completed in the liquid phase, which may not be representative of the vapour phase cracking for those compounds.

Wu et al. studied thermal cracking kinetics and yields of n-hexadecane in both the liquid and vapour phase [34]. The authors found that the kinetics were similar between both phases, with the primary difference being the product yields. In vapour phase cracking, the products showed a higher selectivity towards light gases, particularly alkenes with no addition reactions occurring. Liquid phase cracking conversely had a lower selectivity to vapour products, while addition reactions were detected [34]. This trend is consistent with the Bu vapour cracking study, which showed negligible coke yield and light gases as a product. Our model will investigate the use of either Gray or Radmanesh's liquid phase kinetic model, adapted for the vapour phase. The Arrhenius constants will remain unchanged; however, the product yields will be adjusted such that the light gases and distillates selectivities match the Bu vapour cracking study.

Both studies published by Gray and Radmanesh reported lumped kinetic models to quantify the liquid phase cracking of vacuum residues [25,26]. In Gray's initial study, thin residue films were used such that the liquid side mass transfer resistance was assumed negligible. Further simplifying assumptions were made, such as heavy and light residue having the same activation energy, and estimating coke formation through a single reaction pathway [25]. Radmanesh's study built off the previous work by adapting the model to include the formation of both intrinsic and extrinsic coke. The activation energy of each residue was also determined individually and consideration to liquid side mass transfer

resistance was given [26]. As Radmanesh's work provides separate Arrhenius parameters for both heavy and light residue, our model will use these parameters to estimate the reaction rate of those fractions in this study [26]. As noted by Wu, since the reaction rate for cracking in both the liquid and vapour is consistent, Radmanesh's liquid cracking kinetics is a reasonable estimate for the vapour cracking rate for this model [34]. However, the product yield must be adjusted to favour the formation of light gases rather than light residue, coker gas oil and distillates as shown in Radmanesh's model [34]. Therefore, the vapour cracking model will assume the heavy and light residue form lights and distillates with the same selectivities as CGO based on the vapour cracking study by Bu [27]. Based off the results from Bu, the selectivity of the cracked products is assumed to be 25% light ends, with the remainder being distillates, as shown in Equations 5 - 7 and Figure 9. As no kinetic model is available for the cracking of the distillate fraction, it is assumed to not crack any further.

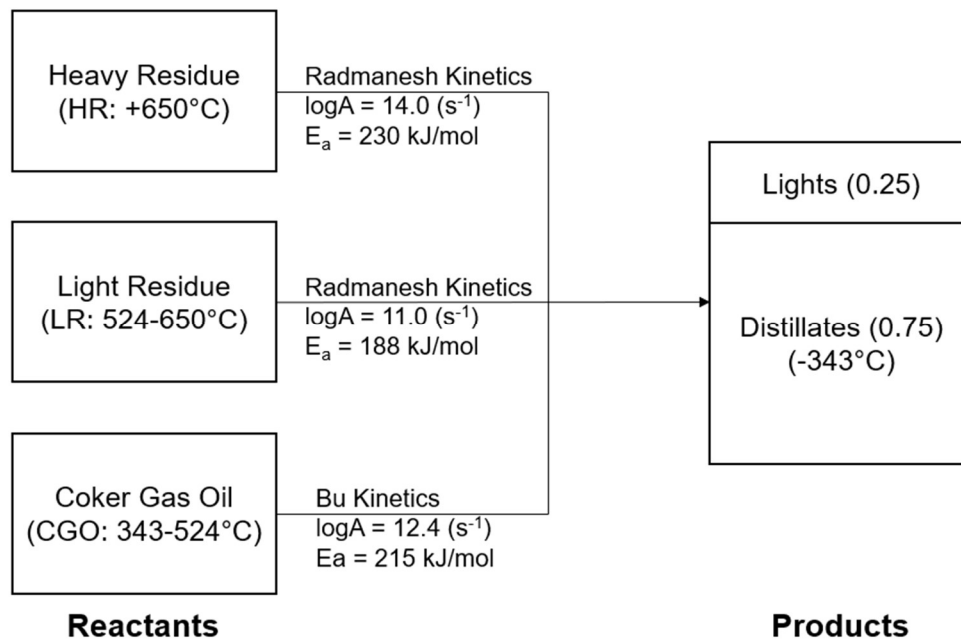
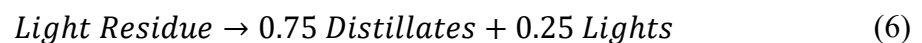
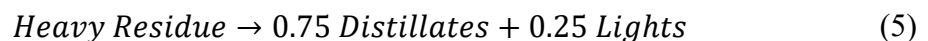
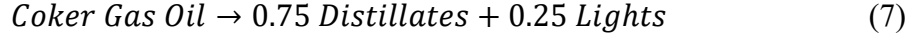


Figure 9. Summary of vapour phase cracking kinetics used in the Aspen Plus freeboard model. Kinetics reported by Radmanesh are used for the residue fractions and kinetics by Bu for the CGO fraction. The products were adapted to match the vapour phase cracking reported by Bu [26,27].





With the reaction network and Arrhenius constants defined, the rate constants at the required temperature and reaction equations can be defined. Using the parameters shown in Figure 9, the Arrhenius equation can be used to determine the rate constant for each fraction as a function of temperature, as shown by Equation 8.

$$k = Ae^{-\frac{Ea}{RT}} \quad (8)$$

The first order reaction rate for each of the cracking components, on a mass basis is shown in Equation 9 based on the mass flow of the applicable component and the rate constant previously defined. Although partial pressure is typically more representative of vapour phase kinetics rather than mass fraction, this simplifying assumption provides a reasonable estimate for the purpose of this study and matches the units basis for lumped kinetics.

$$\frac{d\dot{m}_i}{dt} = -k\dot{m}_i \quad (9)$$

Based on the composition and operating conditions of each control volume, the Aspen Plus model can determine the volumetric flowrate through each region. Using the proprietary geometry data for the reactor, the average residence time of the vapours in each control volume can be determined through Equation 10.

$$\tau = \frac{V}{v} \quad (10)$$

Therefore, by solving the differential shown in Equation 4 from time 0 to tau allows for the final mass flow of the cracking components to be determined, as in Equation 11. Based on the stoichiometry shown in Figure 9, the quantity of lights and distillates formed can be determined using Equations 12 and 13. The sum of the lights and distillates formed and the remaining hydrocarbons exiting a control volume will equal the feed entering, ensuring

continuity through the model. This solution approximates the freeboard as a PFR, which provides a conservative estimate for the vapour cracking reactions.

$$\dot{m}_i = \dot{m}_{i,o} \exp(-k\tau) \quad (11)$$

$$\dot{m}_{lights} = 0.25(\dot{m}_{i,o} - \dot{m}_i) \quad (12)$$

$$\dot{m}_{distillates} = 0.75(\dot{m}_{i,o} - \dot{m}_i) \quad (13)$$

3.2.5 Hydrocarbon Adsorption Estimates

Hydrocarbon adsorption kinetic measurements were completed by Pazoki using mesitylene, n-decane and n-dodecane at temperatures not exceeding 240°C [29]. It was observed that adsorption followed first order kinetics on Fluid Coke, Flexicoke and coconut shell activated carbon [29]. Applying these results to the Fluid Coker is challenging as the hydrocarbons of interest are considerably heavier and are at much higher temperatures. Collecting experimental data at temperatures and with heavy hydrocarbons relevant to the Fluid Coker poses further challenges, as the compounds could readily crack while being heated, complicating the conditions in the adsorption experiment. Based on these limitations, a preliminary estimate for adsorption, based on key assumptions, was determined using the first order kinetic equation:

$$q_t/q^* = (1 - \exp(-t/\tau)) \quad (14)$$

Where q_t (mg/g) is adsorption capacity at time t (s), q^* (mg/g) is equilibrium adsorption capacity, and τ is the time constant. Based on the results from Pazoki, both Fluid and Flexicoke exhibited similar time constants of approximately 75 seconds. It is assumed both coke samples would continue to have equal time constants. As hydrocarbon adsorption is the result of pore filling, it will be assumed that the q_t/q^* ratio is approximately equal to the pore volume fraction filled at a given time. The filled pore volume at a given time can thus be estimated by multiplying this fraction by the total pore volume. It will also be assumed that only the heavy residue, light residue and coker gas oil fractions participate in adsorption. As the coker operates at a temperature much higher than the boiling points of the distillates (above 343°C) and permanent gases, these compounds are less likely to

condense or adsorb within the coke particles. Although the heavy residue would be expected to be preferentially adsorbed, it is assumed that the distribution of adsorbed products is based on their respective mass fractions in the vapour phase. By multiplying the mass fraction and density of each respective lumped component, the total mass adsorbed can be determined. The mass adsorbed of a given fraction at time t is thus estimated as follows:

$$m_{i,ads} = \rho_i V_{pore} m_{coke} \left(\frac{\dot{m}_i}{\dot{m}_{HR} + \dot{m}_{LR} + \dot{m}_{CGO}} \right) (1 - \exp(-t/\tau)) \quad (15)$$

Where m_i (mg) and ρ_i (kg/m³) are the mass adsorbed and liquid density of component i , m_{coke} (g) is the mass of adsorbent coke and \dot{m}_i (kg/sec) is the vapour mass flow in the given control volume for which adsorption is being calculated. The adsorption quantities are calculated sequentially in Excel such that the outlet of a given control volume is the inlet for the subsequent control volume.

3.2.6 Flowsheet Setup

A series of modules, such as heaters and mixers, as well as material streams can be used in Aspen Plus to model each control volume. Material streams of specified composition, flowrate and operating conditions are combined with mixers to simulate the combination of streams within the Fluid Coker. The predicted stream properties can then be used in conjunction with the Excel add-in to calculate pressure drops through a given control volume, which can then be applied with a heater module. In the previous model by Glatt, the heater module was also used to apply the estimated heat of reaction to cool each control volume. As Aspen Plus does not allow for assays to participate in reactions, the composition change from these reactions or due to hydrocarbon adsorption was however not captured.

The block flow diagram shown in Figure 10 illustrates the key steps in our modelling approach, which modifies the hydrocarbon assays based on the predicted reaction kinetics and adsorption. The first step mixes the necessary input streams into a single stream, representing the inlet of a given control volume. The required physical properties are extracted to complete the relevant pressure drop, cracking and adsorption calculations in Excel. With the necessary properties determined, a series of splitters remove

all components that are not involved in the vapour phase cracking and adsorption calculations (i.e., steam, coke, and light ends).

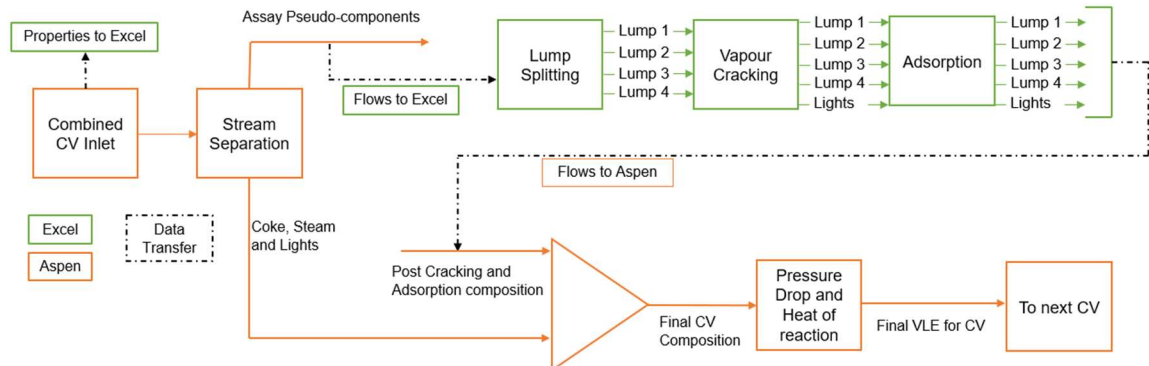


Figure 10. Block flow diagram representation of calculation steps for a single control volume.

The stream containing only the assay pseudo-components, illustrated exiting the top of the “stream separation”, has its information extracted and sent to Excel, where the mass flow of each lump is determined for use in the cracking and adsorption calculations. The composition of the previous stream cannot be changed directly in Aspen Plus, hence it does not connect to any other unit in Aspen, resulting in a discontinuity in the flowsheet. Knowing the flowrates of each hydrocarbon lump and the temperature of the given control volume, cracking reaction kinetic parameters determine the increased flow of distillates and light ends, the reduced heavy residue, light residue and coker gas oil flow rates, as well as the total heat of reaction. Equation 15 is then applied to predict adsorption on the coke particles, reducing the respective flowrates of the heavy residue, light residue, and Coker gas oil. The Excel calculation finally specifies the composition of a new stream in the Aspen flowsheet. As the sum of this new stream and the adsorbed hydrocarbons will equal the total mass originally removed, continuity in the model is maintained.

The stream information sent from the Excel calculations can be combined with the steam, coke, and light ends that were previously separated, determining the outlet composition for the control volume. A heater unit is finally used to apply the calculated pressure drop and heat of reaction for that control volume. Thermodynamic calculations in Aspen Plus then determine the vapour-liquid composition of the control volume before the stream is connected to the inlet of the subsequent control volume. An example of the Aspen

Plus flowsheet for BD1 and BD2 is shown in Figure 11, with remaining control volumes following a similar configuration.

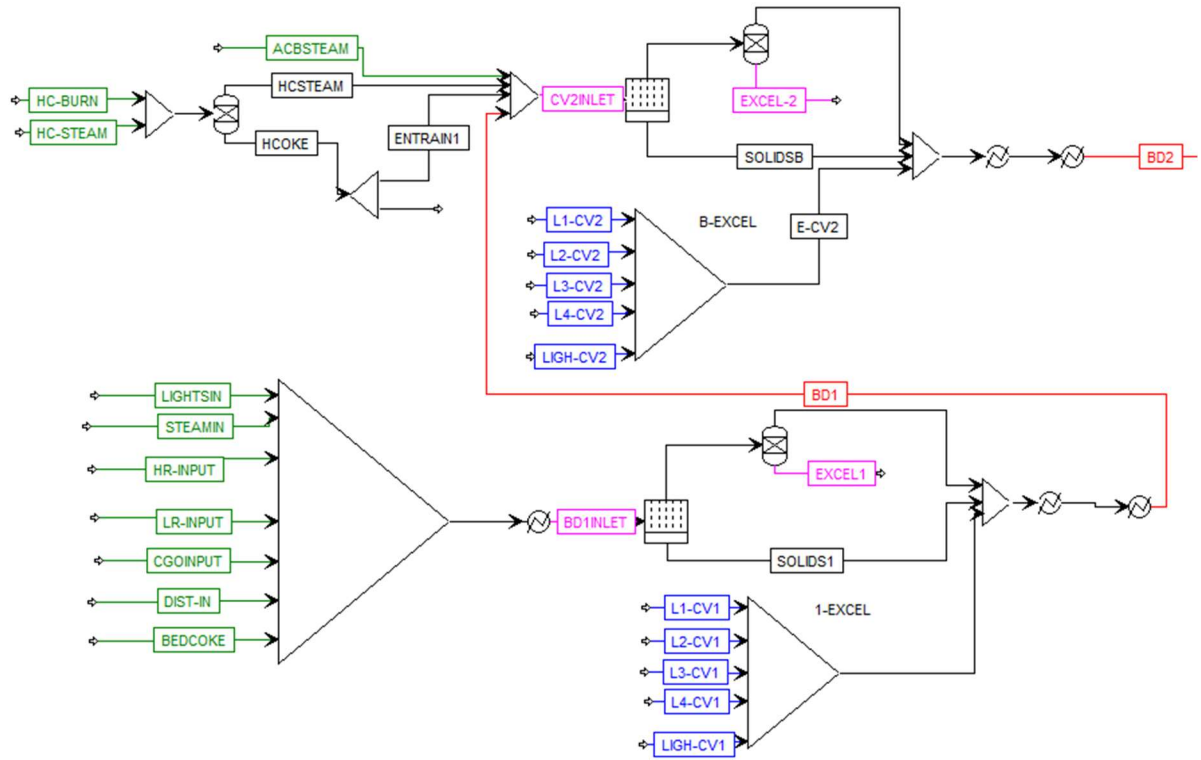


Figure 11. Aspen flowsheet for the first two control volumes, BD1 and BD2. Green streams indicate inputted values, pink and blue streams indicate exported and imported data from excel respectively, black streams indicate an intermediate process stream while red indicate the final control volume composition and operating conditions.

3.2.7 Base Case Parameters

The model requires the inlet stream composition, flowrate and operating condition to estimate vapour cracking, adsorption, and finally cyclone condensation. The total steam flow and distribution of hydrocarbons between the light ends and defined lumps were comparable to industrial values reported by Gray [3]. Bed coke and entrained hot coke flowrates into the freeboard region were selected based on industry estimates. Case studies were performed to determine the impact of transfer line temperature, scouring coke flowrate, entrained bed coke and steam to determine their impact on cyclone condensation. An additional case study repeated the scouring coke test using Flexicoke properties to compare adsorption quantities and condensation predictions. A summary of the base conditions and case study envelopes are summarized in Table 8.

Table 8. Summary of base case parameters and operating envelopes for case studies.

Parameter	Base Case	Units	Case Study Range
Bed Steam	0.08	g/g of BD1 Fluids	0.08 - 0.16
Light Ends	0.12	g/g of BD1 Fluids	-
Heavy Residue	0.03	g/g of BD1 Fluids	-
Light Residue	0.12	g/g of BD1 Fluids	-
Coker Gas oil	0.47	g/g of BD1 Fluids	-
Distillates	0.18	g/g of BD1 Fluids	-
Entrained Bed Coke	40	ton/min	10 – 40
Scouring Coke Flow	6	ton/min	0 – 12
Hot Coke Flow	60	ton/min	-
Entrained Hot Coke	5	ton/min	-
Transfer Line Temperature	610	°C	590 – 650
Bed Temperature	524	°C	-
Bed Pressure	222	kPa	-
Fluid Coke Pore Volume	0.006	mL/g	-
Flexicoke Pore Volume	0.020	mL/g	-

3.3 Results and Discussion

3.3.1 Preliminary Analysis of Model Assumptions

Before running case studies on the identified operating parameters, our first aim was to better understand the condensation predicted by the model. In particular, a relevant liquid condensation rate that would impact the Fluid Coker run times should first be defined. To estimate this rate, we must first estimate how much deposited coke in a cyclone gas outlet tube would cause the unit to shutdown. Assuming the droplet deposition occurs at a constant rate throughout operation, we can convert the total deposition mass to an hourly value to compare with the results of the Fluid Coker model. Under base case conditions, the pressure drop across the cyclone was calculated while reducing the diameter of the gas outlet tube. The diameter reduction was used to simulate an even deposition of coke throughout the outlet tube, reducing the flow area available. A 90 kPa pressure drop was assumed to be the maximum allowable pressure drop through the cyclone, which

occurred when the diameter was reduced by 40% of the initial value, as shown in Figure 12.

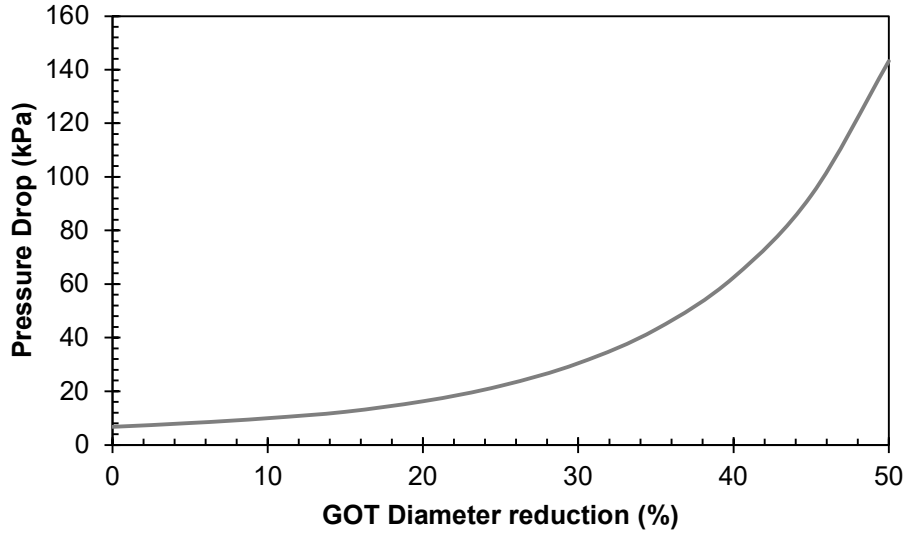


Figure 12. Resulting pressure drop due to reduction in cyclone gas outlet tube diameter.

The total volume of deposited coke can be calculated as a hollow cylinder based on the outlet tube geometry and coke thickness as follows:

$$V_{coke} = \frac{\pi L}{4} (D_{clean}^2 - D_{core}^2) \quad (16)$$

For a desired two-year runtime, a deposition rate of 0.08 kg/hr, or 0.6 ppm of the total hydrocarbon flow (light ends and condensable species) would be required. Figure 13 shows the sensitivity of unit run time relative to the coke deposition rate. If the unit has a runtime of only 1 year, the constant deposition rate would be just 0.16 kg/hr, or 1.2 ppm of the hydrocarbon flow. Reducing the deposition rate by 0.13 kg/hr (or a reduction of 80%) would increase the run time to 5 years. Operating the model such that the base case conditions predict these low levels of condensation would not be effective. If this were the case, small changes to operating parameters could result in no condensation being predicted, making it impossible to quantify and compare the impact of different process levers. The heaviest components of the assay data were modified (as described in Section 3.2.1) such that a non-negligible liquid flow would be predicted, allowing for the relative impact of operating parameters to be quantified. The condensation flowrates presented

throughout the remaining case studies will be notably higher than those provided here; however the relative change should demonstrate the effectiveness of a given lever at reducing cyclone fouling.

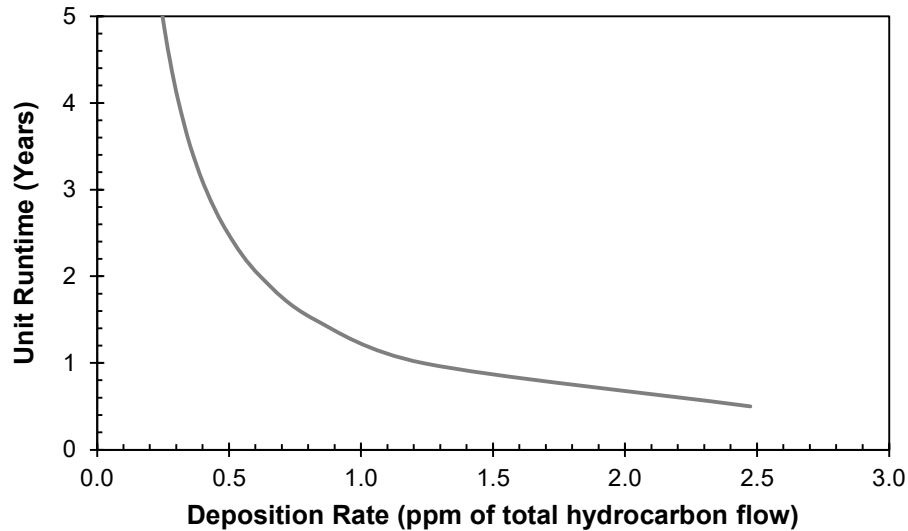


Figure 13. Estimated unit runtime based on hydrocarbon deposition rate assuming maximum pressure drop of 90 kPa before unit shutdown.

The addition of vapour phase cracking to the model has two key impacts on cyclone condensation. First, cracking of the hydrocarbons present in the freeboard will reduce the boiling point of the overall product. Although this change negatively impacts the value of the product, reducing the heavy components would lower the risk of condensation by shifting their dew points to lower temperatures. Second, endothermic cracking reactions will also cool the freeboard and cyclone regions, thereby increasing the likelihood of condensation. Furthermore, as vapour phase cracking of the freeboard model had not been modelled before, it is not known whether there is a sufficient residence time to allow for the cracking reactions to occur at an impactful rate. The base case model was thus run with and without vapour phase cracking to estimate the resulting temperature profile and cyclone liquids. As shown in Figure 14, the inclusion of vapour phase cracking reduced the temperature of each control volume by 3 to 4°C.

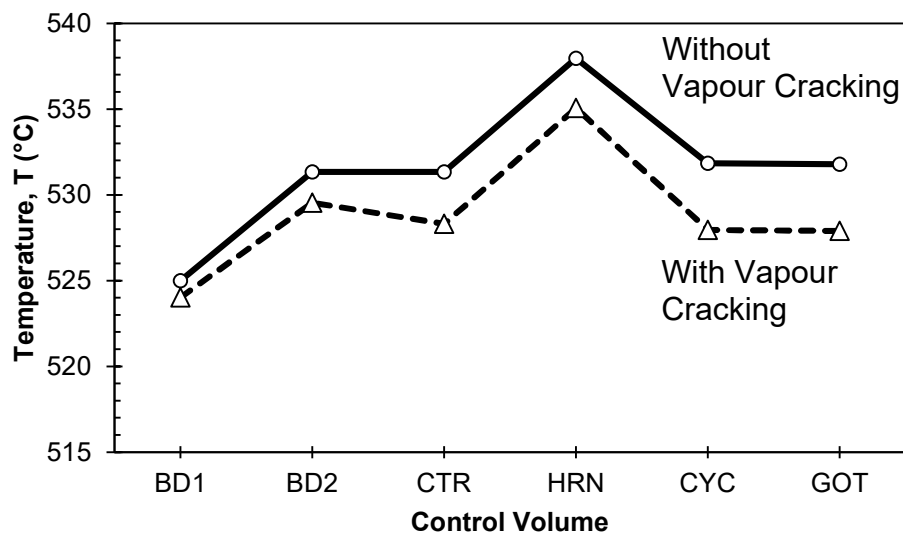


Figure 14. Freeboard temperature profile with (bottom) and without (top) vapour cracking.

Despite the short vapour residence times in this region of the Fluid Coker, the observed temperature reduction demonstrates that vapour phase cracking occurred at impactful levels. Despite being at a lower temperature, the model with vapour cracking still predicted less condensation compared to the non-reacting model, as shown in Figure 15. This demonstrates that the composition change dominated over the resulting temperature drop when considering vapour cracking's impact on the vapour-liquid equilibrium in the cyclones. This phenomenon will be considered throughout the case studies, as minimizing cracking is desired for the product value, while it reduces the cyclone condensation.

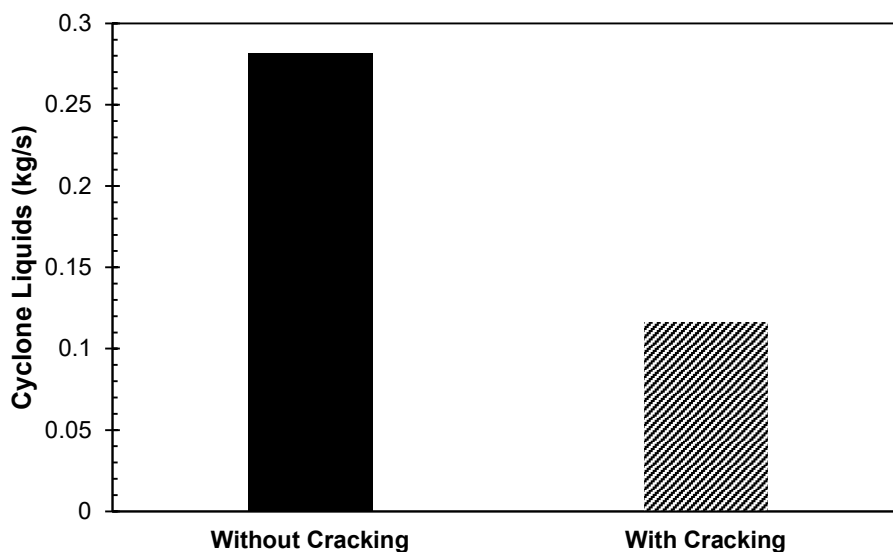


Figure 15. Impact of vapour cracking on model prediction of cyclone liquids.

The final modification is the addition of adsorption kinetics based on Pazoki's work [29]. As previously shown in Equation 2, the model will apply first order kinetics to estimate the mass adsorbed based on the pore volume of the coke particles. An initial comparison between fluid coke and flexicoke is shown in Figure 16, based on the assumed hydrocarbon composition used in the model. Even within the 10-15 second timescale relevant to the freeboard region, the flexicoke adsorption exceeds that of fluid coke. Although flexicoke is shown to adsorb more hydrocarbons, case studies will be required to determine their impact on condensation in the cyclone region. The pore volume estimate was compared to the first order rate equation based on Pazoki's results. As shown with the dashed lines in Figure 16, the pore volume method matched the first order kinetic model using the parameters for dodecane well for flexicoke, but underestimated adsorption by fluid coke. This likely demonstrates that sufficient adsorption occurs on the outer surface of the Fluid Coke particles when compared to the pore volume. The adsorption case studies may thus overestimate the impact of flexicoke adsorption on cyclone liquids relative to fluid coke. Improvements to the adsorption estimation method can be an area of focus for future work.

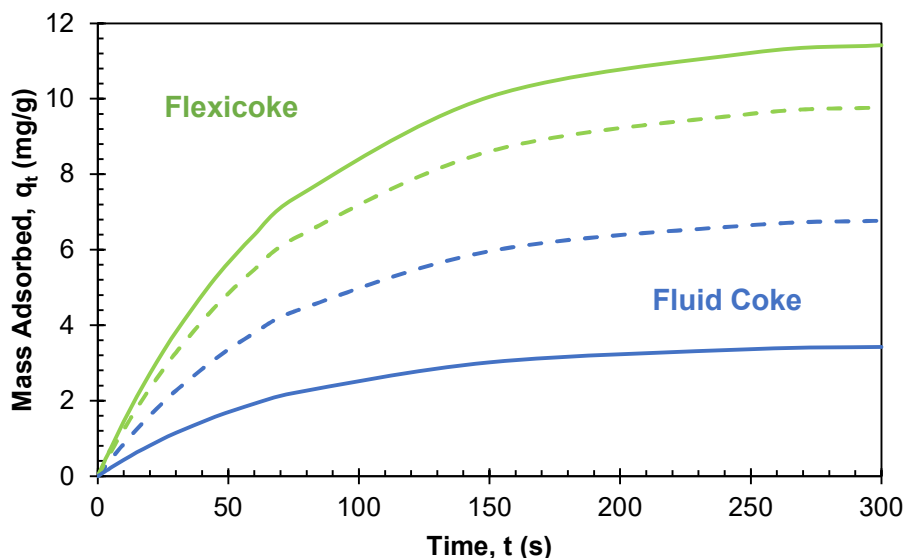


Figure 16. Comparison of pore volume-based adsorption estimates to first order kinetics. Solid lines represent pore volume kinetics, dashed lines represent first order kinetics.

We have demonstrated the impact of adding vapour phase cracking to the freeboard model and developed a method to estimate hydrocarbon adsorption over relevant time scales. Selected process levers, including scouring coke flow, coke porosity, transfer line temperature, bed coke entrainment and steam flowrates can now be varied to determine their relative impact on cyclone liquids while monitoring the impact of vapour cracking on product quality.

3.3.2 Scouring Coke Flowrate

Based on the Glatt et al. study, increased scouring coke flow was found to be an effective method to reduce cyclone fouling [8]. As that model did not include vapour phase cracking, the efficacy of scouring coke flow while accounting for these reactions should be considered. Adding scouring coke will increase the local temperatures; however, the resulting increase in cracking reaction rate needs to be compared to the scouring coke sensible heat addition. Furthermore, the increased vapour cracking due to scouring coke addition is expected to reduce the quality of Fluid Coker products.

Figure 17 compares the energy changes due to the added scouring coke and the cracking heat of reaction. Increasing the scouring coke flow from 0 to 12 ton/min resulted in additional 230 kW of heat consumed by the endothermic reactions as shown in Figure

17. However, the sensible heat of the scouring coke more than compensates for the endothermic cracking, resulting in a steady increase in cyclone temperature and reduction of cyclone liquids, as shown in Figure 18. Compared to the base case value of 6 ton/min, doubling the scouring coke flow to 12 ton/min reduces cyclone liquids by 75%, while removal of all scouring coke flow increases condensation by 73%.

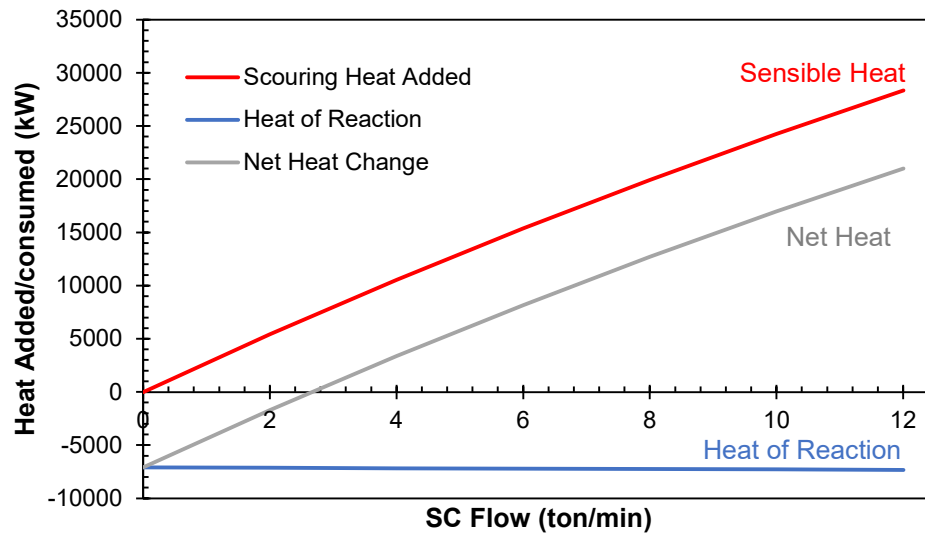


Figure 17. Comparison of sensible and reaction heat as a function of scouring coke flowrate.

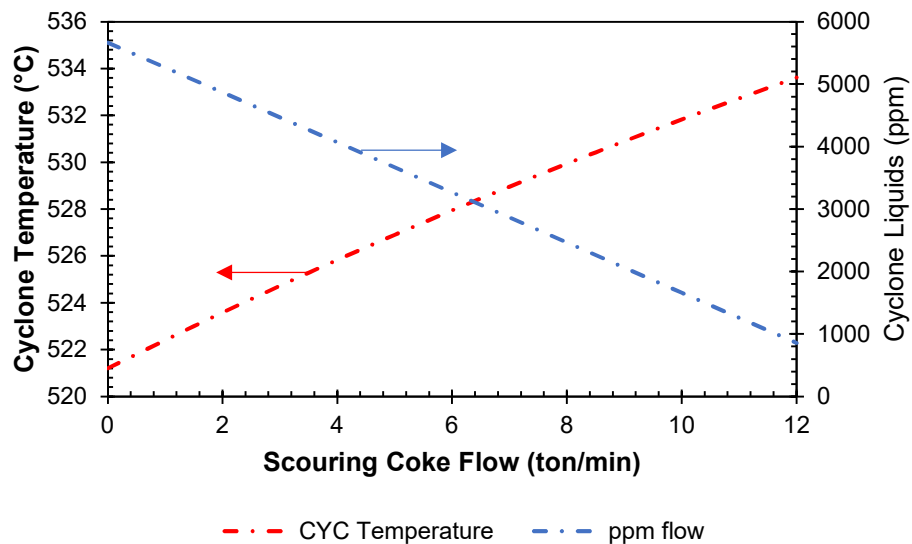


Figure 18. Impact of scouring coke flow on cyclone temperature and liquids.

The final consideration for the increased scouring flow is the impact on the products exiting the gas outlet tube. As the vapour cracking products are the light end and distillate fractions, over cracking will be quantified by the change in flowrate of these fractions through the gas outlet tube. The distribution of the hydrocarbon fractions with varying scouring coke flowrates is presented in Figure 19, with the composition exiting the fluidized bed reactor (i.e., entering BD1) shown for comparison. The prediction with no scouring coke flow demonstrate that the elevated temperatures of the freeboard, due to the coke addition from the HCTL, result in a tangible amount of vapour cracking, increasing the light and distillate mass fraction from 32 to 42 wt%. The more reactive heavy and light residue fractions experience the greatest relative decrease, highlighting the impact of their increased kinetics and the reduced condensation predicted compared to previous non-reactive modelling. It should be noted that although CGO has the smallest relative change due to vapour cracking, its absolute value is the largest as it comprises the majority of the flow through the freeboard region. Figure 19 thus shows that the impact of increasing the scouring flow coke is minor with respect to vapour cracking when compared to the cracking that is already predicted within the freeboard. Although the scouring coke flow rate does increase the temperature of the horn chamber and cyclone, the residence times through these regions is sufficiently short that it minimizes the impact of the increased temperature on the product quality. Increasing the scouring coke flow from 6 to 12 TPM increases the light and distillates by only 1.6 wt%, while this change reduces cyclone liquids by 75%. The improved modeling capabilities further demonstrate that scouring coke is an effective lever to reduce cyclone fouling when considering the potential impact of overcracking the vapour products.

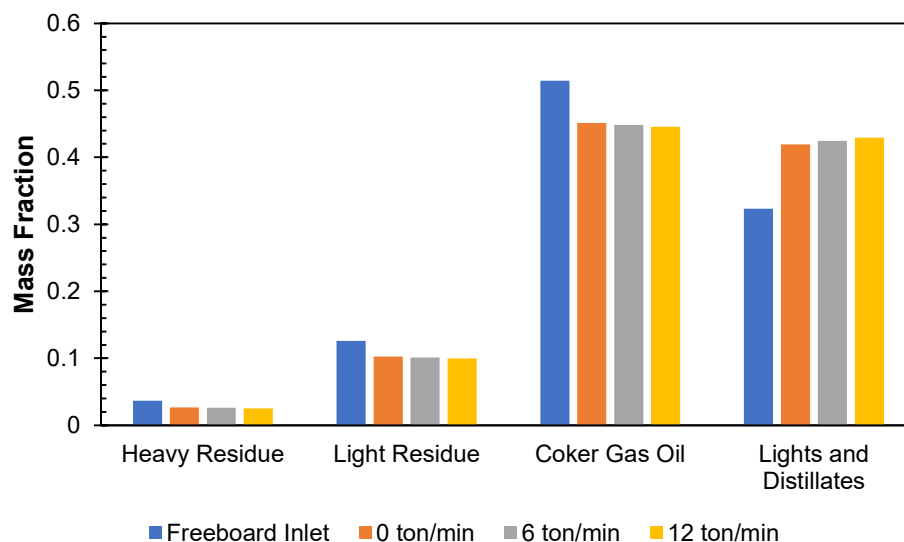


Figure 19. Inlet and resulting gas outlet tube products with varying scouring coke flowrate. The majority of cracking occurs without the presence of scouring coke, with minor increase in cracking as scouring flowrate is increase.

3.3.3 Fluid vs Flexicoke Adsorption

As demonstrated in section 3.1, adsorption by flexicoke exceeds that of fluid coke, even at the short timescales relevant to the freeboard region. Since small changes in the cyclone liquids could have a significant impact on unit runtimes, there is an interest to determine to what extent increased porosity of coke could be beneficial. Coke entrained from the fluidized bed region is assumed to have been in contact with hydrocarbon vapours for a sufficient time, such that they have reached their maximum adsorption capacity. Therefore, only the adsorption done by the entrained hot coke and scouring coke will be quantified.

The total hydrocarbon mass adsorbed is shown in Figure 20. In each case, the entrained hot coke flowrate remained at the base case value of 5 ton/min, while scouring coke flow varied from 0-12 ton/min. For both coke samples, the adsorption by the entrained hot coke is the primary contributor to the total adsorption mass, shown by the initial values with no scouring flow. This can be attributed to the longer residence times of the entrained hot coke in the freeboard regions before the scouring coke is added. Table 9 compares the cyclone liquids predicted in the case of adsorption with either fluid or flexicoke. A

consistent decrease is observed for the fluid and flexicoke cases when compared to the model where no adsorption is considered. Furthermore, flexicoke outperforms fluid coke in reducing cyclone liquids by 5-6ppm as shown in Table 9. Compared to the quantities adsorbed shown in Figure 20, the liquids reduction is considerably lower. It should be noted that Figure 18 shows the total mass adsorbed through the entire freeboard and all six cyclones, while the liquids in Table 9 are on a per cyclone basis.

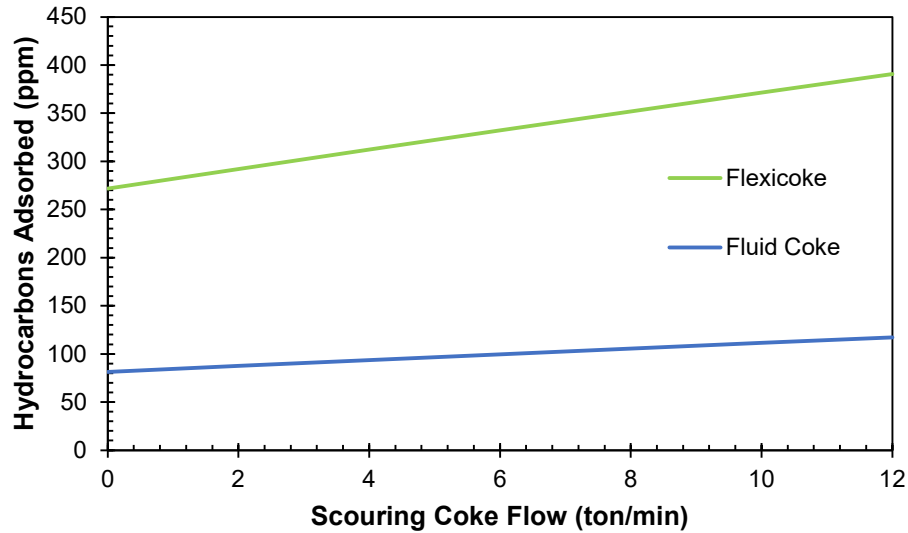


Figure 20. Hydrocarbons adsorbed by fluid and flexicoke in the freeboard region. Adsorption done by entrained hot coke (5 ton/min) and variable scouring coke flow rates. Entrained hot coke is primary contributor due to its increased residence time compared to the scouring coke.

Table 9. Predicted cyclone liquids, per cyclone, with increasing scouring coke flow with and without hydrocarbon adsorption.

Scouring Flow [ton/min]	No Adsorption	Fluid Coke	Flexicoke
	Cyclone liquids [ppm]		
0	5666	5664	5659
6	3269	3266	3261
12	860	857	851

The compositions of the adsorbed hydrocarbons are shown in Figure 21. As nearly 80% of the adsorbed hydrocarbons are modelled as being the lighter CGO fraction, the reduced impact on condensation is expected. The heaviest components are the primary

cause of the cyclone fouling phenomenon, hence a larger percentage of the residue would have to be adsorbed. The heavier fractions would be expected to preferentially adsorb at equilibrium compared to their lighter counterparts; however, it is unknown if the kinetics of adsorption would follow this trend. It is possible that the initial adsorption would be dominated by the lighter fractions which could enter the pores more easily, with the heavier fractions dominating when allowed to reach equilibrium. This highlights the need for further experimental data to quantify the impact of preferential adsorption at the relevant timescales and conditions. The model nonetheless indicates that the more porous flexicoke would reduce cyclone liquids by 5-6 ppm in each cyclone. Based on the initial quantification of relevant deposition rates (refer to Section 3.1), this suggests that the increased porosity are expected to increase unit runtimes. Considering the effectiveness of alternative process levers and the challenges to increase the coke porosity, this may not be the most desirable process lever to reduce cyclone fouling.

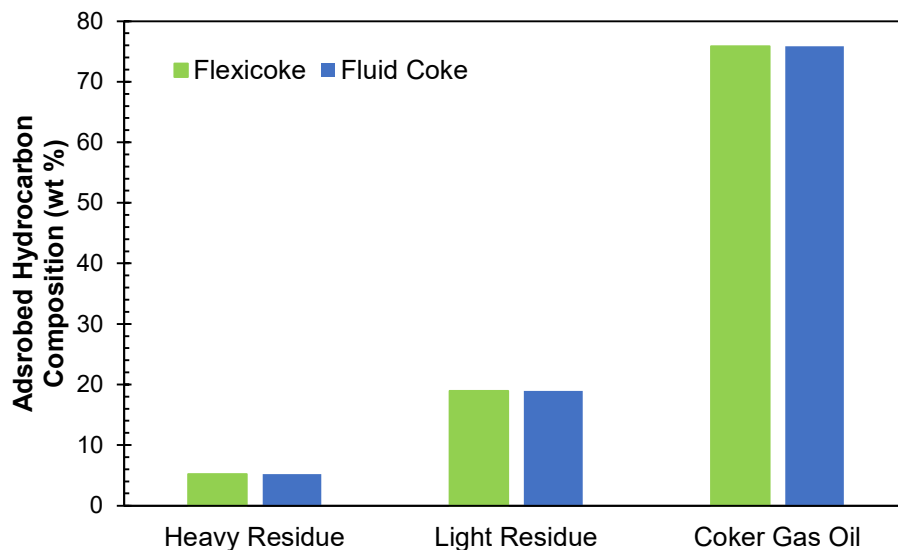


Figure 21. Predicted composition of adsorbed hydrocarbons on fluid and flexicoke. The composition of the adsorbed hydrocarbons remains comparable for both coke samples. As the adsorption was assumed to follow the same mass distribution of the hydrocarbons in the vapour phase, the CGO fraction dominates the adsorbed phase.

3.3.4 Transfer Line Temperature

Rather than varying the scouring coke flow rate into the horn chamber, an increase in cyclone temperature could be achieved by increasing the operating temperature of the

burner and thus the scouring coke itself. The resulting temperature increase of the transfer lines would also impact the entire freeboard and cyclone region, shown in Figure 22, as well as the reactor bed. The impact of increasing the bed temperature is not considered in this section of the thesis. The change in cyclone liquids relative to the base case transfer line temperature of 610°C is presented in Figure 23, where an 81 wt% liquids reduction is achieved with a transfer line temperature of 650°C. This is comparable to the 75 wt% reduction achieved by doubling the scouring coke flow.

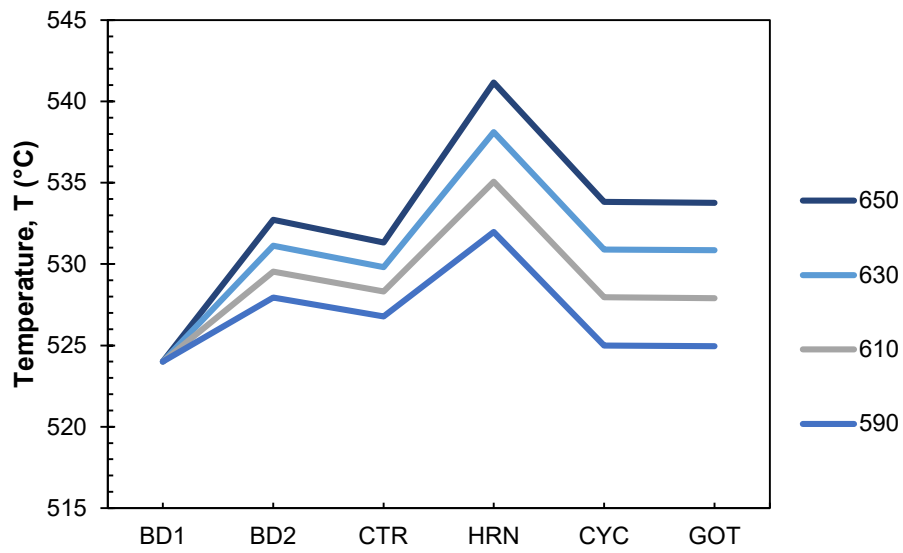


Figure 22. Impact of transfer line temperature on control volume temperature.

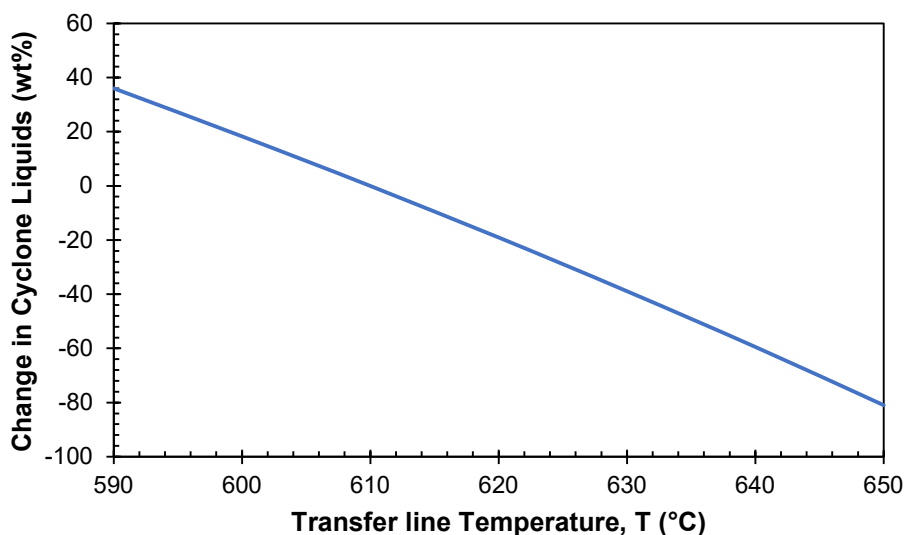


Figure 23. Change in cyclone liquids due to varying the transfer line temperature. Change in liquids reported relative to liquids predicted in the base case with a transfer line temperature of 610°C.

Increasing the transfer line temperature performed similarly to the scouring coke process lever; however, further consideration must be taken to evaluate this option. Due to the increased temperatures seen throughout the freeboard region (excluding BD1), the impact on vapour phase cracking must be considered. This increased transfer line temperature would also have implications on the bed region; however, this is not quantified in this study. The change in composition of vapours exiting the gas outlet tube compared to the feed entering BD1 is shown in Figure 24 for the various transfer line temperatures. The observed 3.5 wt% increase in lights and distillates is more than double the 1.5 wt% produced when doubling the scouring coke flowrate (i.e., for comparable liquids reduction in the cyclone). The over cracking of products resulting from the increased burner temperature limits the efficacy of this process lever to minimize fouling without compromising reactor performance. Increasing the burner temperature may be an easier alternative to implement compared to modifying the scouring coke transfer line.

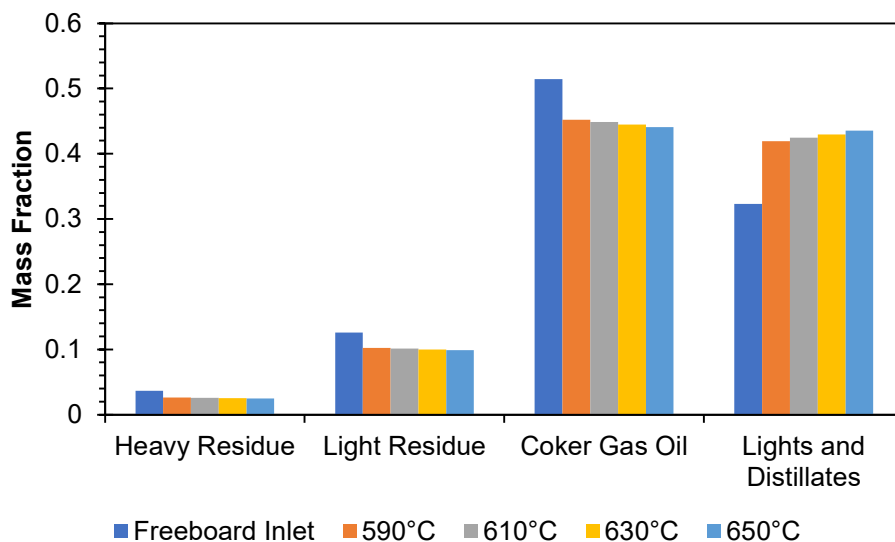


Figure 24. Impact of increasing transfer line temperature on products exiting the gas outlet tube. An additional 3.5 wt% of light and distillate products formed as a result of increasing the temperature to 650°C compared to the base case.

3.3.5 Fluidized Bed Coke Entrainment

Along with the hydrocarbon and steam that travels out of the fluidized bed through the cyclones, a fraction of the coke becomes entrained and is carried into the freeboard region. The height difference between the fluidized bed and the contraction into the horn chamber dictates the fraction of coke that will enter the cyclones to be separated and fed back through the cyclone diplegs or that will fall back down into the bed. As the distance between the freeboard and cyclones increases, the fraction of coke that remains entrained will decrease, up until a critical distance known as the transport disengagement height. At this point, the entrainment rate does not significantly change with height. The coke that is entrained from the fluidized bed is colder than coke particles entering from the transfer lines. The entrained coke will thus be heated along with the hydrocarbon vapours once in contact with the hot coke and scouring coke transfer lines. Reducing the amount of coke entrained from the fluidized bed will increase the freeboard temperature, without modifying coke flowrates or burner temperatures, minimizing the impact on the reactor region.

The resulting cyclone temperature and change in cyclone liquids as a function of bed coke entrainment rate are shown in Figure 25 and Figure 26, respectively. As was the case

with the previous case studies, increasing the cyclone temperature resulted in a reduction of cyclone liquids, and an increase in light products at the expense of the heavy residue, light residue and coker gas oil fractions. Reducing the entrained bed coke from a base case value of 40 to 10 ton/min is predicted to reduce cyclone liquids by 83 wt% compared to the base conditions. However, this is accompanied by an increased light and distillate yield by 2.7 wt%, which is between the predictions for the doubled scouring coke flow and increasing the transfer line temperature to 650°C.

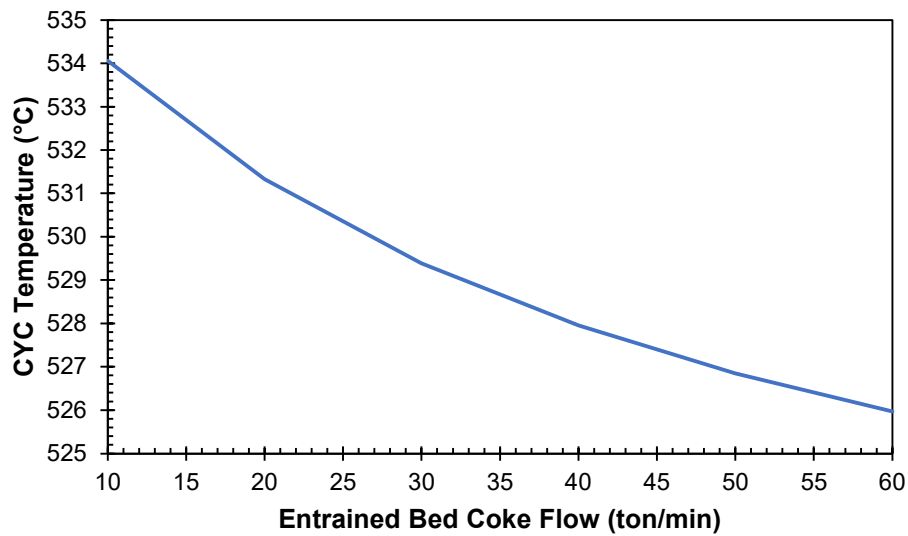


Figure 25. Cyclone temperature vs bed coke entrainment rate. Reducing entrained coke improves the ability of the hot and scouring coke lines to heat the freeboard region, resulting in an increase in cyclone temperature.

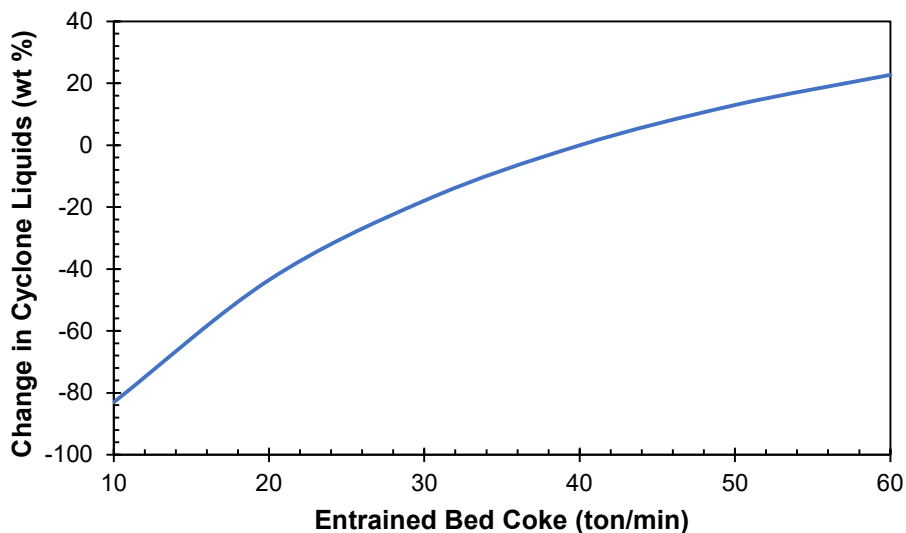


Figure 26. Change in cyclone liquids relative to the base case as a function of entrained bed coke.

3.3.6 Bed Steam Flowrate

Increasing the steam flow rate in the cyclones relative to the base case would dilute the heavy hydrocarbon vapours, shifting them away from their respective dew points. Previous work has noted the effectiveness of diluting hydrocarbons at reducing fouling on a lab scale; however, it is unknown what fraction of steam would be required to significantly reduce or eliminate cyclone fouling [6]. Increasing the volumetric flow, and in turn the fluid velocity through the cyclone could also result in a greater pressure drop. This change could further result in a greater temperature reduction due to the Ranque-Hilsch effect. To estimate the competing effects of increasing the steam flow rate on cyclone condensation, the flowrate entering from the bed was varied to up to twice the base case value.

Figure 27 demonstrates that the dilution of vapours was effective in reducing fouling, with 22 wt% less liquids in the cyclone doubling the steam flowrate. Figure 28 shows that doubling the steam flowrate did result in a larger temperature reduction of 3.6°C relative to the base case due to the increased Ranque-Hilsch cooling. Although the impact on product quality is desirable, the steam requirements to achieve a similar reduction relative to the other process levers could be a limiting factor. Furthermore, increasing the overall steam flowrate through the fluidized bed reactor could strip additional heavy

components from the coke particles, modifying the heavier hydrocarbon composition entering the freeboard region, and ultimately the cyclone. Although this study does not quantify the impact of the changed process parameters on the hydrocarbons entering BD1, further consideration should be given to the potential increase of heavy residues that would be present and their impact on cyclone fouling.

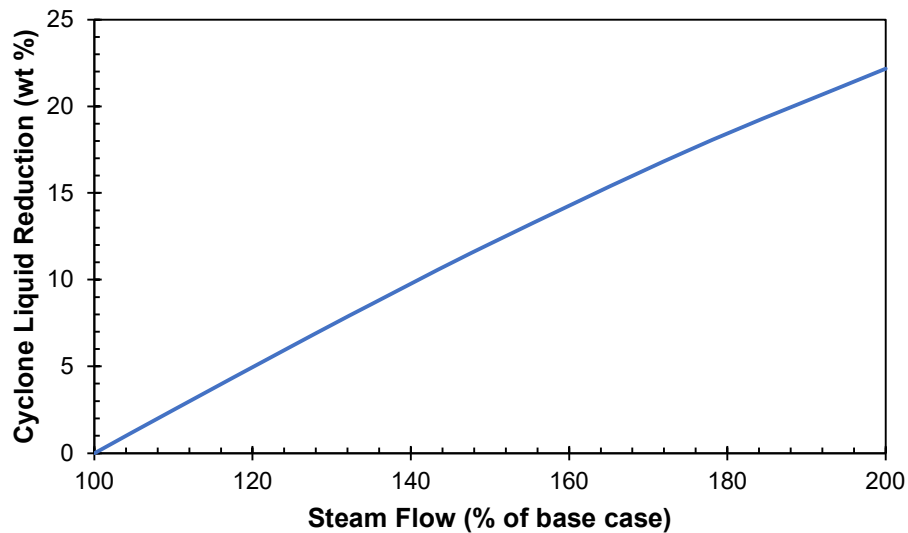


Figure 27. Reduction of cyclone liquids compared to change in bed steam flow rate relative to the base case flows.

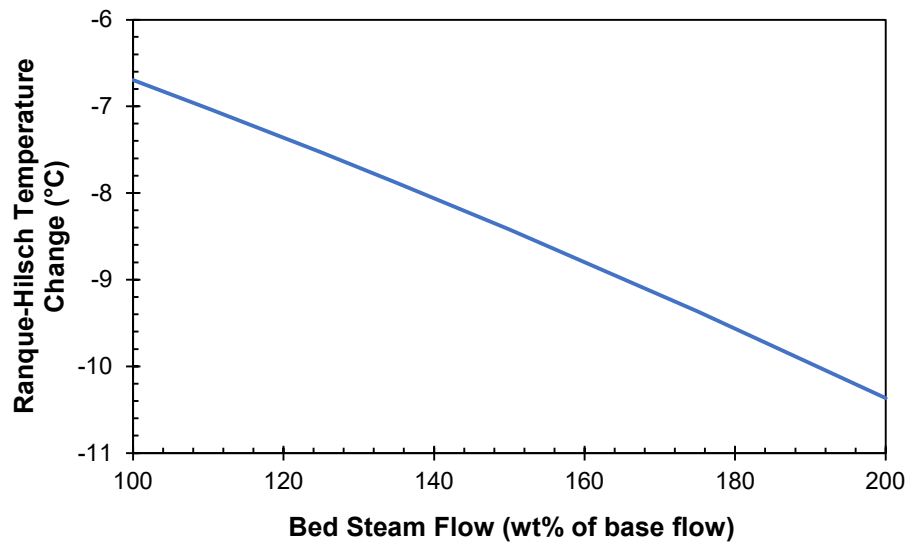


Figure 28. Impact of increased steam flowrate on the Ranque-Hilsch cooling predicted in the cyclone.

3.3.7 Case study comparison

The previous case studies illustrated the benefits in changing various process levers on reducing cyclone fouling, while also predicting the resulting vapour phase cracking in each case. In order to select the best mitigation strategy, the impact of each process lever must be compared. The change in light products and cyclone liquids relative to the base case conditions is shown in Figure 29 for the range of values tested. Increasing the bed steam was the only lever to reduce both fouling and vapour phase cracking. Although this is the desired outcome, there is only a 20% reduction in cyclone liquids relative to the base case. As the desired reduction was upwards of 80% of the base liquids, this process lever alone would not be sufficient in reducing cyclone liquids. The remaining process levers all increase the quantity of light products while reducing the cyclone liquids. Of these three conditions, increasing the scouring coke flowrate was able to achieve the desired liquids reduction with the least impact on light products. As reducing the entrained bed coke would require an increase in height between the bed and cyclone inlets, this lever would result in increased freeboard volume and residence times. Due to limitations in publicly available data, the height increase required for the reduced entrainment flux could not be approximated. Therefore, the relative increase in light products would likely be greater than those reported in this study if this additional residence time were accounted for.

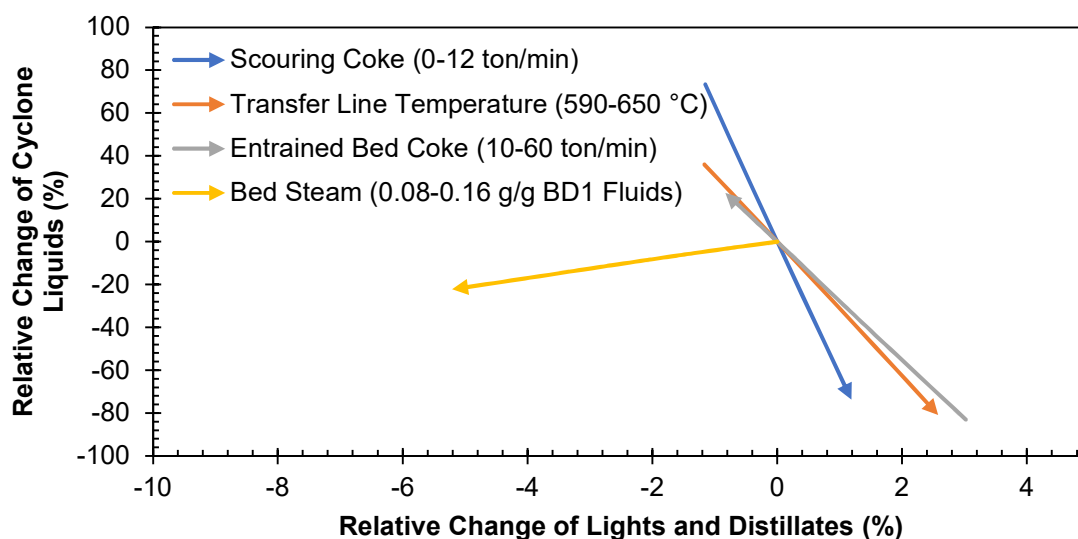


Figure 29. Comparison of the relative change of cyclone liquids and light product formation for each of the four case studies investigated. Arrows indicate the direction of

increased flow, with the upper and lower limits the extremes of the case studies as shown in Table 8

3.4 Summary

To improve Fluid Coker reliability, there is an interest to identify methods to reduce cyclone fouling to increase unit run times. A previous study by Glatt et al. modelled the freeboard region in Aspen Plus, identifying the scouring coke flow and transfer line temperatures as effective means to reduce fouling [8]. This study improved on this work by considering the impact of vapour phase cracking on product quality as well as hydrocarbon adsorption while identifying process levers to reduce cyclone fouling.

Four process levers, being scouring coke flow rate, transfer line temperature, entrained bed coke flow and bed steam flowrate were investigated in this study. Of these four variables, only increasing bed steam flow yielded the ideal result of decreasing both cyclone liquids and vapour phase cracking. However, as the liquids reduction was below the desired 75-80% relative to the base case, this factor alone would not be able to improve unit reliability. Of the remaining three factors, scouring coke flowrate achieved the desired liquids reduction with the smallest impact on over cracking vapours. Consideration should be given to increase both of these parameters to maximize the cyclone liquid reduction while minimizing the vapour phase cracking. Compared to these levers, the impact of adsorption on cyclone fouling was minimal. The increased adsorption capacity of the flexicoke did result in a minor liquids reduction compared to Fluid Coke, however it is not clear if that change would have a tangible impact on unit reliability. Further studies on preferential adsorption and kinetic estimates should be considered before the concluding whether or not adsorption can be used as a method to increase unit run times.

Chapter 4: Fluid Coker Reactor Region Model

4.1 Background Information

The Canadian oil sands consist of over 50 wt% vacuum residues, which are low value heavy hydrocarbons in their current form. To extract value from these reserves, the vacuum residues must be upgraded to synthetic crude oil, which are lighter and higher value products that can be used in traditional refinery operations. The focus of this study is on the Fluid Coker, as shown in Figure 2, which converts the residue feed via thermal cracking reactions in the absence of catalysts. The reactor operates at temperatures between 510-540°C and near atmospheric pressure, where vacuum residue is injected through six rings of nozzles and comes into contact with a fluidized bed of hot coke particles. The heat required for the endothermic cracking reactions is provided via partial combustion of coke particles in a parallel fluidized bed burner. The cracked residue products flash off the coke surface and these vapours then travel up and out of the bed through a set of 6 parallel cyclones, which send any entrained particles back to the fluidized bed. Meanwhile, coke travels downwards in the bed, where it is removed and sent to the separate fluidized bed burner unit. The burner is fed with a controlled amount of air, allowing for the partial combustion of coke that heats the particles to temperatures of 590-650°C.

Run lengths for commercial Fluid Coker units generally depend on the rate of cyclone fouling in the reactor. The parallel cyclones experience coke deposition or fouling throughout standard operation runs. Fouling within the gas outlet tubes particularly impacts the operation as this decreases the available flow area, thus increasing the pressure drop across the cyclone. The previous operating change results in a slow pressure increase within the reactor and burner regions. As a result, the air fed into the burner must be reduced due to limitations in the maximum blower power, thus reducing the available heat for the thermal cracking reactions. The feed rate is hence slowly reduced to maintain the required bed temperature. Eventually, feed rate reductions require the unit to be shut down for cleaning.

Fluid Coker cyclone fouling is primarily due to physical condensation of heavy hydrocarbon vapours. Prior work has investigated methods to mitigate this phenomenon, including work by Glatt et al. [8], and the study presented in Chapter 3. Glatt et al.

developed an Aspen Plus model of the freeboard and cyclone region of the Fluid Coker to identify the impact of key operating parameters on cyclone condensation. This model considered vapour-liquid thermodynamics, heat of liquid phase endothermic cracking and pressure changes on a series of defined control volumes [8]. The Chapter 3 study expanded this model by considering composition changes and cooling effect of vapour phase cracking as well as the impact of hydrocarbon adsorption. This study confirmed the benefit of increased scouring coke flow and transfer line temperature as predicted by Glatt et al, while predicting a small increase in light products because of vapour phase cracking. As this model was limited to the freeboard, the impact of increasing the temperature or flowrate of hot coke into the reactor bed has not been quantified.

Previous studies on vacuum residue have established kinetic models to predict thermal cracking products at conditions relevant to FLUID COKING™; however, no study has applied these kinetics to a reactor model to predict the impact of operating parameters on the Fluid Coker products. A CFD model, validated by pilot scale experiments by Song et al., studied the flow dynamics within the reactor region, observing a vapour rich core surrounded by a solid rich annulus [4]. It is not known whether this flow pattern is beneficial for reactor performance when compared to standard ideal mixing or continuous stirred tank reactor (CSTR) model. Alternatively, the gas and solid phases could act as countercurrent plug flow reactors (PFR), which may allow for cracking product vapours to be swept from the reactor with short of a residences, minimizing the vapour phase over-cracking. This study aims to develop a model of the fluidized bed reactor region that considers vapour and liquid phase cracking, vapour-liquid thermodynamics and the residence time distributions of the liquid, solid and vapours present in the Fluid Coker reactor. This study will determine the impact of varying residence time distributions and bed temperatures on the resulting product yields, in an attempt to identify the ideal flow pattern and temperature to maximize the yield of high value products and minimize light ends, coke and liquid reactants lost to the burner.

4.2 Fluid Coker Reactor Model

Modelling the Fluid Coker reaction network poses several challenges. The vacuum residue feed is a complex mixture of hydrocarbons that cannot be defined as convectional

chemical compounds. Instead, these mixtures are generally defined as assays or boiling point curves. Defining a kinetic reaction network which predicts the specific compounds from cracking residues is thus experimentally and numerically challenging. The vapour-liquid equilibrium must also be accounted for in a Fluid Coker model for key reasons. First, vaporization of the cracked products from the liquid phase coating the hot coke particles is required to transfer them to the gas phase, thus leaving the reactor through the cyclones. If not properly modeled, the products would remain as liquid coated on the coke particles and would exit to the burner and be lost. Second, the cracking products depend on whether the cracking occurs in the liquid or vapour phases, which continue as long as the hydrocarbons are exposed to the elevated reactor temperatures. It is therefore necessary to differentiate between the hydrocarbons present in each phase to apply the relevant kinetic models. Finally, the liquid-solid (i.e., coated coke particles) and vapour phases behave differently within the Fluid Coker. The liquid-solid phase has a considerably longer average residence time when compared to the vapour phase, which must be accounted when modelling the reactor. Within the vapour phase modeling, residence times also depend on the location within the bed that a given vapour is formed. For example, vapours which flash off a particle in the top ring will exit faster compared to those formed at the bottom of the reactor. This will affect the composition of the vapour phase products formed. A model of the Fluid Coker reactor must thus be able to estimate vapour-liquid equilibrium, account for the impact of changing residence times for each phase present in the reactor, and compute the compositional changes based on lumped kinetic models.

4.2.1 Residence Time Distributions

Residence time distributions (RTD) describe the probability distribution function for the time a given particle or fluid spends within a unit in a continuous flow. The RTD can be used to diagnose problems in reactor operation, or predict the effluent concentrations based on reaction kinetics [35]. In non-ideal reactors, flow patterns rarely fit an ideal CSTR or PFR RTD directly. Instead, deviations from ideal flow can be measured and quantified using tracer experiments, where a known tracer step or pulse can be injected at the reactor inlet while measuring the concentration at the exit over time. With a pulse injection, the E-Curve can be determined by normalizing the tracer exit concentration with the total amount injected, as shown in Equation 17.

$$E(t) = \frac{C(t)}{\int_0^\infty C(t)dt} \quad (17)$$

In situations where a tracer measurement is not possible or data is unavailable, it may be necessary to estimate the RTD of a real reactor mathematically. As noted by Fogler and Levenspiel, there are several methods to model the RTD of a non-ideal reactor [28,35]. An initial method involves splitting the reactor into a system of defined regions which can be approximated as an ideal CSTR or PFR. By connecting these regions in series or parallel and combining their respective RTD curves, a non-ideal reactor model can be approximated. Another approach is the one parameter tanks-in-series model which divides a given reactor volume into a series of n evenly divided CSTRs. The resulting RTD curve for the tanks in series model is as follows:

$$E(t) = \frac{t^{n-1}}{(n-1)! \tau_i^n} e^{-\frac{t}{\tau_i}} \quad (18)$$

$$\tau_i = \frac{\tau}{n} \quad (19)$$

Where n is the number of tanks, τ is the average residence time of the reactor (s), τ_i is the residence time of a given tank (s), and t is time (s). The tanks-in-series model allows for the residence time distribution to be varied between an ideal CSTR (when $n = 1$) and a PFR (when n approaches infinity). An example of the tanks in series prediction with varying tanks is shown in Figure 30. As the liquid and vapour phase have different behaviours within the reactor, RTD models will be used for these phases based on the assumed reactor geometry and operating conditions.

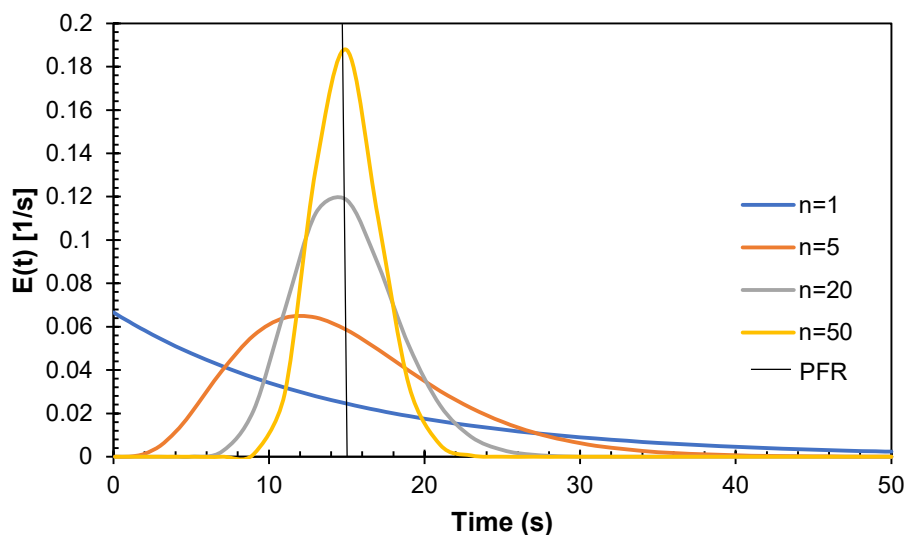


Figure 30. Residence time distributions modelled with a tanks-in-series approach for an average residence time of 15 seconds. As the number of tanks increases from 1 to 50, the model behaviour shifts from that of an ideal CSTR to an increasingly PFR like output.

4.2.2 Kinetic Equations

Reaction rate equations for the liquid and vapour phases must be defined for use with the RTDs. As discussed in Chapter 3, lumped kinetic models have been developed by Gray and Radmanesh that predict the conversion of vacuum residues at FLUID COKING™ conditions [25,26]. Radmanesh's model improved the work by Gray by defining the coke formation mechanism and identifying separate activation energies for the heavy and light residues, which had previously been assumed to be equal [26]. The kinetic model proposed by Radmanesh is illustrated in Figure 31. This model estimates intrinsic coke formation from the heavy residue fraction, which is the result of large aromatic cores in the feed that cannot thermally crack or vaporize. Radmanesh showed that the intrinsic coke forming fraction can be approximated as 26 wt.% of the heavy residue fraction. The heavy residue fraction will thus be split into two components when defining variables for the kinetic equations: the first which undergoes cracking reactions, and a second which forms intrinsic coke. The reaction equations based on the kinetic network shown in Figure 31 are shown in Equations 20 - 23 with updated stoichiometry used in this study, while the rate constant for each first order reactions are based on the Arrhenius equation, with the parameters summarized in Table 10.

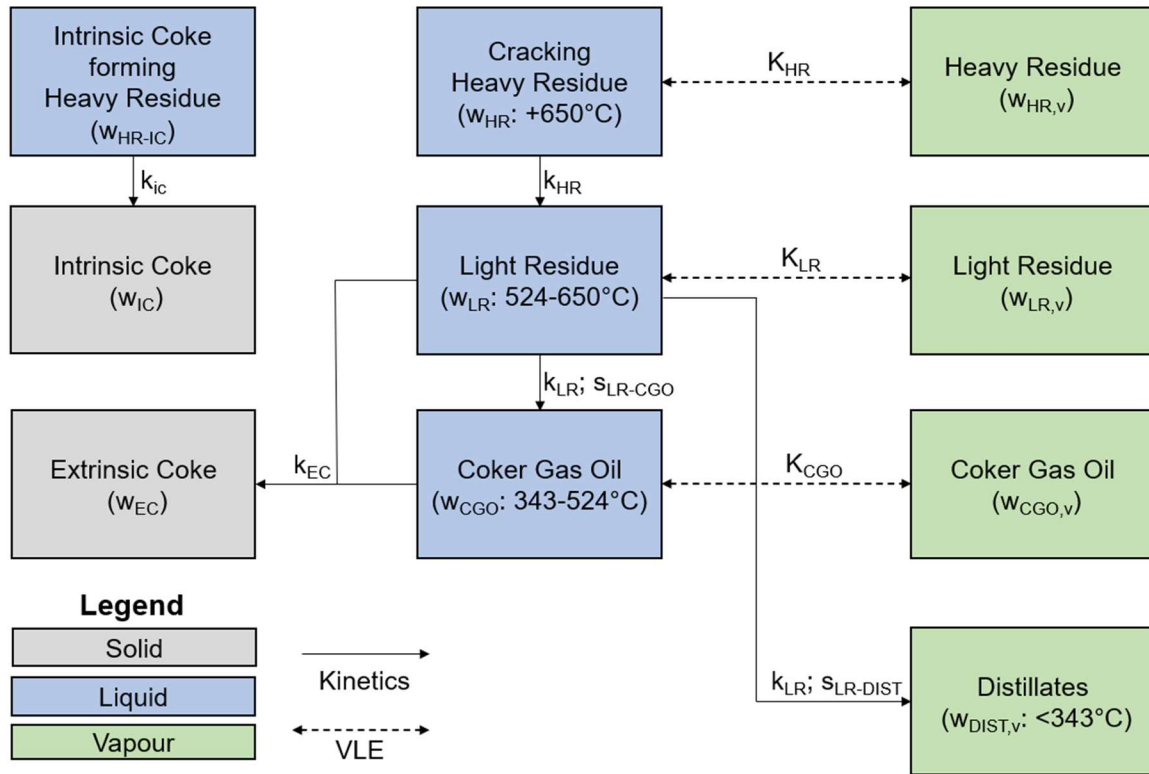


Figure 31. Thermal cracking reaction network diagram based on the weight fraction of each lump, modified from Radmanesh [26]. Stoichiometry (s_{ij}) and first order reaction rate constants determined with Arrhenius constants as presented by Radmanesh, while equilibrium values (K) estimated based on Aspen Plus estimates.

Table 10. Arrhenius constants for the liquid phase cracking reactions [26].

Kinetic Constant	Activation Energy (kJ/mol)	logA (s ⁻¹)
k_{HR}	230	14.0
k_{LR}	188	11.0
k_{IC}	33.7	1.0
k_{EC}	99.6	5.0

$$\text{Intrinsic Coke forming Heavy Residue} \rightarrow \text{Intrinsic Coke} \quad (20)$$

$$\text{Heavy Residue} \rightarrow \text{Light Residue} \quad (21)$$

$$\text{Light Residue} \rightarrow 0.7\text{Coker Gas Oil} + 0.3\text{Distillates} \quad (22)$$

$$\text{Light Residue} + \text{Coker Gas Oil} \rightarrow \text{Extrinsic Coke} \quad (23)$$

Radmanesh's model also accounted for the impact of film thickness on the liquid side mass transfer via a mass transfer coefficient that varies with time. As the impact of film thickness on the coke particles is outside the scope of this study, a simplified approach assuming thin films with negligible liquid side mass transfer resistance, similar to Gray's study, will be applied [25]. Light ends and distillates are also assumed to immediately flash into the vapour phase, due to their high volatility compared to the remaining hydrocarbon components. The mass transfer coefficient reported by Gray and equilibrium ratios for each of the hydrocarbon lumps, as estimated by Aspen Plus, are shown in Table 11. Inputting the assays defined in Chapter 3 into Aspen Plus, the equilibrium ratios at each temperature were reported using the Peng-Robinson equation of state. The values estimated by Aspen Plus were between those reported by Gray and Radmanesh in their respective studies.

Table 11. Equilibrium Values for the heavy residue, light residue and coker gas oil fractions as predicted by Aspen Plus. Mass transfer coefficient as reported by Gray is assumed to be independent of temperature and constant for all fractions [25].

Temperature (°C)	515	520	525	530	535
K_{HR}	0.0163	0.0185	0.0209	0.0236	0.0266
K_{LR}	0.2534	0.2753	0.2985	0.3233	0.3495
K_{CGO}	1.8149	1.9028	1.9926	2.0840	2.1768
k_{Ga} [1/s]	3.80				

The change in each mass fraction shown in Figure 31 is the result of thermal cracking kinetics and the mass transfer from the liquid to vapour phase. Similar to the equations presented by Gray and Radmanesh in their respective studies, the system of kinetic equations for the liquid phase cracking is presented in Equations 24 - 33. Both previous studies assumed no hydrocarbons were present in the vapour phase as the flashed vapours were immediately swept by an inert gas [25,26]. This simplification cannot be made when modelling the commercial Fluid Coker as the products are present in the gas phase after vaporizing, reducing the driving force for product vaporization. As such, the vapour fraction, y_i , is included in each rate equation.

$$r_{HR} = \frac{dw_{HR}}{dt} = -k_{HR}w_{HR} - k_G a(K_{HR}x_{HR} - y_{HR}) \quad (24)$$

$$r_{HR-IC} = \frac{dw_{HR-IC}}{dt} = -k_{IC}w_{HR-IC} \quad (25)$$

$$r_{LR} = \frac{dw_{LR}}{dt} = k_{HR}w_{HR} - k_{LR}w_{LR} - \frac{k_{EC}w_{LR}w_{CGO}}{2} - k_G a(K_{LR}x_{LR} - y_{LR}) \quad (26)$$

$$r_{CGO} = \frac{dw_{CGO}}{dt} = 0.7k_{LR}w_{LR} - k_{CGO}w_{CGO} - \frac{k_{EC}w_{LR}w_{CGO}}{2} - k_G a(K_{CGO}x_{CGO} - y_{CGO}) \quad (27)$$

$$r_{IC} = \frac{dw_{IC}}{dt} = k_{IC}w_{HR-IC} \quad (28)$$

$$r_{EC} = k_{EC}w_{LR}w_{CGO} \quad (29)$$

The resulting vapour phase formation rates are defined as:

$$r_{HR,v} = \frac{dw_{HR,v}}{dt} = k_G a(K_1x_1 - y_1) \quad (30)$$

$$r_{LR,v} = \frac{dw_{LR,v}}{dt} = k_G a(K_{LR}x_{LR} - y_{LR}) \quad (31)$$

$$r_{CGO,v} = \frac{dw_{CGO,v}}{dt} = k_G a(K_{CGO}x_{CGO} - y_{CGO}) \quad (32)$$

$$r_{DIST,v} = \frac{dw_{DIST,v}}{dt} = 0.3k_{LR}w_{LR} \quad (33)$$

The previous set of equations will determine the change in liquid and vapour products composition over time due to the liquid phase cracking reactions. It should be noted that once a component flashes to the vapour phase, no additional cracking is modelled in this set of reactions. The vapour composition exiting the liquid phase is assumed to be the initial feed for the vapour cracking reactions for the given control volume. The vapour phase cracking reaction rates are based on the same premise as Chapter 3. As such, the Radmanesh kinetics will be applied for the heavy and light residue fractions with the predicted products being light gases [26]. Once again, the Bu kinetics will be applied to the vapour phase cracking for the coker gas oil fraction [27]. Although the distillate fraction would be expected to crack to form light ends, there is no relevant kinetic study available to model this reaction. A preliminary estimate will apply the same kinetics as the coker gas oil to the distillate fraction. The ratio of lights to distillates, previously assumed to be 1:3, was reviewed when establishing the model base case and will be entirely

lights for this study, as shown in the reaction Equations 34 - 37. Without this change in stoichiometry, the predicted light gases were significantly lower than the reported commercial products, while consistently over predicting the distillate fraction. The vapour phase reaction network and parameters are shown in Figure 32. Although partial pressure is typically more representative of vapour phase kinetics than mass fraction, the rate equations for vapour phase cracking are estimated on a mass basis to reduce model complexity. The resulting rate equations for each mass fraction are defined in Equations 38 - 42:



$$r_{HR,p} = \frac{dw_{HR,p}}{dt} = -k_{HR}w_{HR,p} \quad (38)$$

$$r_{LR,p} = \frac{dw_{LR,p}}{dt} = -k_{LR}w_{LR,p} \quad (39)$$

$$r_{CGO,p} = \frac{dw_{CGO,p}}{dt} = -k_{CGO}w_{CGO,p} \quad (40)$$

$$r_{DIST,p} = \frac{dw_{DIST,p}}{dt} = -k_{CGO}w_{DIST,p} \quad (41)$$

$$r_{lights} = \frac{dw_{lights}}{dt} = k_{HR}w_{HR,p} + k_{LR}w_{LR,p} + k_{CGO}w_{CGO,p} + k_{CGO}w_{DIST,p} \quad (42)$$

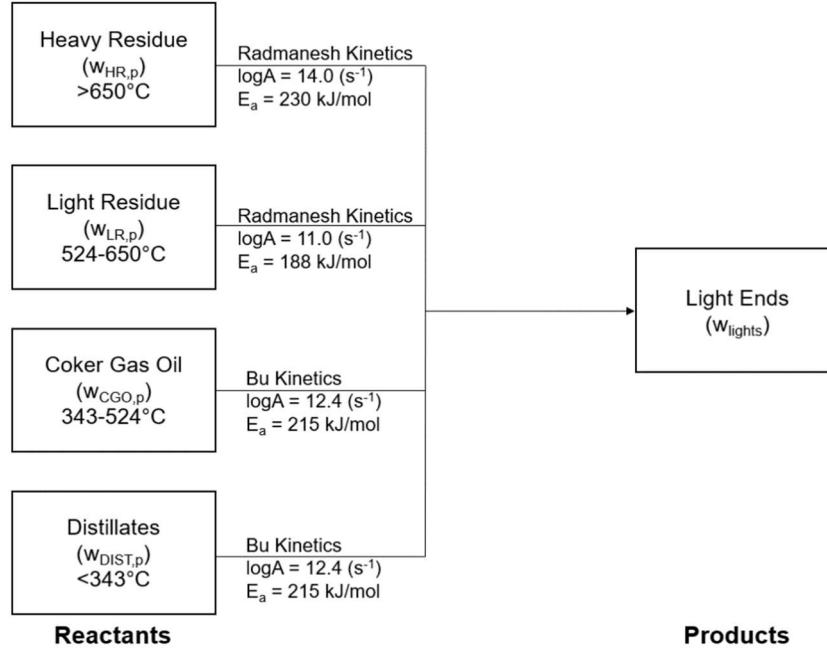


Figure 32. Vapour Phase Reaction model, including kinetic parameters.

4.2.3 Application of RTD and Rate Equations

With the RTD and rate equations defined, a method to model the conversion as a function of these two parameters is required. When the liquid phase residue enters the reactor, it contacts the solid coke particles, creating a thin film where cracking reactions occur. The liquid feed remains on these particles until it flashes into the vapour phase after cracking. These residue films are assumed to not interact with one another after entering and are thus considered segregated from one another. As such, we consider flow through the reactor as a series of volumes which do not interact with other particles and remain isolated throughout their residence time in the reactor. Each volume acts as an individual batch reactor which spends a specified amount of time reacting. Knowing the RTD for the liquid phase, the time that feed fraction spends within the reactor is known. Using the initial feed composition and rate equations, the products composition after a given time can be determined. The products concentration can thus be determined based on the RTD and component concentration at that time by integrating over the entire RTD time interval for each component, as follows:

$$\bar{C}_i = \int_0^{\infty} C_i(t)E(t)dt \quad (43)$$

As the rate equations defined based on the Radmanesh kinetics are in terms of weight fraction rather than concentration, we can convert the previous equation to an average mass flow by multiplying by the feed rate for the control volume:

$$\overline{m}_i = \int_0^{\infty} \dot{m}_{in} w_i(t) E(t) dt \quad (44)$$

Where \overline{m}_i is the average mass flow [kg/s] of component i exiting the reactor, \dot{m}_{in} is the total inlet mass flow rate [kg/sec], w_i is the mass fraction of the component at a given time [kg/kg], and $E(t)$ is the fraction of the inlet feed exiting at a given time [s^{-1}]. The total mass of coke formed and remaining liquids are sent to the next control volume or exit the reactor to be sent to the burner, while vapour products are set as the initial composition of the subsequent control volume for the vapour cracking calculations. The same concept is applied to the vapour cracking while considering that vapours formed lower in the bed will reside in the reactor longer than those formed at the top. Varying RTDs will be applied to the vapours formed in each ring, allowing for this parameter to be considered.

4.3 Software Selection

An appropriate software package must be chosen to implement the necessary reaction kinetics, RTD estimates and VLE method. Aspen Plus and HYSYS have previously been used to model the scrubber and freeboard regions of the Fluid Coker. Aspen has been shown to be effective at the required VLE calculations, successfully matching operational data shown by Jankovic [20]. Although Aspen Plus was effectively used for vapour phase cracking in Chapter 3 through the Excel add-in, the liquid phase reactions are not easily solved in the same manner. Due to the complexity of the liquid phase reaction network, numerical integration techniques are required to solve. As Excel does not have a numerical differential equation solver built in, it would be challenging to model the reactor in Aspen Plus. Alternatively, Aspen HYSYS can react assays as the software splits hydrocarbon assays into a series of smaller pseudo-components which represent hydrocarbons between a set of boiling points. The boiling point ranges represented by the pseudo-components are significantly smaller than those shown in the lumped kinetics. Although this increases the accuracy of the VLE calculations, implementing the lumped kinetic model would be challenging as the kinetics would need to be converted to the correct units and individually applied to each pseudo component.

With over 60 pseudo components used for the studied hydrocarbon residue, converting and applying the kinetics limits this simulation method. Furthermore, applying non-ideal or complex residence time distributions in both Aspen Plus and HYSYS presents another challenge. A series of ideal CSTR and PFRs could be used to estimate deviations from ideal flow; however, each additional CSTR or PFR added in the liquid or vapour increases the model complexity and computational demand. An alternative modelling method that allows for the lumped kinetic model to be applied while considering vapour liquid equilibrium and various residence time distributions is therefore required.

MATLAB is a programming platform that that can be used for data analysis, graphing and complex numerical computation. MATLAB is highly customizable, allowing for the development of a model that will consider the rate equations, VLE predictions, and application of user defined residence time distributions. MATLAB also contains built in ordinary differential equation solvers that allow for the solution of the rate equation network. ODE45 and ODE23s are two ordinary differential equation solvers based on the Runge-Kutta method. By providing the initial composition of the feed entering the reactor, rate laws can determine the change in each of the defined weight fractions over time while accounting for the flashing of components to the vapour phase. Once the liquid phase cracking products are determined, a second set of initial conditions using the flashed products can be established before applying the vapour phase kinetic equations. This determines the product distribution exiting the cyclone gas outlet tube for a given injection ring. Vapour residence times will differ depending on the ring being modelled and will include the freeboard region in each case. Any components that remain in the liquid phase after the first ODE solver are assumed to remain on the coke particles as they travel to the next region of the reactor, where they are re-coated with fresh feed. This process is repeated for each ring in the reactor. By summing the vapour products from all six rings, the total products exiting the cyclones can be determined. Any liquid remaining after the bottom ring is assumed to be sent to the burner and lost. The previous approach is illustrated in the block flow diagram shown in Figure 33.

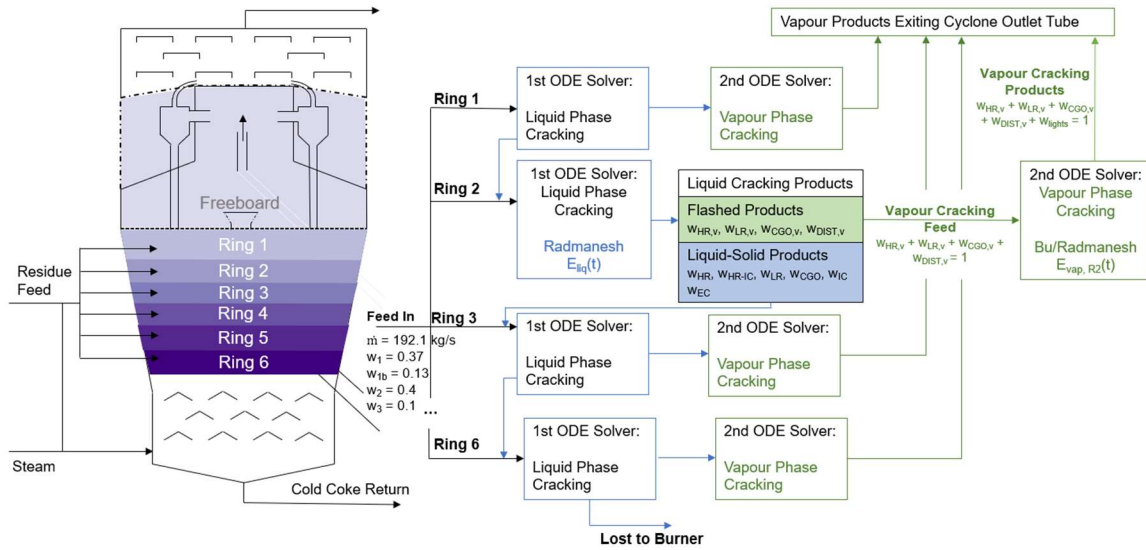


Figure 33. Schematic of Fluid Coker reactor (left) and proposed MATLAB model block flow diagram (right), with detailed schematic of Ring 2. Fresh liquid feed of a known composition enters a given ring, where liquid and vapour cracking reactions are applied using a series of ODE solvers, with vapour products exiting the cyclone, while liquid products carry on down to next ring.

4.4 Base Case Conditions

The model requires the physical characteristics of the reactor, operating conditions and inlet compositions to predict the outlet flows. These parameters are used to determine the average residence time in each ring, and provide the initial conditions required for the ODE solver to compute the cracking reactions. To simplify the calculations, the reactor bed will be assumed isothermal, with a base case temperature of 525°C.

4.4.1 Fluid Inputs

The vacuum residue feed is composed of heavy residue, light residue and coker gas oil, based on the mass distribution shown in Table 12. The heavy residue must be split between the highly aromatic fraction, which does not crack and forms intrinsic coke, and the less aromatic fraction which undergoes thermal cracking. The distribution between these two fractions is based on data presented by Radmanesh [26]. The total hydrocarbon feed for the Fluid Coker is assumed as 762.3 ton/h or 192.1 kg/s, based on Gray [3]. This flowrate represents the total flow entering the reactor, which will be either a single input or distributed between each of the rings as required.

Table 12. Composition of vacuum residue feed to the Fluid Coker [26].

Component	Mass Fraction
Intrinsic Coke Forming Heavy Residue	0.13
Cracking Heavy Residue	0.37
Light Residue	0.4
Coker Gas Oil	0.1

In addition to the residue, steam is injected through the nozzles to assist in the atomization of the feed. Steam is also used in the stripper section at the bottom of the reactor to remove hydrocarbons still coating the coke particles and assist in the fluidization of the bed. Based on the Exxon FLUID COKING™ patent, the steam injected into the coking and stripping zones of the reactor can range between 5 to 30 wt% of the liquid hydrocarbon feed, with typical values between 6 and 15 wt% [14]. A steam flowrate equal to approximately 10 wt% of the liquid hydrocarbon feed was used in the model. The residue-steam mixture the feed nozzles ranges from 25-80 vol% steam. The steam flowing through each nozzle was approximated based on the volumetric flowrate of steam at an intermediate value between those listed in the patent, with the remaining being assumed to enter through the stripper. The steam is assumed to travel upwards through the bed, therefore the steam in a given region is equal to the steam entering through its nozzle, as well as all regions below it in the reactor. As the specific steam flowrates were chosen based on input from Syncrude, specific flowrates cannot be presented.

4.4.2 Average Residence Time Estimates

The average residence time through each region of the model will impact their RTD. The average residence times will be different for the vapour and liquid-solid phases and must be estimated based on their respective volumetric flows through each region. The reactor region will be split into 6 control volumes, one around each nozzle, as shown in Figure 33. Based on the geometry of the 1/20th pilot scale model reported by Song, the reactor geometry can be approximated for the commercial reactor [4]. This allows for the total volume and cross-sectional area for flow around each nozzle to be estimated. This study also found an average voidage in the pilot scale system of 0.6. Therefore, 40% of the

total volume is occupied by the solid phase, with the remaining volume occupied by the vapour phase as summarized in Table 13.

Table 13. Volume of each control volume for the commercial reactor based on dimensions of 1/20th scale lab model [4].

	Total Volume [m ³]	Solid Volume [m ³]	Vapour Volume [m ³]
Ring 1	231.7	92.7	139.0
Ring 2	203.2	81.3	121.9
Ring 3	176.7	70.7	106.0
Ring 4	152.0	60.8	91.2
Ring 5	129.1	51.7	77.5
Ring 6	108.2	43.3	64.9

The average vapour residence time was first estimated using the typical vapour velocity at the bottom and top of the bed as 0.3 and 1 m/s (1 ft/s to 3.5 ft/s), respectively [14]. Assuming a linear change in velocity through the bed, the resulting velocity at each ring and ultimately residence time in each control volume can be determined as follows:

$$\tau_i = \frac{V_{i,vap}}{u_i A_i} \quad (32)$$

Where for a given control volume, $V_{i,vap}$ is the volume of the vapour phase [m³], u_i is the superficial gas velocity (m/s), and A_i is the cross-sectional area [m²]. Average residence times are summarized in Table 14. The average residence time in the freeboard region was estimated based on proprietary geometries, as used in the freeboard model presented in Chapter 3. It should be noted that vapours formed in the lower regions of the bed then travel upwards through all regions in the bed before exiting through the cyclones. The average residence time for vapours formed in a given ring is thus given by the cumulative time spent in that ring plus all regions downstream until reaching the cyclone outlet.

Table 14. Average residence time of each reactor control volume.

Region	Residence time by Region	
	Residence time within region [s]	Cumulative before exiting [s]
Freeboard	6.2	-
Ring 1	1.9	8.1
Ring 2	2.1	10.2
Ring 3	2.3	12.5
Ring 4	2.5	15
Ring 5	2.8	17.8
Ring 6	3.2	21

For the solid phase, the total coke flow entering the top of the fluidized bed reactor is 66 tonne/min, which includes the hot coke and scouring coke transfer lines. Based on the coke density, and volume for the solid phase, the average residence time through each ring control volume was approximately 100 seconds, or a total of 10 minutes for the entire reactor.

4.4.3 Reaction Products and Stoichiometry

The products leaving the Fluid Coker range from light permanent gases to heavy hydrocarbon compounds with normal boiling points exceeding 650°C. The distribution between these different components will be predicted by the kinetic model; however, the composition of the actual product is necessary to validate the estimates of the kinetic model. Gray reported the yield of coke in a typical Fluid Coker was 21.7 wt% of the hydrocarbons fed [3]. The study published by Jankovic provided an assay of the products exiting the Fluid Coker cyclone. This boiling point curve was used to estimate the distribution between each boiling point lump, shown in Table 15. The stoichiometry in Radmanesh's reaction network specifies that 20 wt.% of the light residue cracked in the liquid phase forms CGO, with no other reaction yielding CGO as a product. Based on these parameters, it would not be possible to predict the product distribution shown in Table 15. The stoichiometry of the reaction network was thus modified to obtain a more comparable product distribution, with the modified coefficients summarized in Table 16. The Arrhenius constants used to determine the reaction rate as a function of temperature are unchanged, as shown in Table 10.

Table 15. Composition of product exiting the Fluid Coker based on data reported by Jankovic [20].

Component	Mass fraction (wt.%)
Lights	25
Distillates	16
Coker Gas Oil	44.5
Light Residue	10.5
Heavy Residue	4

Table 16. Liquid phase reaction stoichiometry used in each case study.

Stoichiometric Coefficient	Radmanesh [26]	Modified
S_{HR-LR}	1	1
S_{HR-CGO}	0	0
$S_{HR-DIST}$	0	0
S_{LR-CGO}	0.2	0.7
$S_{LR-DIST}$	0.8	0.3

When considering the vapour phase cracking kinetics established in Chapter 3, it was found that the light products were underpredicted compared to Jankovic's results, due to an over prediction of the distillate fraction. This was attributed to the assumption that vapour phase cracking products were split between the light and distillate fractions. Jankovic showed the light ends were a significant portion of the Fluid Coker product, comprising 25 wt.% of the vapours exiting the cyclones. As the only way for lights to be formed is through vapour phase cracking, this study will model light ends as the only product formed from vapour phase cracking, allowing for a better alignment with Jankovic's results.

4.5 Results and Discussion

4.5.1 Basic CSTR Model

The reactor model was first implemented assuming the reactor behaved like an ideal CSTR. This model considered the entire reactor region as a well mixed CSTR, where the solid-liquid phase (i.e., the residue coated coke particles) had an average residence time of 600 seconds. The vapour phase was modelled with an average residence time of 15 seconds, based on the parameters shown in Table 14. Figure 34 provides the predicted liquid and flashed vapour mass fractions when modelling the solid-liquid phases. Based on

the liquid phase cracking, it is observed that the only component left in the liquid phase, with sufficient time to crack, is the solid coke formed. Meanwhile, CGO is the primary component flashed to the vapour phase, along with some light residue and distillates, and negligible heavy residue. It should be noted the data in Figure 34 are the mass fractions based on the combined liquid and vapour phases, as such the sum of the mass fractions from both plots will be 1.

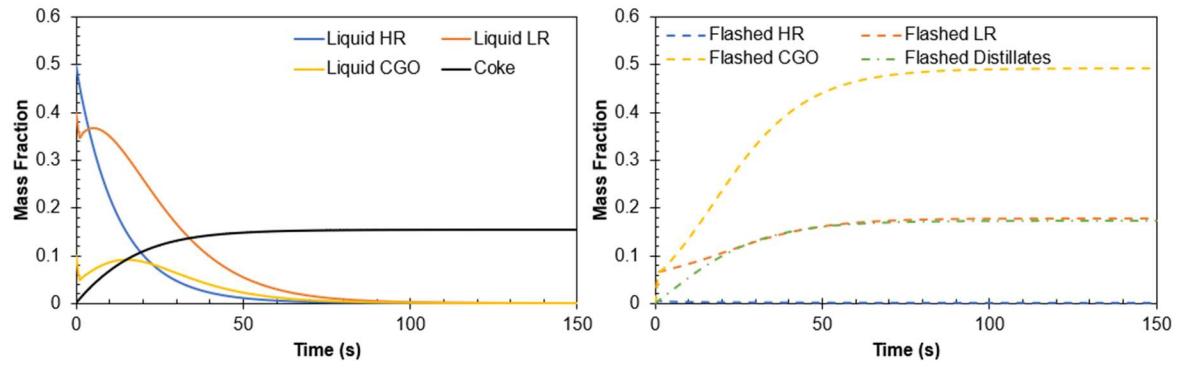


Figure 34. Resulting liquid and vapour phase products as a function of time due to liquid phase cracking of residue feed. The left plot reflects the remaining liquid film and solids formed from the initial residue feed, while the right shows the increasing vapours composition over time.

Using the mass fractions determined from the liquid phase reaction rates, in conjunction with the ideal CSTR RTD, the initial composition of the products entering the vapour phase can be estimated. These conditions are used with the vapour phase rate equations, yielding the product distribution over time shown in Figure 35. As expected, increasing the reaction time increase the yield of light products, at the expense of the other hydrocarbon fractions.

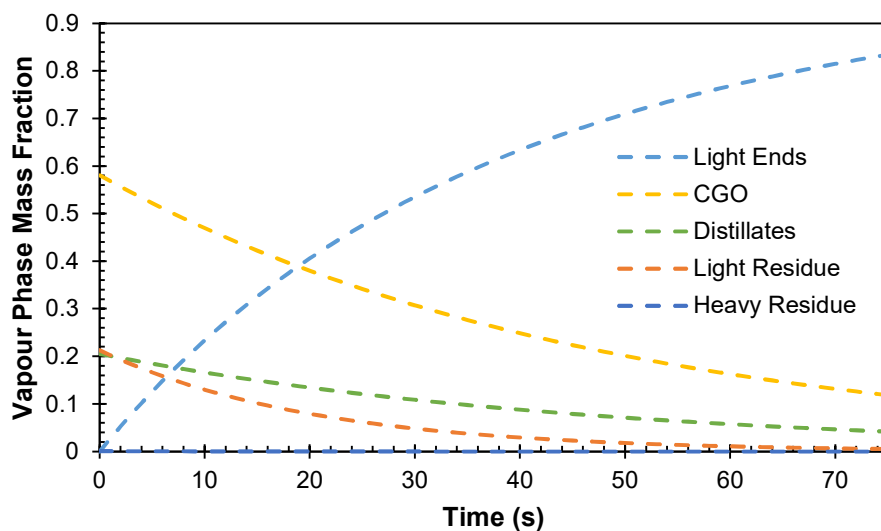


Figure 35. Change in predicted hydrocarbon fractions over time as a product of vapour phase cracking.

Figure 34 and Figure 35 show the predicted hydrocarbon compositions as a function of time based on the defined rate equations. Nonetheless, the actual composition of the hydrocarbons exiting the reactor via the cyclone gas outlet tubes depend on their respective residence times. By applying the ideal CSTR RTD equation to both the liquid and vapour phases, the resulting product distribution is shown in Figure 36. A high vapour product yield is observed for the ideal CSTR reactor model. The vapours exit the top of the reactor through the cyclone outlet tubes, whereas the liquid and coke products are sent to the burner. The predicted vapour composition aligns well with the vapour composition seen exiting the commercial Fluid Coker reported by Jankovic [20]. A comparison of this model and the Jankovic data is shown in Table 17. Although the composition of vapours closely matches Jankovic, the total yield of vapour products is predicted to be nearly 80 wt.%, compared to a typical commercial yield of 70 wt.% [3]. The increased vapour products yield comes at the expense of coke formation, where the simple CSTR model predicts a yield of approximately 15 wt.%, compared to 20-30 wt.% seen commercially [3].

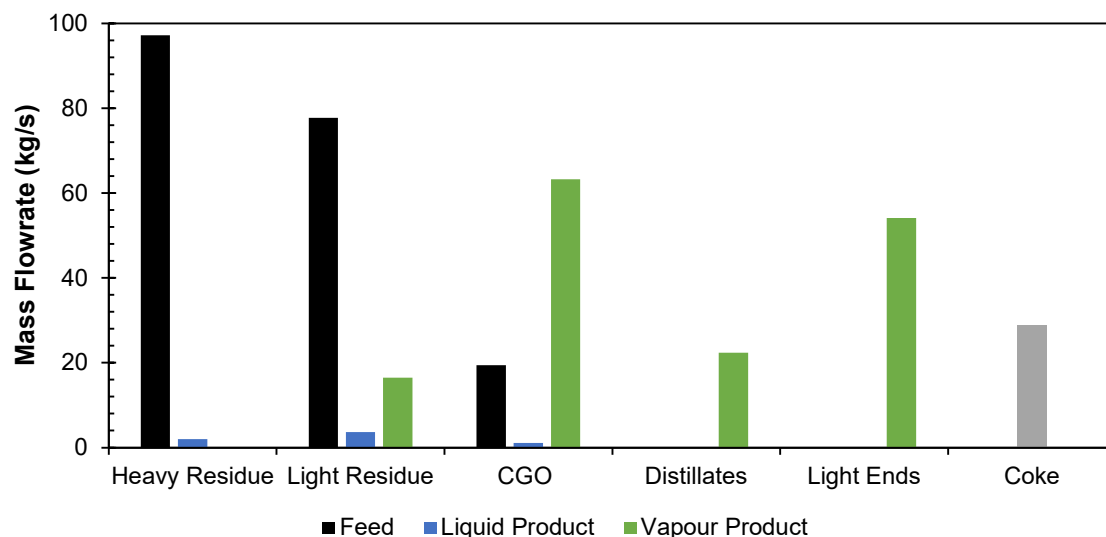


Figure 36. Predicted mass flowrates of hydrocarbon lumps for a two-phase ideal CSTR Fluid Coker model. Cracking reactions converted the feed into lighter fractions, with CGO, light ends and distillates dominating the final composition. Minimal products remained in liquid phase lost to the burner, while CGO, light gases and distillates dominate the vapour product.

Table 17. Composition of the vapour products exiting the single CSTR Fluid Coker Model. Overall, model shows a reasonable alignment with operational data, providing an initial baseline to compare further models against.

	Jankovic wt %	MATLAB Single CSTR wt%
Heavy Residue	4	0.04
Light Residue	10.5	12.3
Coker Gas Oil	44.5	44.3
Distillates	16	15.7
Light Ends	25	27.7

The low coke yield observed in the single CSTR may be the result simplifying assumptions. For example, the long average residence time (600 s) used for the liquid-solid phase in the simplified model provides a significant amount of time for liquid films to crack and leave as vapours. Reducing the residence time by splitting the reactor into smaller regions, while also adding fresh feed throughout the reactor, could increase the coke yield. These changes would provide less time for liquid phase cracking to occur, potentially increasing the fraction that remains in the liquid phase after exiting the reactor. Any

remaining liquid fraction would be coated with fresh feed when introduced to another ring, increasing the quantity of hydrocarbons present in the liquid phase and allowing for more extrinsic coke to form.

4.5.2 Reactor Ring Model

The next model considered split the reactor region into six control volumes based on each feed injection nozzle, as shown in Figure 33. The liquid phase residence time within each control volume was approximated at 100 seconds, while the vapour produced in each ring will have the cumulative residence time shown in Table 14. The previous model assumed each phase was an ideal CSTR; however, it is unknown whether this is preferred configuration for the Fluid Coker based on the products distribution. Therefore, a tanks-in-series approach will be used to vary the flow behaviour between an ideal CSTR and an increasingly PFR like flow pattern.

First, the tanks-in-series model was applied to the liquid phase while maintaining the vapour phase as a CSTR. By maintaining the vapour phase as a CSTR, the impact of changing liquid-solid residence time distribution can be evaluated. The products exiting the Fluid Coker reactor in the liquid, vapour and solid phases are presented in Figure 37, with the liquid-solid region modelled as 1, 5 and 50 tanks in series. Compared to the single CSTR model, the multi-ring configuration yields similar results regardless of the number of tanks-in-series used. Despite the previous hypothesis about transferring unreacted liquids to subsequent rings, the coke yield was lower in the multi-ring model, ranging between 14.0-14.3 wt.%, when compared to the single CSTR at 15.1 wt.%. Furthermore, as the number of tanks increased, the liquid lost to the burner decreased, corresponding with a marginal increase in vapour products. The overall mass fraction distribution between the vapour products remained relatively unchanged as shown in Figure 38. This suggests that for the residence times seen by the liquid-solid phase, the liquid-solid RTD has a minimal impact on the reactor product composition.

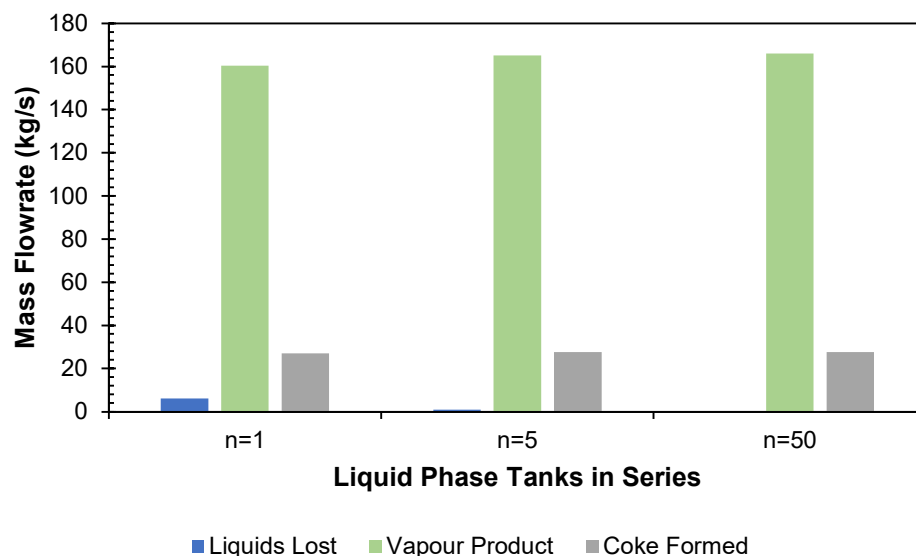


Figure 37. Product distribution between solids and liquids exiting bottom of reactor and vapours exiting top when modelling liquid-solid phase as the tanks-in-series approximation with 1, 5 and 50 tanks.

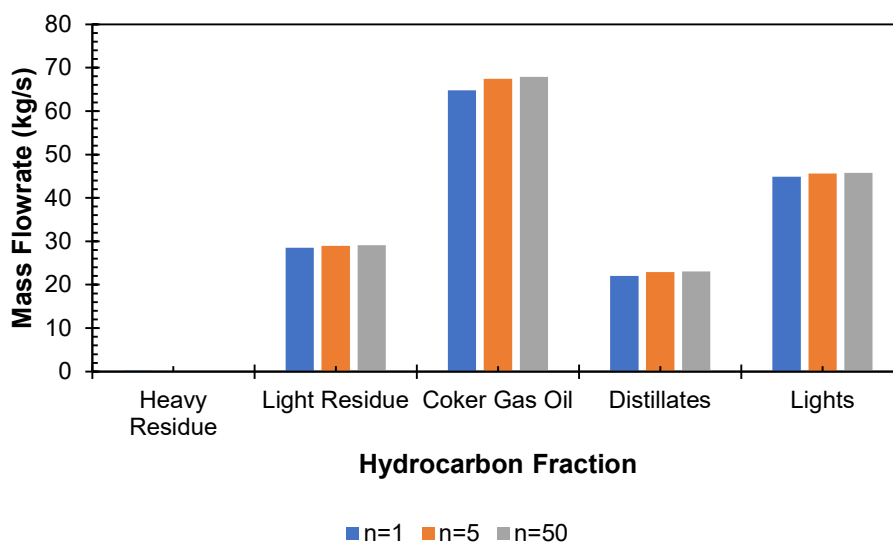


Figure 38. Composition of the vapour phase products when modelling the liquid-solid phase as the tanks-in-series approximation with 1, 5 and 50 tanks.

The subsequent case study investigates the impact of the vapour phase residence time distribution on Fluid Coker products. As the vapours exiting a given ring are modelled as a CSTR with an average residence time matching the cumulative times listed in Table 14, we can apply the tanks in series approximation to simulate an increasingly plug flow behaviour. The impact of the tanks-in-series approach on the residence time distributions

of these regions is shown in Figure 39. As the liquid-solid phase remains constant as a single CSTR for each ring, the predicted coke yield and liquids remained constant, as depicted by the $n = 1$ case in Figure 37. The resulting increase in light products with increasing the number of tanks-in-series is shown in Figure 40. When the vapours follow an RTD comparable to an ideal CSTR, a fraction leaves immediately without cracking. As the flow shifts towards that of a PFR, this “by-passing” fraction is reduced or removed, which results in vapour phase residing in the reactor to continue crack. Comparing this case study to the vapour product distribution shown in Jankovic, an increasing number of tanks-in-series shifts the lights, distillates, and CGO fractions further from the reported operating data.

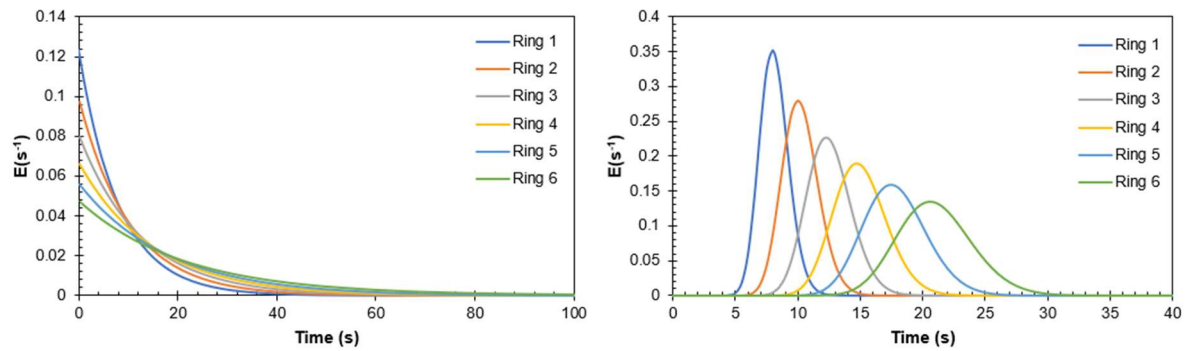


Figure 39. Comparison of ideal CSTR model (left, $n=1$) and tanks in series (right, $n=50$) on vapour phase residence time distribution for products of each ring before exiting the cyclone outlet tube.

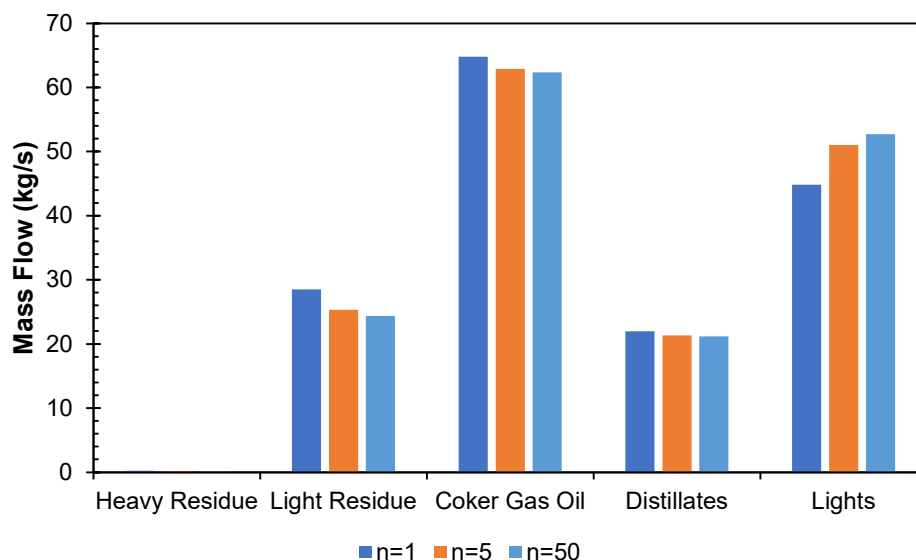


Figure 40. Composition of vapour products with varying tanks-in-series for the vapour phase components.

Table 18. Vapour composition of the tanks-in-series vapour phase compared to operational data reported by Jankovic [20].

Component	Jankovic wt%	n=1 wt%	n=5 wt%	n=50 wt%
Lights	25	28.0	31.7	32.8
Distillates	16	13.7	13.3	13.2
CGO	44.5	40.4	39.1	38.8
LR	10.5	17.8	15.8	15.2
HR	4	0.13	0.10	0.09

4.5.3 Complex Vapour Residence Time

The RTD for vapours formed in a given ring has so far been estimated by summing the residence times of each control volume from the given ring to the reactor outlet. With the average residence time, the vapour phase was either treated as a CSTR or with a tanks-in-series approximation for CSTR's of varying sizes based on the specific ring. Assuming the vapour phase is well mixed in the bed region is a reasonable assumption due to the highly turbulent nature of the fluidized bed. Once the vapours enter the freeboard, however, the flow characteristics may be more plug flow in nature. As such, a more accurate RTD

for the vapour phase could be considered based on a system of CSTRs and PFRs in series. Considering the Fluid Coker reactor freeboard region, the flow through the BD1 and CTR control volumes was modelled as ideal PFRs, assuming the lack of new feed or mixing would result in plug flow. Conversely, the introduction of the hot and scouring coke would result in well mixed regions for BD2 and the horn chamber, with the both regions and the cyclone modelled as an ideal CSTR. Similarly, each reactor ring was modelled as an ideal CSTR, as shown in Figure 41. Based on the resulting transfer functions for a pulse input in each ring, the residence time distributions for the vapours formed in each ring can be solved. This work was completed in collaboration with an undergraduate thesis student, Niall Murphy, with the resulting RTDs for each ring shown in Figure 42.

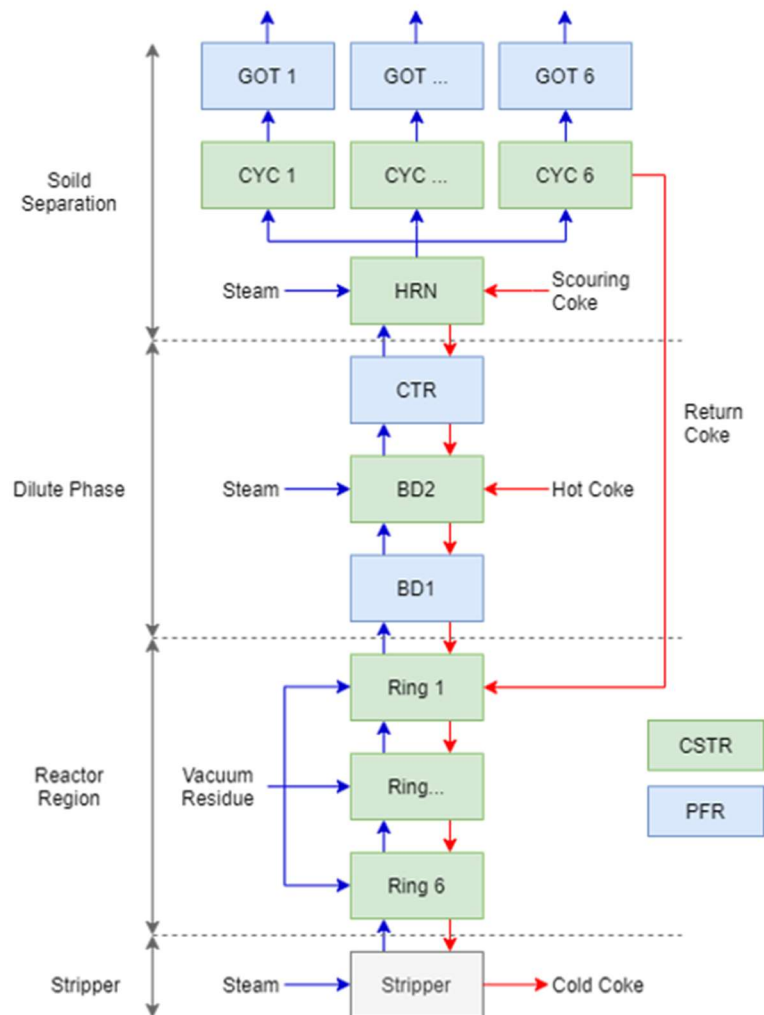


Figure 41. Block flow diagram for complex RTD based on modeling individual control volumes as either a CSTR or PFR.

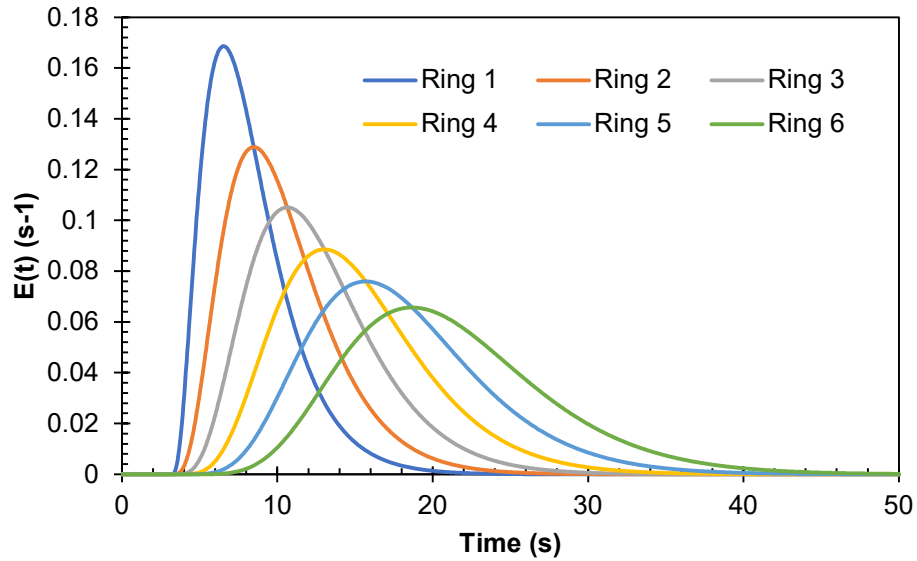


Figure 42. RTDs for each ring based on complex CSTR-PFR vapour model.

Assuming the feed is evenly split between the six rings, the residence time for all vapours entering the reactor can be estimated by taking the average of these RTDs. The overall RTD for the complex model, as well as an ideal CSTR and 50 tanks-in-series approximation models are shown in Figure 43. By using a combination of CSTRs and PFRs, the complex case falls in between the two ideal cases. For the ideal CSTR RTD, a fraction of the feed is predicted to bypass the Coker and exit immediately. In practice, due to the distance between the bed and cyclone outlet tubes, this would not be the case. The addition of the PFR regions into the RTD calculation improves upon this shortcoming of the CSTR model. When considering the product composition, the complex model once again is similar to the 50 tanks-in-series (i.e., PFR) model as shown in Figure 44. As the 50 tanks-in-series model is not a true PFR, rather an approximation between an ideal CSTR and PFR, it exhibits qualities of a mixed model. Results are thus comparable between it and the complex model, which shows higher light ends flow due to increased vapour phase cracking.

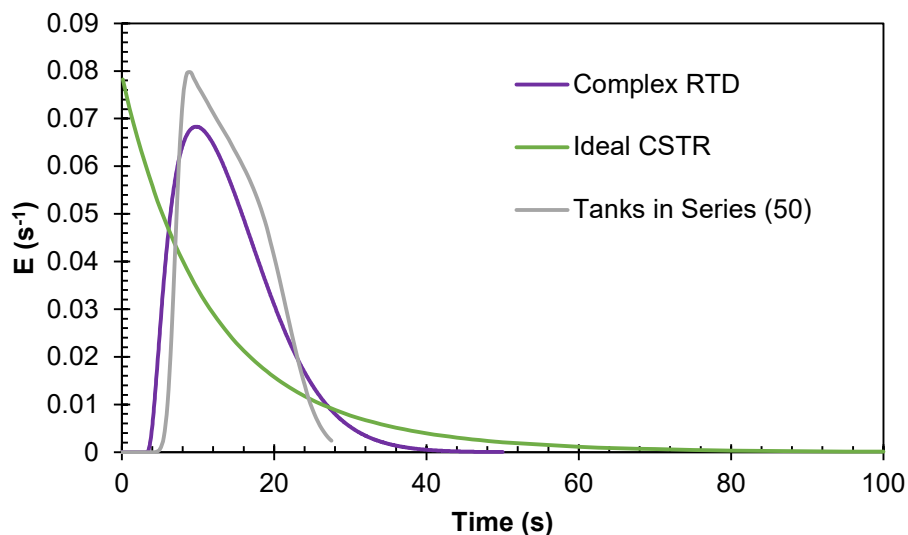


Figure 43. Overall vapour phase residence time distributions for the ideal CSTR, 50- tanks-in-series and complex flow pattern approximations.

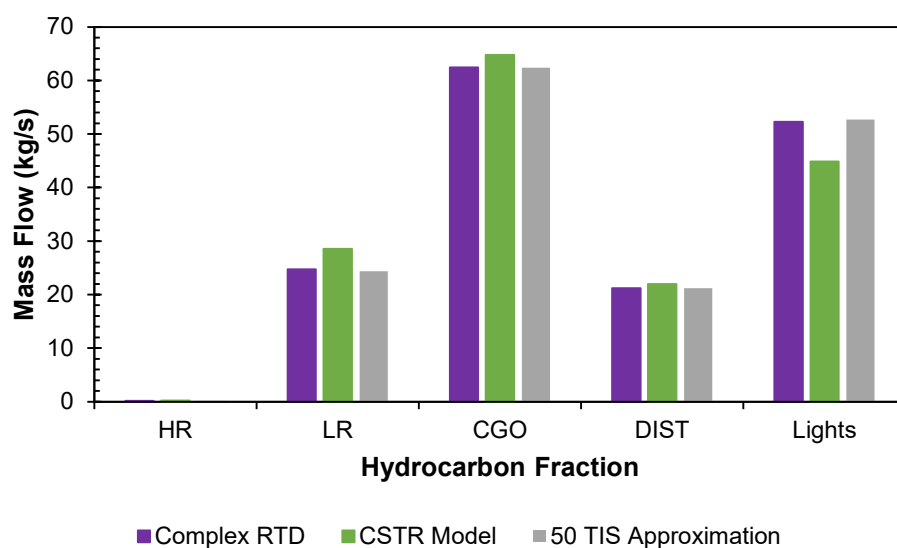


Figure 44. Impact of complex RTD on vapour products, compared to CSTR and PFR (50 tanks-in-series) cases.

4.5.4 Impact of hydrocarbon vapours on VLE

Each model previously presented has been solved sequentially starting with the top ring (ring 1) and working down to the bottom ring (ring 6). This was done to estimate the

effect of particles being recoated with fresh feed, thus considering liquids that remained on the particles to determine their impact on coke yield. As the composition of vapours travelling up the bed are not solved for this case until the bottom rings are solved, each ring has been assumed to contain only steam until products flashed in each respective ring are determined. Nonetheless, hydrocarbon vapours travelling up the bed would impact the VLE of each ring by reducing the driving force to transfer from the liquid to the vapour phase. The model may have thus overestimated the amount of vapours flashing from the liquid-solid phase. The previous simplifications could explain the increased vapour yields relative to those seen commercially. An ideal model would iterate between the liquid and vapour rate equations to solve for both phases simultaneously, while accounting for liquids travelling down the reactor, and vapours travelling upwards. As a preliminary verification, the composition of vapours travelling through each region was estimated based on the product distribution of the complex model (refer to Figure 44). The resulting overall vapour product flows are compared to the original predictions in Figure 45. This change to the VLE calculations resulted in a reduction of vapour products by 2.25 kg/s, or 1.2 wt% of the overall feed. This reduction came primarily at the expense of CGO, which is the primary vapour product, and would therefore be most impacted by the updated VLE estimates, and increased the total coke yield from 14 to 15 wt% of the overall feed.

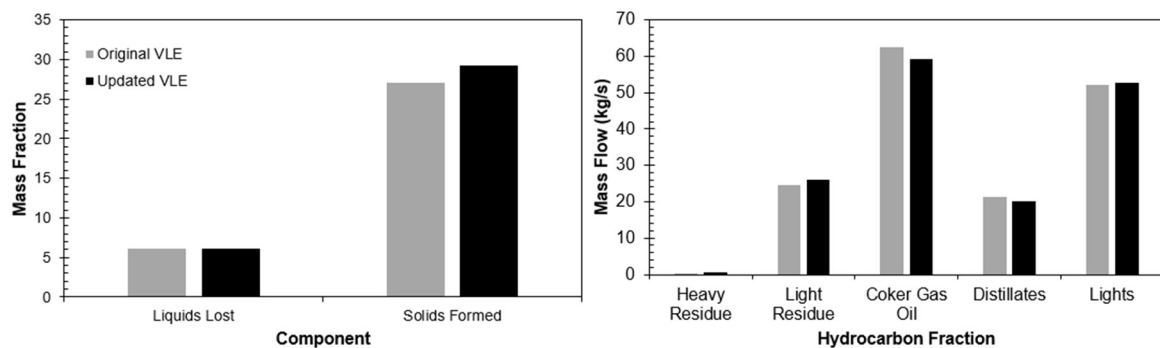


Figure 45. Impact of updated VLE on Fluid Coker products. By considering the vapours flowing upwards through the reactor, there is a reduction in vapours predicted compared to the original model, resulting in increased coke yield.

4.5.5 Impact of mixing between gas and liquid-solid phases

One additional consideration given for the complex RTD was mass transferring between the solid-liquid (i.e., solid-rich region) and vapour (gas-rich region) phases.

Previous models have considered these two phases separate and independent; however, it is likely for a fraction of the vapour phase to mix into the solids-rich region and vice-versa. As the solids region has a considerably longer residence time, the a gas fraction that becomes entrained in the solid would remain in the reactor for a considerably longer residence time, increasing the conversion to light products. In collaboration with Niall Murphy, a Simulink model was setup based off the complex CSTR-PFR approximation, previously shown in Figure 41, by adding separate liquid-solid regions in parallel with the vapours in the reactor bed as shown in Figure . A 5% mixing of the vapours moving between each phase was assumed, resulting in the RTDs for each ring shown in Figure 47. As a result of the gas-solid mixing modelled in each ring, a portion of the vapours remain in the reactor for much longer than previously modelled. The fraction that mixes into the solid phase results in a long tail on the residence time distribution, increasing the lights formed as demonstrated in Figure 48.

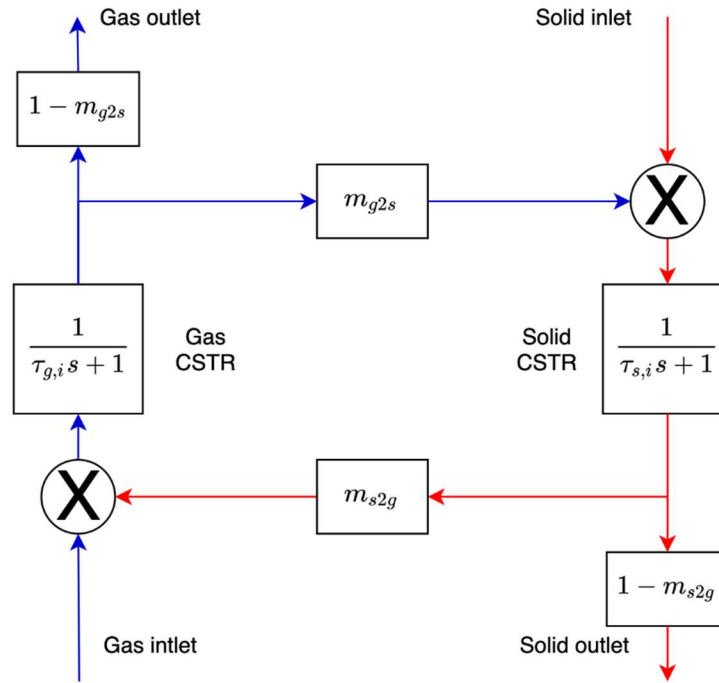


Figure 46. Block flow diagram for one ring of the proposed Simulink model to estimate RTD with 5% mixing of vapours between each region as prepared by Niall Murphy.

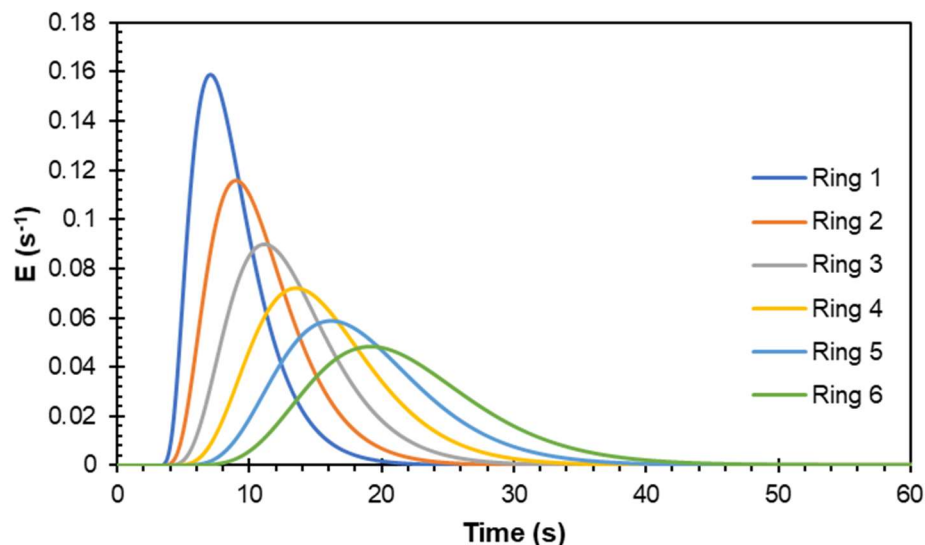


Figure 47. RTD for vapour phase for each ring with 5% mixing between solid-rich and gas-rich phases. Results part of a collaboration with Niall Murphy.

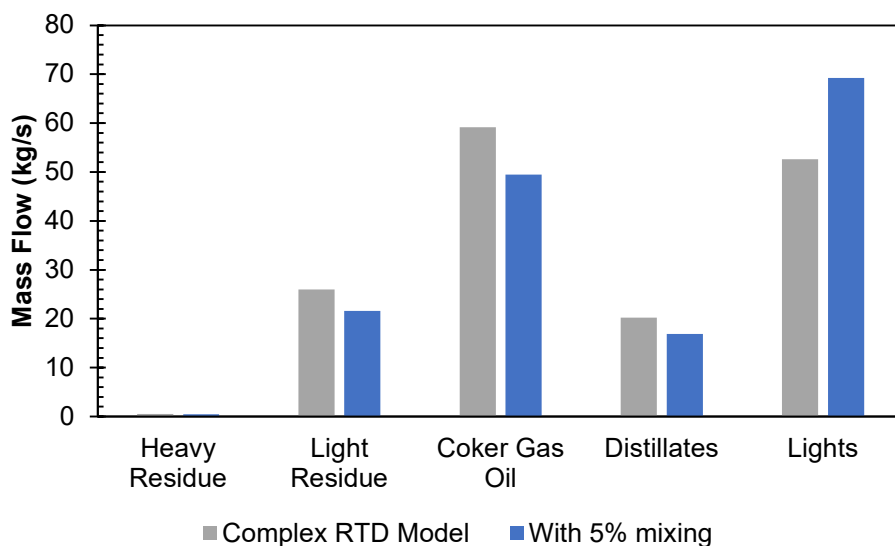


Figure 48. Impact of vapour-solid mixing on Fluid Coker products. Mixing of the vapours into the solid phase increases the resulting residence time, and ultimately the light products formed.

4.5.6 Impact of Bed Temperature

Chapter 3 demonstrated the effectiveness of increasing both scouring coke flow and transfer line temperature on reducing cyclone fouling. It was however noted that both process levers would provide more heat to the reactor bed, potentially increasing the reactor temperature. As a result, this case study aims to approximate the impact of bed temperature

on the Fluid Coker product quality. The temperature change will impact the model in two primary ways. First, the liquid and vapour phase rates of reaction will change as a function of temperature, as governed by the Arrhenius equation. In addition, the equilibrium constants, K , will change such that vaporization is more favourable as temperature increases. The values estimated from Aspen Plus are shown in Table 11 for temperatures ranging from 515-535°C. As the reactor temperature increases, Figure 49 shows a predicted decrease in Coke formation and liquids lost to the burner, which can be attributed to an increase in hydrocarbons flashing to the vapour phase.

With increasing reactor temperature, the product light gases also increase in flow, as shown in Figure 49. The vapour products distribution highlights the detriment with increasing the bed temperature. The total yield of vapour products does increase, where the total vapour mass flow increases from 153 to 162 kg/s when increasing the bed temperature from 515 to 535°C. However, the light ends ultimately dominate the vapour products, as the lights comprise 44 wt% of the vapour products at 535°C compared to 28 wt.% at 515°C. Although the temperature increase does reduce the liquids lost to the burner, the temperature increase ultimately reduces the quality of the products, negated the benefits of the increased yield.

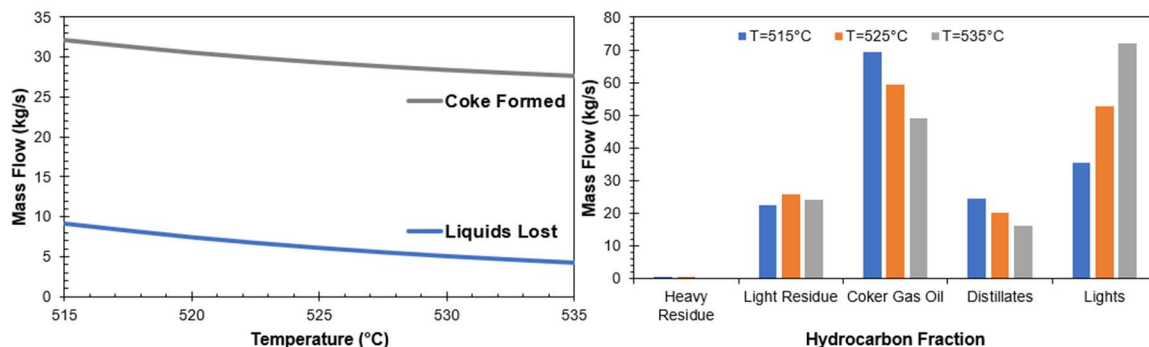


Figure 49. Change in coke formation and liquids lost to the burner and distribution of vapour products with increasing reactor temperature.

4.5.7 Impact of bed steam flowrate

As noted in the freeboard study reported in chapter three, increasing the steam flowrate had a positive impact on cyclone fouling. Therefore, a case study to determine the impact of changing steam flowrates on the reactor region is of interest. Theoretical impacts

of changing the steam was modelled, which considered the impact of steam on the vapour-liquid equilibrium in the reactor region was performed. This study did not consider the impact of steam on the dynamics (i.e. fluidization) of the bed, or the impact on vapour residence time at this time. The results shown in Figure 50 show minimal impact of steam flow on the resulting liquids lost and solids formed. The minor changes in solid-liquid yield result in a minimal change in vapour yields, however the distribution of vapour products is largely unchanged as a function of steam flowrate. As this model did not dynamically change the average residence times in response to the variable steam flowrate, the impact of steam may not be captured in this iteration of the model. The results from chapter three indicated that increased steam reduced vapour phase cracking by reducing the overall residence time, therefore future studies on the reactor region should estimate the resulting residence time as operating conditions change to improve the vapour phase cracking predictions.

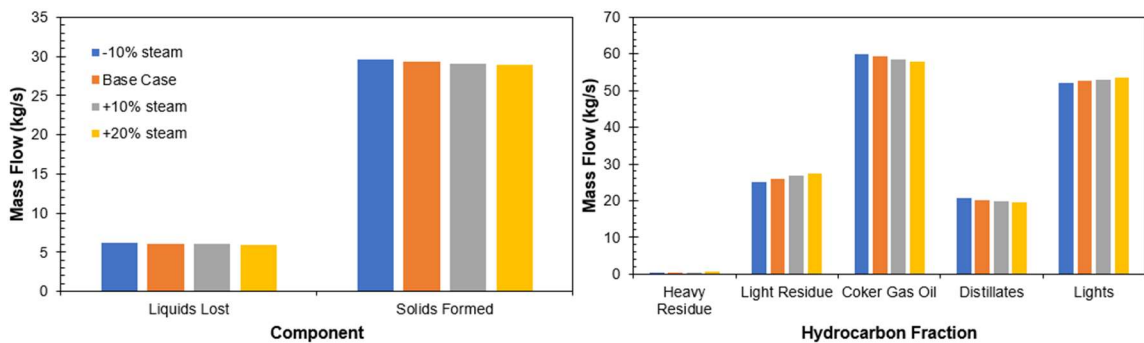


Figure 50. Change in coke formation and liquids lost to the burner and distribution of vapour products with variable steam flowrate.

4.6 Summary

This study was completed as an extension of the modelling efforts to reduce Fluid Coker cyclone to improve unit reliability as shown in Chapter 3. Previous modelling efforts found increased scouring coke flow and transfer line temperature were effective strategies to mitigate against cyclone fouling. However, as the previous models were limited to the freeboard region, the impact on reactor performance was unknown. The primary objective of this study was thus to develop a novel model of the reactor region of a commercial Fluid Coker to investigate the impact of operating conditions on reactor performance. Overall, this study found

- Increased reactor temperature increased the yield of light gases exiting the Fluid Coker, with an additional 37 wt% lights formed due to a 10°C increase in reactor temperature.
- Variations in the liquid-solid phase RTD had minimal impact on composition of reactor products.
- Variations in the vapour phase RTD impacted the composition of reactor products, with a 17.5 wt% increase in light ends in the complex RTD compared to the ideal CSTR base case
- Simplifying assumptions to the increased steam flowrate case study limited the impact of this factor. Future iterations should consider the change on residence time caused by increased steam flow rates.

Chapter 5: Conclusions and Recommendations

The main objective of this thesis was to advance the modelling efforts for the Fluid Coker to improve unit reliability. Due to the condensation of heavy ends, cyclone fouling is a limiting factor in the run length of commercial Fluid Cokers. A previous study modeled the freeboard region and identified the scouring coke flow rate and transfer line temperature as effective methods to mitigate this phenomenon. This thesis improved upon this work with two contributions. First, the freeboard model was expanded to include vapour phase cracking and hydrocarbon adsorption to predict their impact on the products exiting the Fluid Coker. Second, a novel model of the reactor region was developed to predict the impact of various process parameters on the fluidized bed reactor region and the subsequent products exiting the reactor, which had not previously been considered.

5.1 Freeboard Model

The updated model highlighted the relevance of vapour phase cracking on the Fluid Coker, as seen by the predicted temperature drop of approximately 2°C compared to the model without vapour cracking. Despite the cooler temperatures, the compositional change due to vapour phase cracking shifted the cracked heavy hydrocarbons to the light and distillate fractions, reducing cyclone liquids compared to the non-cracking reference point. With the updated model, strategies to reduce cyclone fouling while considering product quality could be performed. Ideal process levers would reduce fouling by upwards of 80%, while maintaining or reducing the light products formed compared to base case conditions.

Four process levers were investigated to determine their impact on reactor performance: scouring coke flow rate, transfer line temperature, entrained bed coke flow and bed steam flowrate. Of these four parameters, only increasing the bed steam flowrate yielded the ideal result of decreasing both cyclone liquids and vapour phase cracking; however, doubling the steam flow rate only reduced the predicted liquids by 20% relative to the base case. Increasing the steam flowrate alone would therefore not be sufficient to reduce cyclone liquids by the desired amount. Of the remaining three process levers, scouring coke flowrate achieved the desired liquids reduction with the smallest impact on over cracking vapours. As the scouring coke only resulted in a temperature increase of the horn chamber, cyclone and gas outlet tube control volumes, the vapour residence time was

sufficiently short to minimize the vapour phase cracking. When compared to increasing the transfer line temperature, increased scouring flow achieves a comparable cyclone liquid reduction with 1.5 wt% less light gases formed. Consideration should be given to increasing both parameters to maximize the cyclone liquid reduction, while minimizing the vapour phase cracking. Compared to these levers, the impact of adsorption on cyclone fouling in the freeboard region appeared to be minimal. The increased adsorption capacity of the flexicoke did result in a minor liquids reduction compared to fluid coke, however it is not clear if that change would have a tangible impact on unit reliability.

5.2 Reactor Model

The reactor region model was used to determine the impact of liquid-solid and vapour residence time distribution, reactor temperature and steam flowrate on the resulting coke yield, liquids lost to the burner and vapour product composition. Using a tanks-in-series approximation, it was found that the liquid-solid phase was less impacted by the residence time distribution, with minimal variance in reactor products between cases. The vapour phase composition showed some sensitivity to its RTD, with a 7.9 kg/s (17.5 wt%) increase in light gases due to the 50 TIS and complex RTD model compared to the ideal CSTR approximation. As anticipated from the Chapter 3 results, vapour product yield was sensitive to changes in reactor temperature, as this correlated with light gas yield. Increasing the reactor temperature by 10°C above the base conditions resulted in a 37 wt% increase in light gases exiting the Fluid Coker. Due to the promise shown for increased steam flow as a method to reduce fouling, a case study was performed to estimate its impact on reactor performance. Increased steam was shown to have a minor change to the coke yield and lost liquids, however as its impact on the vapour phase residence time was not captured in the model, its ultimate impact on vapour product composition was not effectively represented by this iteration of the model.

5.3 Recommendations for Future Work

5.3.1 Freeboard Model

Estimating the Ranque-Hilsch effect using proprietary equations provided by Syncrude allows for a dynamic estimate of the temperature change while varying the

operating conditions of the reactor; however, the temperature change predicted may be inaccurate based on the simplifying assumptions made in its derivation. A detailed derivation, or approximation using a computational fluid dynamic model may provide a better estimate for this temperature change.

Aspen Plus has the ability to complete a rigorous simulation of a cyclone separation operation. Incorporating this detail may enhance the accuracy of the pressure drop calculations applied to the model, while allowing for the investigation of the impact of changing cyclone geometry on fouling.

Finally, the impact of adsorption was estimated using many simplifying assumptions as a foundation for its calculation. Further experimental studies could improve the modelling effort. The first recommendation would be to perform kinetic studies on preferential adsorption to determine if the problematic heavy residue fraction would be preferentially adsorbed by coke, thereby reducing fouling. Further studies with heavier hydrocarbons and at temperatures closer to FLUID COKING™ conditions would provide further justification for the assumptions made, while an alternative method to the pore-volume based estimate could improve the overall accuracy of the model.

5.3.2 Reactor Model

While the entire complexity of the commercial Fluid Coker was not captured in this numerical model, this study was effective in demonstrating the impact of reactor performance with varying temperature and flow patterns. The method to calculate the reaction kinetics, equilibrium and residence time distributions for both the vapour and liquid-solid regions can be used as a foundation for future Fluid Coker models. Nonetheless, a number of simplifying assumptions were made when developing the model which can be investigated in subsequent studies.

When considering the injection of feed into the bed, the model assumed that a given set of particles was coated at the top of the control volume and travelled through this region unchanged until being coated again by the following nozzle. In reality, it is possible for mixing to occur which would result in particles being coated multiple times by a nozzle, resulting in thicker liquid films which could increase the formation and yield of extrinsic coke. Similarly, the formation of larger agglomerates has been shown to occur in the

commercial reactor. Again, these agglomerates would result in increased coke yield, and potentially impact the overall reactor performance.

Although the presence of flashed vapours was considered in the mass transfer calculations, further improvements could be made. Solids and liquids near the centre of the Fluid Coker likely have increased steam flow that helps strip products off the coke particles. However, as you move outwards towards the wall of the Fluid Coker, the region is increasingly solids-rich, with less steam present to strip the products formed. It is thus possible that the solid rich region could be near saturation. Before more products could flash, vapours would need to diffuse out of the solids-rich region, into the core where it can quickly be swept out of the bed. The current model treats all solids as if they are in the presence of the overall vapour composition of the reactor, thus not capturing the variation between the core and annulus regions. A study which considered this mass transfer resistance could determine whether the diffusion is a limiting effect on Coker product formation, and the impact of increasing the solid-vapour mixing.

Finally, the entire reactor, including the freeboard region, was treated as isothermal. Incorporating enthalpy of reaction calculations to the model would allow for the modelling of temperature gradients throughout the reactor region, while better calculating the Fluid Coker products by accounting for the increased cracking following the addition of the hot and scouring coke.

The ultimate goal of these parallel studies would be to combine them into a single model. This could include the addition of the burner region to the model, and allow for case studies on the entire system to be run simultaneously. This would allow for changes in reactor products to be reflected in the freeboard composition as parameters are changed, as well the impact of gradual system pressure increases on reactor performance.

Bibliography

- [1] US Energy Information Administration, International Energy Outlook 2019 with projections to 2050, (2019) 85. doi:10.5860/CHOICE.44-3624.
- [2] BP Stats, Statistical Review of World Energy, 68th edition, Ed. BP Stat. Rev. World Energy. (2019) 1–69. <https://www.bp.com/content/dam/bp/business-sites/en/global/corporate/pdfs/energy-economics/statistical-review/bp-stats-review-2019-full-report.pdf>.
- [3] M. Gray, Upgrading Oilsands Bitumen and Heavy Oil, The University of Alberta Press, Edmonton, 2015.
- [4] X. Song, H. Bi, C. Jim Lim, J.R. Grace, E. Chan, B. Knapper, C. McKnight, Hydrodynamics of the reactor section in fluid cokers, Powder Technol. 147 (2004) 126–136. doi:10.1016/j.powtec.2004.09.033.
- [5] W. Zhang, A.P. Watkinson, Carbonaceous material deposition from heavy hydrocarbon vapors. 2. Mathematical modeling, Ind. Eng. Chem. Res. 44 (2005) 4092–4098. doi:10.1021/ie0490334.
- [6] W. Zhang, P. Watkinson, Carbonaceous Material Deposition from Heavy Hydrocarbon Vapors. 1. Experimental Investigation, Ind. Eng. Chem. Res. 44 (2005) 4084–4091. doi:10.1021/ie049055q.
- [7] S.W. Kim, J.W. Lee, J.S. Koh, G.R. Kim, S. Choi, I.S. Yoo, Formation and characterization of deposits in cyclone dipleg of a commercial residue fluid catalytic cracking reactor, Ind. Eng. Chem. Res. 51 (2012) 14279–14288. doi:10.1021/ie301864x.
- [8] E. Glatt, D. Pjontek, C. McKnight, J. Wiens, M. Wormsbecker, J. McMillan, Hydrocarbon condensation modelling to mitigate fluid coker cyclone fouling, Can. J. Chem. Eng. 99 (2021) 209–221. doi:10.1002/cjce.23830.
- [9] J. Gary, G. Handwerk, M. Kaiser, Petroleum Refining - Technology and Economics, 2007. doi:10.3775/jie.67.11_972.

- [10] CAPP, Canada's Oil and Natural Gas Industry Energy Tomorrow, (2017).
- [11] L.C. Castañeda, J.A.D. Muñoz, J. Ancheyta, Combined process schemes for upgrading of heavy petroleum, *Fuel*. 100 (2012) 110–127. doi:10.1016/j.fuel.2012.02.022.
- [12] R. Sahu, B.J. Song, J.S. Im, Y.P. Jeon, C.W. Lee, A review of recent advances in catalytic hydrocracking of heavy residues, *J. Ind. Eng. Chem.* 27 (2015) 12–24. doi:10.1016/j.jiec.2015.01.011.
- [13] M.S. Rana, V. Sámano, J. Ancheyta, J.A.I. Diaz, A review of recent advances on process technologies for upgrading of heavy oils and residua, *Fuel*. 86 (2007) 1216–1231. doi:10.1016/j.fuel.2006.08.004.
- [14] D.S. Borey, C.E. Jahng, R.W. Pfeiffer, D.S. Borey, *Fluid Coking of Heavy Hydrocarbons*, (1959).
- [15] C.B. Solnordal, K.J. Reid, L.P. Hackman, R. Cocco, J. Findlay, Modeling coke distribution above the freeboard of a FLUID COKING reactor, *Ind. Eng. Chem. Res.* 51 (2012) 15337–15350. doi:10.1021/ie3010176.
- [16] I.A. Wiehe, Mitigation of the fouling by popcorn coke, *Pet. Sci. Technol.* 21 (2003) 673–680. doi:10.1081/LFT-120018546.
- [17] D.G. Mallory, S.A. Mehta, R.G. Moore, S. Richardson, The role of the vapour phase in fluid coker cyclone fouling: Part 1. Coke yields, *Can. J. Chem. Eng.* 78 (2000) 330–336. doi:10.1002/cjce.5450780207.
- [18] P. Gonzalez, *Mechanisms of Aerosol Formation in Bitumen Cracking*, Univ. Alberta. (2004).
- [19] B. Lakghomi, F. Taghipour, D. Posarac, A.P. Watkinson, CFD simulation and experimental measurement of droplet deposition and hydrocarbon fouling at high temperatures, *Chem. Eng. J.* 172 (2011) 507–516. doi:10.1016/j.cej.2011.06.046.
- [20] J. Jankovic, *Simulation of the Scrubber Section of a Fluid Coker*, (1996).
- [21] J. Singh, S. Kumar, M.O. Garg, Kinetic modelling of thermal cracking of petroleum

- residues: A critique, *Fuel Process. Technol.* 94 (2012) 131–144. doi:10.1016/j.fuproc.2011.10.023.
- [22] I.A. Wiehe, A Phase-Separation Kinetic Model for Coke Formation, *Ind. Eng. Chem. Res.* 32 (1993) 2447–2454. doi:10.1021/ie00023a001.
- [23] R.P. Dutta, W.C. McCaffrey, M.R. Gray, K. Muehlenbachs, Use of ¹³C tracers to determine mass-transfer limitations on thermal cracking of thin films of bitumen, *Energy and Fuels.* 15 (2001) 1087–1093. doi:10.1021/ef0002694.
- [24] W.N. Olmstead, H. Freund, Thermal conversion kinetics of petroleum residua, *AIChE Spring Meet.* (1998).
- [25] M.R. Gray, W.C. McCaffrey, I. Huq, T. Le, Kinetics of cracking and devolatilization during coking of Athabasca residues, *Ind. Eng. Chem. Res.* 43 (2004) 5438–5445. doi:10.1021/ie030654r.
- [26] R. Radmanesh, E. Chan, M.R. Gray, Modeling of mass transfer and thermal cracking during the coking of Athabasca residues, *Chem. Eng. Sci.* 63 (2008) 1683–1691. doi:10.1016/j.ces.2007.11.019.
- [27] W. Bu, M.R. Gray, Kinetics of vapor-phase cracking of bitumen-derived heavy gas oil, *Energy and Fuels.* 27 (2013) 2999–3005. doi:10.1021/ef4009407.
- [28] O. Levenspiel, *Chemical reaction engineering*, Third Edit, 1999. doi:10.1021/ie990488g.
- [29] E.P. Toroudi, Adsorption kinetics of C9-C12 hydrocarbons on carbonaceous materials, (2018).
- [30] J.G. Polihronov, A.G. Straatman, Thermodynamics of angular propulsion in fluids, *Phys. Rev. Lett.* 109 (2012) 1–4. doi:10.1103/PhysRevLett.109.054504.
- [31] M.J. Parker, A.G. Straatman, Experimental Study on the Impact of Pressure Ratio on Temperature Drop in a Ranque-Hilsch Vortex Tube, *Appl. Therm. Eng. (In Rev.* 189 (2021) 116653. doi:10.1016/j.applthermaleng.2021.116653.
- [32] D. Green, R. Perry, *Perry's Chemical Engineers' Handbook* 8th Edition, 2008.

- [33] Wen-Ching Yang, Handbook of Fluidization and Fluid-Particle Systems, Marcel Dekker, Inc, New York, 2003.
- [34] G. Wu, Y. Katsumura, C. Matsuura, K. Ishigure, J. Kubo, Comparison of Liquid-Phase and Gas-Phase Pure Thermal Cracking of n-Hexadecane, Ind. Eng. Chem. Res. 35 (1996) 4747–4754. doi:10.1021/ie960280k.
- [35] H.S. Fogler, Elements of Chemical Reaction Engineering, 5th Editio, Pearson, 2016.

Appendix

Copyright Permissions for Figure 4.

JOHN WILEY AND SONS LICENSE TERMS AND CONDITIONS

Apr 05, 2021

This Agreement between Western University -- Andrew Heaslip ("You") and John Wiley and Sons ("John Wiley and Sons") consists of your license details and the terms and conditions provided by John Wiley and Sons and Copyright Clearance Center.

License Number	5042540395367
License date	Apr 05, 2021
Licensed Content Publisher	John Wiley and Sons
Licensed Content Publication	Canadian Journal of Chemical Engineering
Licensed Content Title	The role of the vapour phase in fluid coker cyclone fouling: Part 1. Coke yields
Licensed Content Author	Donald G. Mallory, S. A. (Raj) Mehta, R. Gordon Moore, et al
Licensed Content Date	Mar 27, 2009
Licensed Content Volume	78
Licensed Content Issue	2
Licensed Content Pages	7
Type of use	Dissertation/Thesis
Requestor type	University/Academic
Format	Electronic
Portion	Figure/table
Number of figures/tables	1

Will you be translating?	No
Title	Mitigation of Fluid Coker Cyclone Fouling with Consideration to Reactor Performance
Institution name	Western University
Expected presentation date	Apr 2021
Portions	Figure 1. Locations of coke formations in cyclones. Western University 500 Proudfoot Lane Apartment 206
Requestor Location	London, ON N6H5G7 Canada Attn: Western University
Publisher Tax ID	EU826007151
Total	0.00 USD
Terms and Conditions	

TERMS AND CONDITIONS

This copyrighted material is owned by or exclusively licensed to John Wiley & Sons, Inc. or one of its group companies (each a "Wiley Company") or handled on behalf of a society with which a Wiley Company has exclusive publishing rights in relation to a particular work (collectively "WILEY"). By clicking "accept" in connection with completing this licensing transaction, you agree that the following terms and conditions apply to this transaction (along with the billing and payment terms and conditions established by the Copyright Clearance Center Inc., ("CCC's Billing and Payment terms and conditions"), at the time that you opened your RightsLink account (these are available at any time at <http://myaccount.copyright.com>).

Terms and Conditions

- The materials you have requested permission to reproduce or reuse (the "Wiley Materials") are protected by copyright.
- You are hereby granted a personal, non-exclusive, non-sub licensable (on a stand-alone basis), non-transferable, worldwide, limited license to reproduce the Wiley Materials for the purpose specified in the licensing process. This license, **and any CONTENT (PDF or image file)**

purchased as part of your order, is for a one-time use only and limited to any maximum distribution number specified in the license. The first instance of republication or reuse granted by this license must be completed within two years of the date of the grant of this license (although copies prepared before the end date may be distributed thereafter). The Wiley Materials shall not be used in any other manner or for any other purpose, beyond what is granted in the license. Permission is granted subject to an appropriate acknowledgement given to the author, title of the material/book/journal and the publisher. You shall also duplicate the copyright notice that appears in the Wiley publication in your use of the Wiley Material. Permission is also granted on the understanding that nowhere in the text is a previously published source acknowledged for all or part of this Wiley Material. Any third party content is expressly excluded from this permission.

- With respect to the Wiley Materials, all rights are reserved. Except as expressly granted by the terms of the license, no part of the Wiley Materials may be copied, modified, adapted (except for minor reformatting required by the new Publication), translated, reproduced, transferred or distributed, in any form or by any means, and no derivative works may be made based on the Wiley Materials without the prior permission of the respective copyright owner. **For STM Signatory Publishers clearing permission under the terms of the [STM Permissions Guidelines](#) only, the terms of the license are extended to include subsequent editions and for editions in other languages, provided such editions are for the work as a whole in situ and does not involve the separate exploitation of the permitted figures or extracts**, You may not alter, remove or suppress in any manner any copyright, trademark or other notices displayed by the Wiley Materials. You may not license, rent, sell, loan, lease, pledge, offer as security, transfer or assign the Wiley Materials on a stand-alone basis, or any of the rights granted to you hereunder to any other person.
- The Wiley Materials and all of the intellectual property rights therein shall at all times remain the exclusive property of John Wiley & Sons Inc, the Wiley Companies, or their respective licensors, and your interest therein is only that of having possession of and the right to reproduce the Wiley Materials pursuant to Section 2 herein during the continuance of this Agreement. You agree that you own no right, title or interest in or to the Wiley Materials or any of the intellectual property rights therein. You shall have no rights hereunder other than the license as provided for above

in Section 2. No right, license or interest to any trademark, trade name, service mark or other branding ("Marks") of WILEY or its licensors is granted hereunder, and you agree that you shall not assert any such right, license or interest with respect thereto

- NEITHER WILEY NOR ITS LICENSORS MAKES ANY WARRANTY OR REPRESENTATION OF ANY KIND TO YOU OR ANY THIRD PARTY, EXPRESS, IMPLIED OR STATUTORY, WITH RESPECT TO THE MATERIALS OR THE ACCURACY OF ANY INFORMATION CONTAINED IN THE MATERIALS, INCLUDING, WITHOUT LIMITATION, ANY IMPLIED WARRANTY OF MERCHANTABILITY, ACCURACY, SATISFACTORY QUALITY, FITNESS FOR A PARTICULAR PURPOSE, USABILITY, INTEGRATION OR NON-INFRINGEMENT AND ALL SUCH WARRANTIES ARE HEREBY EXCLUDED BY WILEY AND ITS LICENSORS AND WAIVED BY YOU.
- WILEY shall have the right to terminate this Agreement immediately upon breach of this Agreement by you.
- You shall indemnify, defend and hold harmless WILEY, its Licensors and their respective directors, officers, agents and employees, from and against any actual or threatened claims, demands, causes of action or proceedings arising from any breach of this Agreement by you.
- IN NO EVENT SHALL WILEY OR ITS LICENSORS BE LIABLE TO YOU OR ANY OTHER PARTY OR ANY OTHER PERSON OR ENTITY FOR ANY SPECIAL, CONSEQUENTIAL, INCIDENTAL, INDIRECT, EXEMPLARY OR PUNITIVE DAMAGES, HOWEVER CAUSED, ARISING OUT OF OR IN CONNECTION WITH THE DOWNLOADING, PROVISIONING, VIEWING OR USE OF THE MATERIALS REGARDLESS OF THE FORM OF ACTION, WHETHER FOR BREACH OF CONTRACT, BREACH OF WARRANTY, TORT, NEGLIGENCE, INFRINGEMENT OR OTHERWISE (INCLUDING, WITHOUT LIMITATION, DAMAGES BASED ON LOSS OF PROFITS, DATA, FILES, USE, BUSINESS OPPORTUNITY OR CLAIMS OF THIRD PARTIES), AND WHETHER OR NOT THE PARTY HAS BEEN ADVISED OF THE POSSIBILITY OF SUCH DAMAGES. THIS LIMITATION SHALL APPLY NOTWITHSTANDING ANY FAILURE OF ESSENTIAL PURPOSE OF ANY LIMITED REMEDY PROVIDED HEREIN.

- Should any provision of this Agreement be held by a court of competent jurisdiction to be illegal, invalid, or unenforceable, that provision shall be deemed amended to achieve as nearly as possible the same economic effect as the original provision, and the legality, validity and enforceability of the remaining provisions of this Agreement shall not be affected or impaired thereby.
- The failure of either party to enforce any term or condition of this Agreement shall not constitute a waiver of either party's right to enforce each and every term and condition of this Agreement. No breach under this agreement shall be deemed waived or excused by either party unless such waiver or consent is in writing signed by the party granting such waiver or consent. The waiver by or consent of a party to a breach of any provision of this Agreement shall not operate or be construed as a waiver of or consent to any other or subsequent breach by such other party.
- This Agreement may not be assigned (including by operation of law or otherwise) by you without WILEY's prior written consent.
- Any fee required for this permission shall be non-refundable after thirty (30) days from receipt by the CCC.
- These terms and conditions together with CCC's Billing and Payment terms and conditions (which are incorporated herein) form the entire agreement between you and WILEY concerning this licensing transaction and (in the absence of fraud) supersedes all prior agreements and representations of the parties, oral or written. This Agreement may not be amended except in writing signed by both parties. This Agreement shall be binding upon and inure to the benefit of the parties' successors, legal representatives, and authorized assigns.
- In the event of any conflict between your obligations established by these terms and conditions and those established by CCC's Billing and Payment terms and conditions, these terms and conditions shall prevail.
- WILEY expressly reserves all rights not specifically granted in the combination of (i) the license details provided by you and accepted in the course of this licensing transaction, (ii) these terms and conditions and (iii) CCC's Billing and Payment terms and conditions.

- This Agreement will be void if the Type of Use, Format, Circulation, or Requestor Type was misrepresented during the licensing process.
- This Agreement shall be governed by and construed in accordance with the laws of the State of New York, USA, without regards to such state's conflict of law rules. Any legal action, suit or proceeding arising out of or relating to these Terms and Conditions or the breach thereof shall be instituted in a court of competent jurisdiction in New York County in the State of New York in the United States of America and each party hereby consents and submits to the personal jurisdiction of such court, waives any objection to venue in such court and consents to service of process by registered or certified mail, return receipt requested, at the last known address of such party.

WILEY OPEN ACCESS TERMS AND CONDITIONS

Wiley Publishes Open Access Articles in fully Open Access Journals and in Subscription journals offering Online Open. Although most of the fully Open Access journals publish open access articles under the terms of the Creative Commons Attribution (CC BY) License only, the subscription journals and a few of the Open Access Journals offer a choice of Creative Commons Licenses. The license type is clearly identified on the article.

The Creative Commons Attribution License

The [Creative Commons Attribution License \(CC-BY\)](#) allows users to copy, distribute and transmit an article, adapt the article and make commercial use of the article. The CC-BY license permits commercial and non-

Creative Commons Attribution Non-Commercial License

The [Creative Commons Attribution Non-Commercial \(CC-BY-NC\) License](#) permits use, distribution and reproduction in any medium, provided the original work is properly cited and is not used for commercial purposes.(see below)

Creative Commons Attribution-Non-Commercial-NoDerivs License

The [Creative Commons Attribution Non-Commercial-NoDerivs License](#) (CC-BY-NC-ND) permits use, distribution and reproduction in any medium, provided

the original work is properly cited, is not used for commercial purposes and no modifications or adaptations are made. (see below)

Use by commercial "for-profit" organizations

Use of Wiley Open Access articles for commercial, promotional, or marketing purposes requires further explicit permission from Wiley and will be subject to a fee.

Further details can be found on Wiley Online

Library <http://olabout.wiley.com/WileyCDA/Section/id-410895.html>

Other Terms and Conditions:

v1.10 Last updated September 2015

Curriculum Vitae

Name	Andrew Heaslip
Post-Secondary Education and Degrees	<p>B.E.Sc. - Chemical Engineering The University of Western Ontario 2013-2018</p> <p>M.E.Sc. – Chemical Engineering The University of Western Ontario 2019-2021</p>
Honours and Awards	<p>Ontario Graduate Scholarship 2019, 2020</p> <p>Dean’s Honour List 2014-2016</p>
Related Work Experience	<p>Teaching Assistant The University of Western Ontario 2019-2021</p> <p>Pipeline Engineer in Training Enbridge Gas Distribution 2018-2019</p> <p>Stations Engineering Intern Union Gas 2016-2017</p>